111-15

NASA Contractor Report 202325

Summary Report of Mission Acceleration Measurements for STS–79

Launched September 16, 1996

Melissa J.B. Rogers, Milton E. Moskowitz,
Kenneth Hrovat, and Timothy A. Reckart
Tal-Cut Company
North Olmsted, Ohio

March 1997

Prepared for
Lewis Research Center
Under Contract NAS3–27254

National Aeronautics and
Space Administration

SUMMARY REPORT OF MISSION ACCELERATION MEASUREMENTS FOR STS-79

Launched September 16, 1996

Authors:

Melissa J.B. Rogers
Tal-Cut Company
North Olmsted, Ohio

Milton E. Moskowitz
Tal-Cut Company
North Olmsted, Ohio

Kenneth Hrovat
Tal-Cut Company
North Olmsted, Ohio

Timothy A. Reckart
Tal-Cut Company
North Olmsted, Ohio

Abstract

The Space Acceleration Measurement System (SAMS) collected acceleration data in support of the Mechanics of Granular Materials experiment during the STS-79 Mir docking mission, September 1996. STS-79 was the first opportunity to record SAMS data on an Orbiter while it was docked to Mir. Crew exercise activities in the Atlantis middeck and the Mir base module are apparent in the data. The acceleration signals related to the Enhanced Orbiter Refrigerator Freezer had different characteristics when comparing the data recorded on Atlantis on STS-79 with the data recorded on Mir during STS-74. This is probably due, at least in part, to different transmission paths and SAMS sensor head mounting mechanisms. Data collected on Atlantis during the STS-79 docking indicate that accelerations due to vehicle and solar array structural modes from Mir transfer to Atlantis and that the structural modes of the Atlantis-Mir complex are different from those of either vehicle independently. A 0.18 Hz component of the SAMS data, present while the two vehicles were docked, was probably caused by the Mir solar arrays. Compared to Atlantis structural modes of about 3.9 and 4.9 Hz, the Atlantis-Mir complex has structural components of about 4.5 and 5.1 Hz. After docking, apparent structural modes appeared in the data at about 0.8 and 1.8 Hz. The appearance, disappearance, and change in the structural modes during the docking and undocking phases of the joint Atlantis-Mir operations indicates that the structural modes of the two spacecraft have an effect on the microgravity environment of each other. The transfer of structural and equipment related accelerations between vehicles is something that should be considered in the International Space Station era.

Table of Contents

List of Tables

List of Figures

Abbreviations and Acronyms

$accel_{avg}$	root-sum-square of averaged triaxial data
$accel_{RMS}$	root-sum-square of RMS of triaxial data
ARIS	Active Rack Isolation System
CG	Center of Gravity
DMT	Decreed Moscow Time
EDT	Eastern Daylight Time
EORF	Enhanced Orbiter Refrigerator Freezer
GMT	Greenwich Mean Time (day/hour:minute:second)
ISS	International Space Station
k	number of time series interval used in analysis
LeRC	NASA Lewis Research Center
M	number of points in time series interval used in analysis
MET	Mission Elapsed Time (day/hour:minute:second)
PIMS	Principal Investigator Microgravity Services
PSD	Power Spectral Density
RME	Risk Mitigation Experiment
RMS	root mean square
SAMS	Space Acceleration Measurement System
TSH	Triaxial Sensor Head
VRCS	Vernier Reaction Control System
X_h, Y_h, Z_h	SAMS sensor head coordinate system axes
X_o, Y_o, Z_o	Orbiter structural coordinate system axes

Acknowledgments

Shannon Lucid, Board Engineer 2 on the Mir Space Station between 22 March and 26 September 1996, provided valuable information about crew exercise on Mir and on Atlantis during STS-79. Manny Avila, Code EA at NASA JSC, provided useful information about refrigerator/freezer systems used on different Orbiter missions.

1. Introduction

Microgravity science experiments are conducted on the NASA Space Shuttle Orbiters to take advantage of the reduced gravity environment provided by low earth orbit. Accelerometer systems are flown in conjunction with these experiments to record the microgravity environment that the experiments experience. The Mechanics of Granular Material experiment flew in the SPACEHAB module on the Orbiter Atlantis on mission STS-79 in September 1996. The Space Acceleration Measurement System (SAMS), managed by the NASA Lewis Research Center (LeRC), collected acceleration data in support of this experiment. This report was prepared by the Principal Investigator Microgravity Services (PIMS) project at NASA LeRC as a summary of the microgravity environment during this Orbiter mission. In addition, PIMS provides internet-based file server access to SAMS data and specialized analyses of data upon request. For information on how to obtain SAMS data and request analysis, see Appendix A.

2. Mission Overview

At 4:54:49 a.m. EDT on 16 September 1996, the Space Shuttle Atlantis launched on the STS-79 mission from NASA Kennedy Space Center. Landing was at Kennedy Space Center on 26 September at 8:13:20 a.m. EDT. In terms of other time conventions used in this report, launch was at Greenwich Mean Time (GMT) 260/08:54:49 or mission elapsed time (MET) 000/00:00:00 and landing was at GMT 270/12:13:20 or MET 010/03:18:31. Both GMT and MET are recorded in day/hour:minute:second format. STS-79 was the fourth Shuttle-Mir docking mission. During the docked phase, resupply items, such as water and food, and research hardware and equipment were transferred from Atlantis to Mir. Atlantis returned Russian, European, and American science samples and hardware to Earth.

The goals of the STS-79 and Shuttle-Mir experiments were to provide valuable information about space flight and long term exposure to the microgravity environment. This knowledge will be used in the development of the International Space Station (ISS) and of specific experiment facilities for the Orbiter, Mir, and ISS. The major STS-79 payloads are listed in Table 1. Development Test Objectives, Detailed Supplementary Objectives, and Risk Mitigation Experiments are listed in Table 2. The STS-79 crew members are listed in Table 3.

The Mechanics of Granular Materials microgravity experiment was performed in the SPACEHAB module. The goal of this experiment was to develop a quantitative scientific understanding of the behavior of cohesionless granular materials in dry and saturated states at very low confining pressures and effective stresses. Data collected could help scientists understand the behavior of the Earth's surface during earthquakes and landslides.

Several Risk Mitigation Experiments (RME) were performed during STS-79 to obtain data that will reduce the development risk for ISS. An evaluation of the Active Rack Isolation System (ARIS) was conducted in the SPACEHAB module as RME 1313. The ARIS is of significant interest to the microgravity community at large. ARIS is a rack level isolation system to be used on ISS. ISS has stringent requirements for its microgravity environment for allowable acceleration disturbance amplitudes, over long periods of time (30 days minimum) and frequency range (down to 0.01 Hz). ARIS was developed to isolate payloads from vibrations in the 0.01 to 300 Hz range.

The primary objective of RME 1313 was to conduct performance and system characterization measurements, and to achieve an early identification of operational risks for the ISS ARIS flight units. The ARIS RME unit was tested for three days prior to docking with Mir, five days while docked, and two days after the undocking. Total testing time in active mode was approximately 130 hours, and the total time in stand-by mode was approximately 58 hours.

3. Space Acceleration Measurement System

SAMS is used to measure the acceleration environment of orbiting laboratories in support of microgravity science payloads. STS-79 was the sixteenth SAMS flight on a NASA Orbiter. The SAMS unit consisted of three remote triaxial sensor heads, connecting cables, and a controlling data acquisition unit with a digital data recording system using optical disks with 200 megabytes of storage capacity per side. The SAMS unit was located in the SPACEHAB module, as indicated in Table 4 and Figure 1. The signals from the three triaxial sensor heads were filtered by lowpass filters with cutoff frequencies of 5 Hz (TSH A), 2.5 Hz (TSH B), and 25 Hz (TSH C). These signals were then sampled at 25, 12.5, and 125 samples per second, respectively. In this report, the SAMS data are presented in terms of the Orbiter structural coordinate system, Figure 2. The SAMS data sign convention is such that a forward thrust of the Orbiter is recorded as a negative X_0 acceleration. We refer to this convention as an inertial frame of reference fixed to a point in space. More detailed descriptions of SAMS are available in the literature [1-4].

SAMS data were collected during the entire mission, between MET 000/23 and 008/22. Approximately 1.4 gigabytes of SAMS data are available. Appendix A describes how these data can be accessed using the internet.

SAMS TSH C was stowed in Atlantis close to launch time as a replacement for a sensor head with a filter card problem. This TSH change necessitated an on-orbit sensor head installation change from bolt mounting to tape mounting. In order to tape the head, the crew used duct tape, placing a number of strips in a crosswise pattern over the head. For example, imagining the head to be the face of an analog clock, tape strips were placed from 12-6, 3-9, 2-8, etc. The gold color of the TSH was no longer visible because of the tape [Helen Brown, personal communication].

Before the decision was made to tape mount TSH C, SAMS data collected during STS-66 were compared for a bolted and a taped sensor head. On STS-66, two 10 Hz cutoff TSHs were placed next to each other on a middeck locker. Analysis of these data showed that there was minimal difference in the data below 10 Hz. Because data above 10 Hz were attenuated by the lowpass filter, no conclusions were drawn about possible mounting-related attenuation above 10 Hz. It is believed that at some frequency the tape will begin to attenuate the signal. However, the exact frequency at which this would happen is unknown and would also depend on the type of tape, how well the TSH was taped, and the structure to which the TSH and tape were attached. We believe that the frequency at which the tape begins to attenuate the signal is above 20 Hz [Allen Karchmer, personal communication].

4. SAMS Data Analysis

The data recorded by SAMS on STS-79 were processed to correct for post-mission bias calibration offsets and to compensate for temperature and gain related errors of bias, scale factor, and axis misalignment. The resulting units of acceleration are g's where 1 g = 9.8 m/s^2. The data were orthogonally transformed from the three SAMS TSH coordinate systems to the Orbiter structural coordinate system (X_O, Y_O, Z_O). After this initial data correction phase, SAMS data were analyzed to characterize the acceleration environment of the mission.

The time domain plots presented in this report are acceleration versus time, interval average acceleration versus time and interval root mean square (RMS) acceleration versus time. Transformation of data to the frequency domain is typically done to gain more insight about the environment and to identify potential acceleration sources. The frequency domain displays in this report show acceleration power spectral density versus frequency and acceleration power spectral density versus frequency versus time (spectrogram). The notation for all the data analysis discussed here is defined in the Abbreviations and Acronyms list.

4.1 Time Domain Analysis

Acceleration versus Time: These are plots of the acceleration in units of g versus time. Among the time domain plots displayed in this report, this one yields the most precise accounting of the variation of acceleration magnitude as a function of time.

Interval Average Acceleration versus Time: A plot of this quantity in units of g versus time gives an indication of net accelerations which last for a number of seconds equal to or greater than the interval parameter. The interval parameter used for STS-79 data analysis was ten seconds. Shorter duration, high amplitude accelerations can also be detected with this type of plot, however, the exact timing and magnitude of specific acceleration events cannot be extracted. The interval average acceleration for generic x-axis data is defined as

$$x_{avg_k} = \frac{1}{M} \sum_{i=1}^{M} x_{(k-1)M+i}$$

Corresponding expressions for y- and z-axis data can be combined with that for the x-axis to form the interval average acceleration vector magnitude as follows:

$$\text{accel}_{avg_k} = \sqrt{x^2_{avg_k} + y^2_{avg_k} + z^2_{avg_k}}.$$

Interval Root Mean Square Acceleration versus Time: A plot of this quantity in units of g_{RMS} versus time gives a measure of the energy in the acceleration signal due to purely oscillatory acceleration sources. Again, the interval parameter used for STS-79 data analysis was ten seconds. The interval RMS acceleration for generic x-axis data is defined as

$$x_{RMS_k} = \sqrt{\frac{1}{M} \sum_{i=1}^{M} \left(x_{(k-1)M+i}\right)^2}.$$

Corresponding expressions for y- and z-axis data can be combined with that from the x-axis to form the interval RMS acceleration vector magnitude as follows:

$$\text{accel}_{RMS_k} = \sqrt{x^2_{RMS_k} + y^2_{RMS_k} + z^2_{RMS_k}}.$$

4.2 Frequency Domain Analysis

Power Spectral Density versus Frequency: Spectral analysis is performed on time series data to identify the relative magnitudes of sinusoidal signals that compose the series. The basis of this computation is the Fourier transform which indicates the magnitude of each frequency (sinusoid) present in the time history signal. The PSD is computed directly from the Fourier transform of a time series so that Parseval's Theorem is satisfied: the RMS of a time signal is equal to the square root of the integral of the PSD across the frequency band represented by the original signal. The PSD is reported in units of g^2/Hz. Welch's Averaged Periodogram Method, or spectral averaging, is often used to produce PSDs that represent the average spectral content of a time period of interest. The PSD of k successive intervals is calculated and the k resulting spectral series are averaged together on a point by point basis.

Power Spectral Density versus Frequency versus Time (Spectrogram): Spectrograms provide a roadmap of how acceleration signals vary with respect to both time and frequency. As such, they are particularly useful in identifying when certain activities begin and end and to get a general feel for changes in the microgravity environment with time. To produce a spectrogram, PSDs are computed for successive intervals of time. The PSDs are oriented vertically on a page such that frequency increases from bottom to top. PSDs from successive time slices are aligned horizontally across the page such that time increases from left to right. Each time-frequency bin is imaged as a color corresponding to the logarithm of the PSD magnitude at that time and frequency. A color bar is included with each plot as a key to the color to $\log_{10}$(PSD) correspondence. To maximize the value of individual PIMS analyses, spectrogram color bars may vary among analyses and among mission reports. For ease of interpretation, however, within an appendix the color maps are kept constant unless otherwise noted.

5. Microgravity Environment—STS-79

This section discusses the microgravity environment of the Orbiter Atlantis during the STS-79 mission for specific events both when Atlantis was freely orbiting and when it was docked to Mir. Particular acceleration phenomena discussed are the docking and undocking of the two vehicles, differences in the apparent structural modes of Atlantis and the docked complex, the effects of Vernier Reaction Control System (VRCS) jets on the acceleration environment of Atlantis and the docked complex, excitation of the Mir solar arrays, crew exercise, and the Enhanced Orbiter Refrigerator Freezer (EORF) compressor. Appendix B provides an overview of the microgravity environment during the entire mission.

5.1 Microgravity Environment of the Mir-Atlantis Complex

One of the primary goals of STS-79 was the rendezvous and docking with Mir. Analysis of SAMS data recorded aboard Mir from the docking with Atlantis on the STS-74 mission showed that the microgravity disturbances caused by the Orbiter's Ku-band communication antenna and the EORF were recorded by SAMS on the Mir station [5].

Complementing the SAMS data from the docking of STS-74, the STS-79 mission gave the opportunity for SAMS to record the acceleration environment of Atlantis during a docking. Figure 3 shows a spectrogram of SAMS data from TSH A for a period containing the docking event. During the time leading up to the physical docking of the two vehicles, the Orbiter's VRCS jets were fired for stationkeeping and rendezvous control. The initial capture of the docking ring (soft mate) was at approximately MET 002/18:19. The docking ring retraction started at MET 002/18:22, the ring was completely retracted around MET 002/18:24, and the docking clamps were all latched (hard mate) around MET 002/18:27.

Figure 3 shows some key features of this docking event. The magenta vertical line 19 minutes into the plot probably indicates the initial capture of the docking ring. Notice that two Orbiter structural modes are initially at about 3.9 Hz and 4.9 Hz (the fuzzy yellow horizontal lines on the plot). Around 23 minutes into the plot, the structural modes begin an upwards shift, towards 4.5 Hz and 5.1 Hz. These higher frequencies are probably representative of the structural modes of the docked Atlantis-Mir complex. Additionally, two structural modes appear in the data at 0.8 Hz and 1.8 Hz. These are believed to be contributions from the Mir portion of the complex.

Figure 4 is a spectrogram of SAMS data recorded during the undocking. Notice the disappearance of the Mir structural modes and the shift of the structural modes back to the known Orbiter structural modes around MET 007/16:37. Similar to the docking operations, the vertical magenta line which appears around 19.5 minutes into Figure 4 is probably related to the release of the docking ring. VRCS activity increased at about 007/16:53 as Atlantis began a fly-around of Mir.

The VRCS consists of six small thruster jets which each deliver approximately 24 pounds of thrust. These VRCS jets may be activated for a minimum of 0.08 seconds or a maximum of 125 seconds at a time [6]. Nominally, SAMS records accelerations around 1×10^{-4} g due to firings of the VRCS jets. For a period during the STS-79 mission in which the Orbiter was not docked to Mir, a simultaneous firing of the L5D and R5D jets [7] produced an acceleration transient of approximately 8.9×10^{-5} g, see Figure 5. In this figure, the jets fire at approximately the 13 second mark and cease at the 15 second mark. Due to the jet directions, this disturbance was primarily in the positive Z_0-axis, but there was also an offset of approximately -4.5×10^{-5} g in the X_0-axis. After the firing, the Z_0-axis shows a ringing behavior, with excited frequencies of approximately 4.6 and 5.1 Hz (related to vehicle structural modes), but no noticeable continued X_0-axis disturbance.

A firing of the same jets while Atlantis was docked to Mir produced the accelerations shown in Figure 6. In this figure, the jets began firing shortly after the 20 second mark and ceased shortly before the 30 second mark. The Z_0-axis excursion was approximately 7.1×10^{-5} g. Again the Z_0-axis shows a ringing behavior, but this time the excited frequencies are approximately 5.0 and 5.2 Hz (related to structural modes of the Atlantis-Mir complex). The X_0-axis behavior shows an oscillatory vibration of approximately 0.18 Hz. This is probably related to a structural mode of the solar arrays on the Mir station.

The extra mass of Mir caused a diminished VRCS acceleration level (8.9×10^{-5} g for Atlantis alone, 7.1×10^{-5} g for the Atlantis-Mir complex). Although Atlantis and Mir are roughly the same mass, the center of gravity (CG) of the complex is in a significantly different location than the CG of Atlantis alone. This fundamental shift in the CG (the rotation point) causes the acceleration recorded on the Atlantis-Mir complex during a VRCS firing to be reduced by somewhat less than half of that predicted by Newton's Second Law, F=ma. Without the rotational consideration, Newton's Second Law predicts the VRCS acceleration of the Atlantis-Mir complex to be approximately 4.5×10^{-5} g.

5.2 Crew Exercise

Crew members on Orbiter and Mir are required to exercise during their time in space to maintain the health of their cardiovascular and musculoskeletal systems. Different types of exercise are often tested to determine which have the most beneficial effects on the crew. Crew members on Mir have three pieces of exercise equipment available for aerobic activities: a treadmill in the Kristall module, a treadmill in the base module, and a bicycle ergometer in the base module. The typical Russian exercise procedure is to exercise for a period of time on one of these pieces of equipment and then stop and do some resistance exercises. This is repeated several times. During the STS-79 mission, a bicycle ergometer was used in the middeck of Atlantis.

While Atlantis and Mir were connected, exercise on Mir occurred on the treadmill in the base module. The cosmonaut crew, including Shannon Lucid, continued to exercise on Mir. A limited amount of exercise occurred on Atlantis during the docked phase of the mission. Figures 7 and 8 are spectrograms of SAMS TSH C data collected during Atlantis ergometer exercise and Mir treadmill exercise, respectively. Both of these exercise periods occurred soon after the docking.

The ergometer exercise accelerations seen in Figure 7 are comparable to what has been seen on previous Orbiter missions. The two primary excited frequencies are due to pedalling (about 2.5 Hz) and body rocking (about 1.25 Hz). The 2.5 Hz pedalling frequency typically excites an Orbiter structural mode, making for a rather sharp frequency disturbance. There is a little more spread in the frequency disturbance than normal, probably due to the increased mass of the complex and the difference in structural modes compared to an Orbiter alone.

In Figure 8, the aerobic-resistance exercise cycle is evident as the 5 to 10 minute periods of 1 and 2 Hz footfall frequencies are broken up by periods of similar length showing no dominant acceleration frequencies. The cause of the increased excitation of the 1.8 Hz structural modes (red spots at the start of the plot, about 7 minutes into the plot, and about 30 minutes into the plot) is unknown. Excitation of structural modes by events such as thruster firings are typically associated with broadband acceleration excitation, obvious in spectrograms by increased magnitude along a vertical strip. These 1.8 Hz spots are not accompanied by any other significant frequency excitation. Throughout this set of SAMS data, this characteristic is only associated with base module treadmill exercise times. The cause of this is under investigation.

5.3 Enhanced Orbiter Refrigerator Freezer Compressor

The EORF was flown on the aft bulkhead of the SPACEHAB module, in position AC04. The EORF operates using a vapor compression freon engine. Figure 9 is a spectrogram of one hour of SAMS data from TSH C, beginning at MET 002/08. These data were collected during a crew sleep period prior to Mir docking. The regularly repeating disturbances radiating vertically from 19 Hz are probably related to the operation of the refrigerator's compressor motor.

SAMS data collected onboard Mir during the STS-74 Atlantis-Mir docking showed a regularly repeating signal around 21 Hz which appeared only when Atlantis was docked to Mir. Figure 10 is a spectrogram of SAMS data recorded on Mir during the STS-74 docking. Notice the regularly recurring signal around 21 Hz, which was attributed to the EORF flown in a forward middeck bulkhead locker during the STS-74 mission. Although the shape and duration of the 21 Hz signals in Figure 10 are somewhat obscured by broadband disturbances, it is clear that the signals did not register on Mir until after the hard mate was established with Atlantis (at approximately DMT 319/08:48 in the plot).

There are several possible explanations for the discrepancy in the EORF signal shape between the STS-74 and STS-79 missions, Figures 10 and 9. First, the SAMS data during the STS-74 docking were recorded aboard Mir. Second, the EORF was located in the middeck during the STS-74 mission and in the SPACEHAB module during the STS-79 mission. Finally, the SAMS sensor head on the STS-79 mission was held in place with duct tape and the SAMS sensor on Mir was taped in place using double-sided tape. The effect of the tape on the signal is unknown, but may be a cause of the discrepancy in the signal shape between the two data sets.

5.4 Unknown Disturbances

Often, accelerometer signals cannot be associated with a specific source. Figure 6 in Appendix B shows a spectrogram of SAMS TSH C data from MET 001/06 to 001/12 (during a crew sleep period, prior to Mir docking). This figure contains three unknown, variable frequency disturbances which appear to ramp down and converge at the zero Hz line around MET 001/10:15. Shortly after this, three similar signals begin to ramp up and diverge upwards on the frequency axis. Further tracking of these signals throughout the spectrograms shows other anomalous behavior, such as the peak and subsequent slope seen around 18 Hz and 6 Hz shortly before MET 002/07 in Figure 14 of Appendix B. These unknown signals persist throughout the docked and undocked portions of the mission, varying in frequency and also repeating the converge-diverge behavior described above. The source for these signals is unknown, but is presumably not related to equipment transferred to or from Mir, because the signals exist before, during, and after the docked period.

SAMS TSH C data can be analyzed up to the Nyquist frequency of 62.5 Hz, although data above the 25 Hz cutoff have been attenuated in magnitude. Analysis of data between 25 and 62.5 Hz indicates a number of isolated unknown signals (which vary in frequency), primarily in the 40 to 60 Hz region.

5.5 Average Acceleration Levels

An analysis of 8.74 minute PSDs representing the entire mission (a total of 1298 PSDs) were used to produce the plot shown in Figure 11. The processing used to produce this plot is somewhat complex and a description is beyond the scope of this report. Users who are interested in the details of this processing are asked to contact the PIMS group as indicated in Appendix A.

Figure 11 shows five lines, corresponding to the percentages of time for which the microgravity environment was at or below the indicated level. For example, the green line around 5 Hz shows that the microgravity environment was about 5×10^{-7} g^2/Hz (or quieter) for 50% of the analyzed time. By plotting 5 lines (1, 25, 50, 75, and 99 percent of the time), data quartiles (the areas between successive lines) may be discerned. The lower (1%) and upper (99%) lines are representative of the best and worst cases for the mission. As is shown bracketed between the blue (25%) and red (75%) lines, the middle 50% of the data falls within a relatively small magnitude spread for any given frequency on the plot. The green (50%) line represents the median of the data, showing the demarcation at which half the data lie above the line and half the data lie below the line. The data median is very close to the data mean, particularly in the 0-10 Hz region.

6.0 Summary

STS-79 was the first opportunity to record SAMS data on an Orbiter while it was docked to Mir. SAMS data collected on Mir during the STS-74 docking indicated that accelerations on Atlantis (Ku-band antenna dither and EORF compressor) were transferred to Mir while the two vehicles were docked. Data collected on Atlantis during the STS-79 docking indicate that the opposite is true, at least for treadmill exercise and vehicle and solar array structural modes. The EORF signal recorded on Atlantis on STS-79 had different characteristics than the signal recorded on Mir during STS-74. This is probably due to different transmission paths and TSH mounting mechanisms.

A 0.18 Hz component of the SAMS data, present while the two vehicles were docked, was probably caused by the Mir solar arrays. Compared to Atlantis structural modes of about 3.9 and 4.9 Hz, the Atlantis-Mir complex has structural components of about 4.5 and 5.1 Hz. After docking, apparent structural modes appeared in the data at about 0.8 and 1.8 Hz. These are related to the Mir complex. Known Mir structural modes are 0.6, 1.0 to 1.3, and 1.9 Hz [8].

The appearance, disappearance, and change in the structural modes during the docking and undocking phases of the joint Atlantis-Mir operations indicates that the structural modes of the two spacecraft have an effect on the microgravity environment of each other. The transfer of accelerations between vehicles is something that should considered in the International Space Station era.

7. References

[1] DeLombard, R., B. D. Finley, Space Acceleration Measurement System description and operations on the First Spacelab Life Sciences Mission. NASA Technical Memorandum 105301, November 1991.

[2] DeLombard, R., B. D. Finley, and C. R. Baugher, Development of and flight results from the Space Acceleration Measurement System (SAMS). NASA Technical Memorandum 105652, January 1992.

[3] Baugher, C. R., G. L. Martin, and R. DeLombard, Low-frequency vibration environment for five shuttle missions, NASA Technical Memorandum 106059, March 1993.

[4] Rogers, M. J. B., C. R. Baugher, R. C. Blanchard, R. DeLombard, W. W. Durgin, D. H. Matthiesen, W. Neupert, and P. Roussel, A Comparison of low-gravity measurements onboard Columbia during STS-40. Microgravity Science and Technology VI/3 (1993) 207 - 216.

[5] DeLombard, R., K. Hrovat, M. Moskowitz, and K. McPherson, SAMS acceleration measurements on Mir from June to November 1995. NASA Technical Memorandum 107312, September 1996.

[6] Shuttle Operational Data Book, Volume 1, JSC-08934, Rev. E, Johnson Space Center, Houston, TX, January 1988.

[7] DeLombard, R., Compendium of information for interpreting the microgravity environment of the orbiter spacecraft, NASA Technical Memorandum 107032, August 1996.

[8] Delombard, R., S. Ryaboukha, K. Hrovat, and M. Moskowitz, Further analysis of the microgravity environment on Mir Space Station during Mir-16. NASA Technical Memorandum 107239, June 1996.

Table 1. STS-79 Payloads

Payloads	***Location***
Orbiter Docking System	Cargo Bay
SPACEHAB Double Module	Cargo Bay
IMAX	In-Cabin
Risk Mitigation Experiments	In-Cabin
SAREX	In-Cabin
Middeck Science Hardware	In-Cabin

Table 2. Developmental Test Objectives/Detailed Supplementary Objectives /Risk Mitigation Experiments

DTO 255	Wraparound Digital Autopilot Flight Test Verification
DTO 301D	Ascent Structural Capability Evaluation
DTO 307D	Entry Structural Capability
DTO 312	ET TPS Performance
DTO 700-5	Trajectory Control Sensor
DTO 700-10	Orbiter Space Vision System Flight Video Taping
DTO 700-14	Single String Global Positioning System
DTO 805	Crosswind Landing Performance
DTO 837	Vernier RCS Reboost Demonstration
DTO 840	Hand-Held Lidar Procedures
DTO 1118	Photographic and Video Survey of Mir space station

DSO 901	Documentary Television
DSO 902	Documentary Motion Picture Photography
DSO 903	Documentary Still Photography

Table 2. Developmental Test Objectives/Detailed Supplementary Objectives /Risk Mitigation Experiments (cont.)

RME 1301	Mated Shuttle and Mir Structural Dynamics Test
RME 1302	Mir Electric Field Characterization Test 1 and 2
RME 1303	Shuttle/Mir Experiment Kit Transport
RME 1310	Shuttle/Mir Alignment Stability Experiment
RME 1312	Intra-Vehicular Radiation Environment Measurement Experiment
RME 1313	Active Rack Isolation System (ARIS)
RME 1319	Inventory Management System

Table 3. STS-79 Crew

Crewmember	***Position***
William Readdy	Commander (CDR)
Terry Wilcutt	Pilot (PLT)
Jay Apt	Mission Specialist 1 (MS 1)
Tom Akers	Mission Specialist 2 (MS 2)
Carl Walz	Mission Specialist 3 (MS 3)
John Blaha	Mission Specialist 4 (MS 4) [Launch-Docking]
Shannon Lucid	Mission Specialist 4 (MS 4) [Docking-Landing]

Table 4. STS-79 SAMS Sensor Head Location and Orientation

Unit C Head A (TSH-A) Serial no.: 821-3 Location: SPACEHAB FS 08		Sample Rate: 25 samples/second Frequency: 5 Hz
ORIENTATION		**LOCATION**
Orbiter Structural Axis	**Sensor Axis**	**Structural Axis**
X_O	$-X_H$	$X_O = 1018.6$ in
Y_O	$-Y_H$	$Y_O = 62.1$ in
Z_O	Z_H	$Z_O = 393.5$ in

Table 4. STS-79 SAMS Head Location and Orientation (cont.)

Unit C Head B (TSH-B) Serial no.: 402-2 Location: SPACEHAB FP 07		Sample Rate: 12.5 samples/second Frequency: 2.5 Hz
ORIENTATION		**LOCATION**
Orbiter Structural Axis	**Sensor Axis**	**Structural Axis**
X_O	$-X_H$	X_O = 1037.8 in
Y_O	$-Y_H$	Y_O = -62.1 in
Z_O	Z_H	Z_O = 393.5 in

Unit C Head C (TSH-C) Serial no.: 821-16 Location:Spacehab FP 02, supporting MGM (TSH was taped, using 6-7 pieces of duct tape, in a cross-type pattern)		Sample Rate: 125 samples/second Frequency: 25 Hz
ORIENTATION		**LOCATION**
Orbiter Structural Axis	**Sensor Axis**	**Structural Axis**
X_O	$-X_H$	X_O = 1037.8 in
Y_O	$-Y_H$	Y_O = -43.0 in
Z_O	Z_H	Z_O = 426.3 in

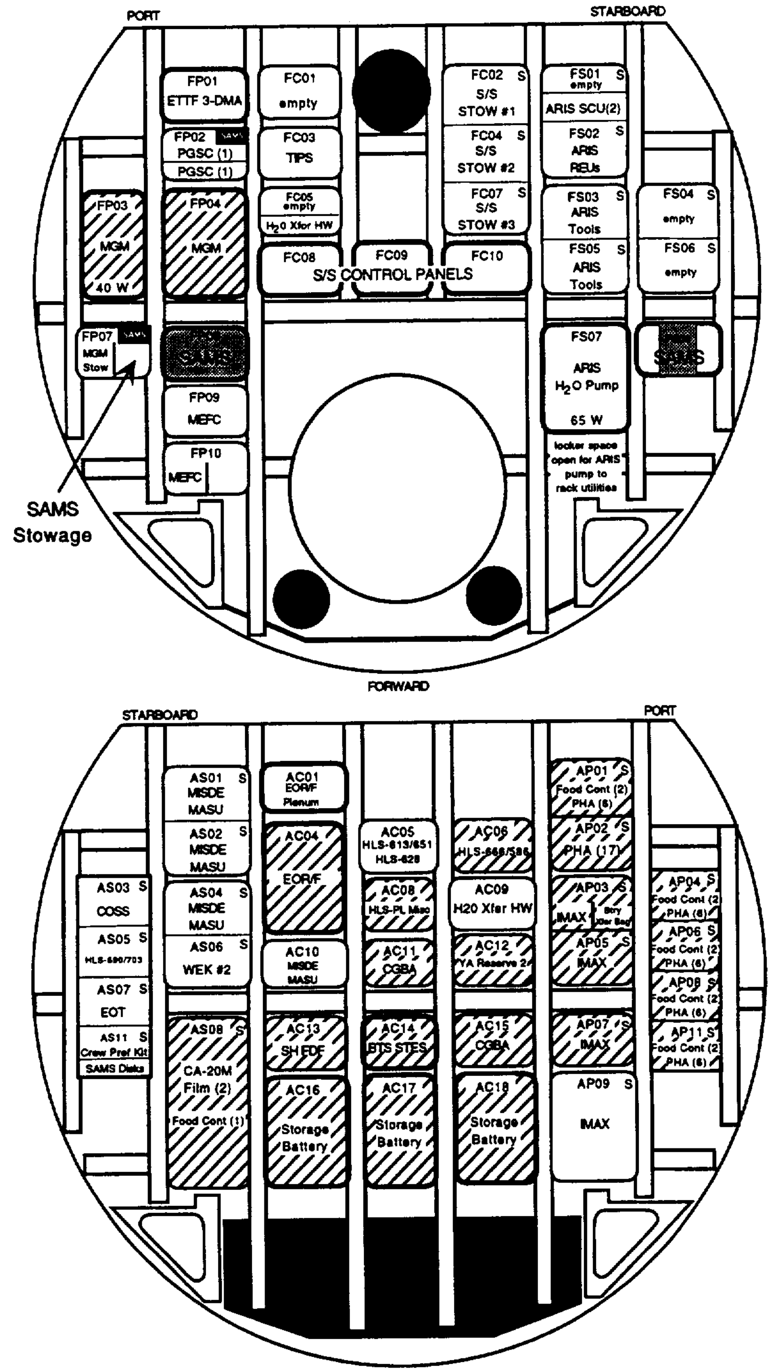

Figure 1. SAMS sensor head and unit location

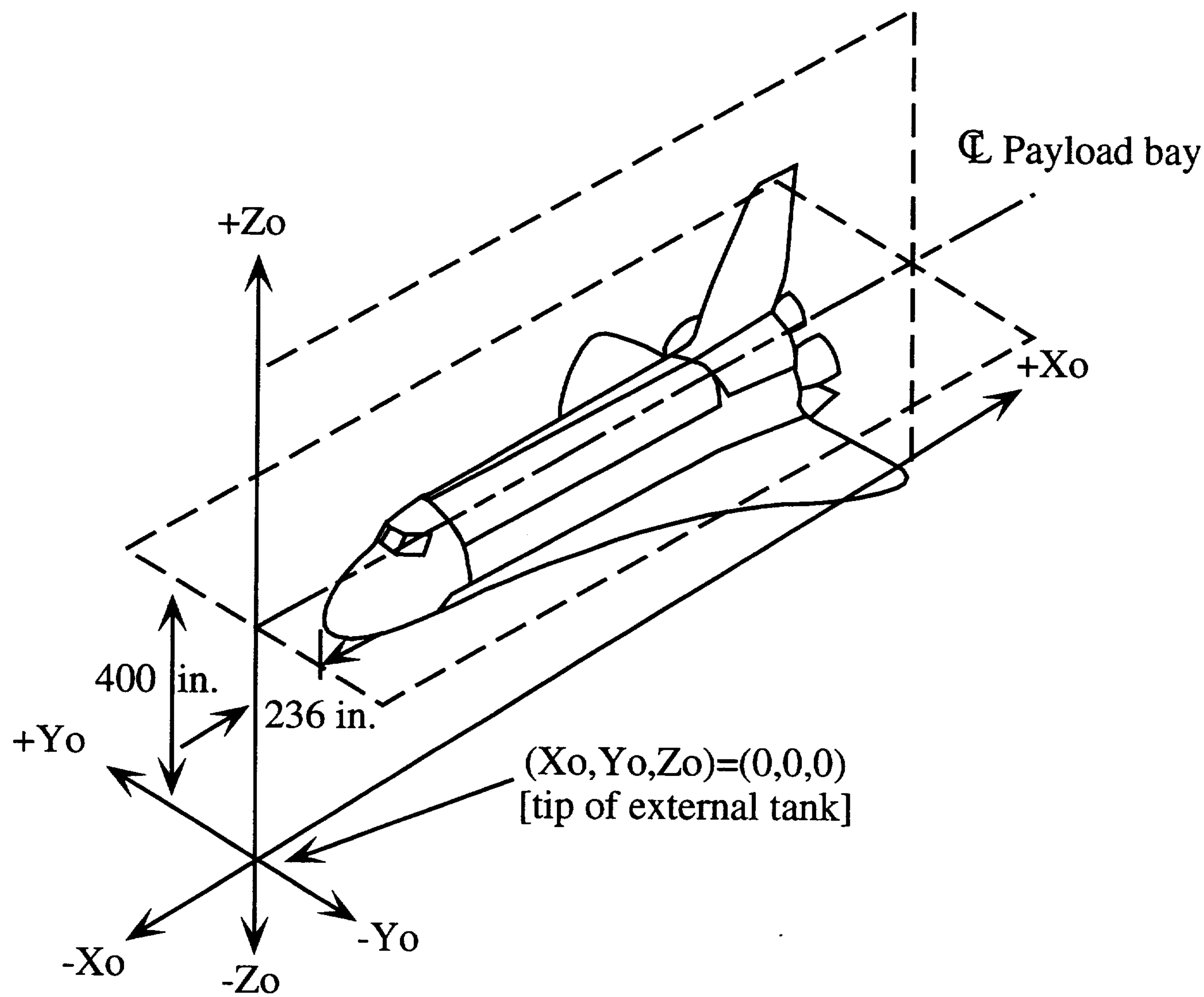

Figure 2. Orbiter structural coordinate system

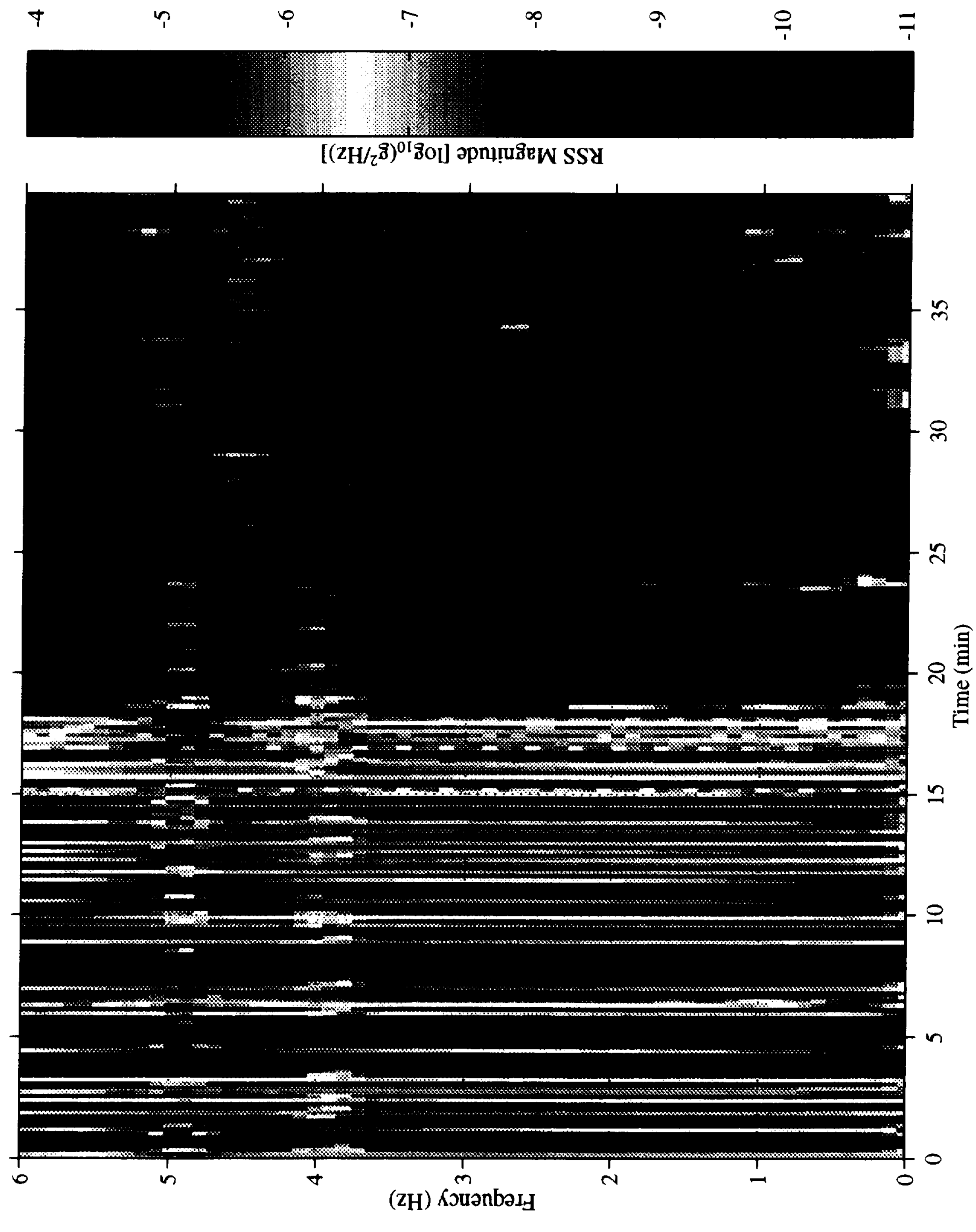

Figure 3. SAMS TSH A data collected on Atlantis during Mir docking. MET start 002/18:00:01. See text for details.

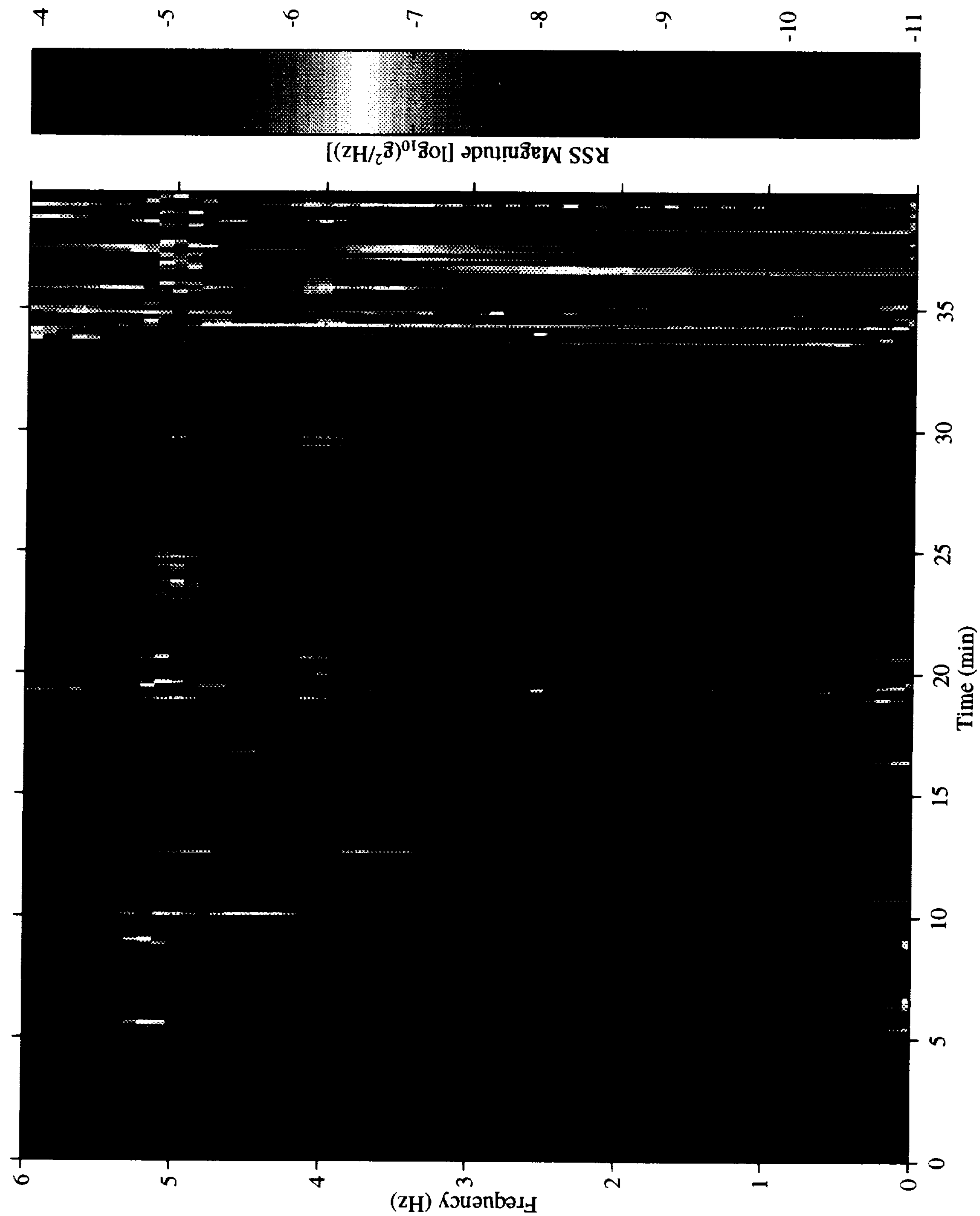

Figure 4. SAMS TSH A data collected on Atlantis during Mir undocking. MET start 007/16:20. See text for details

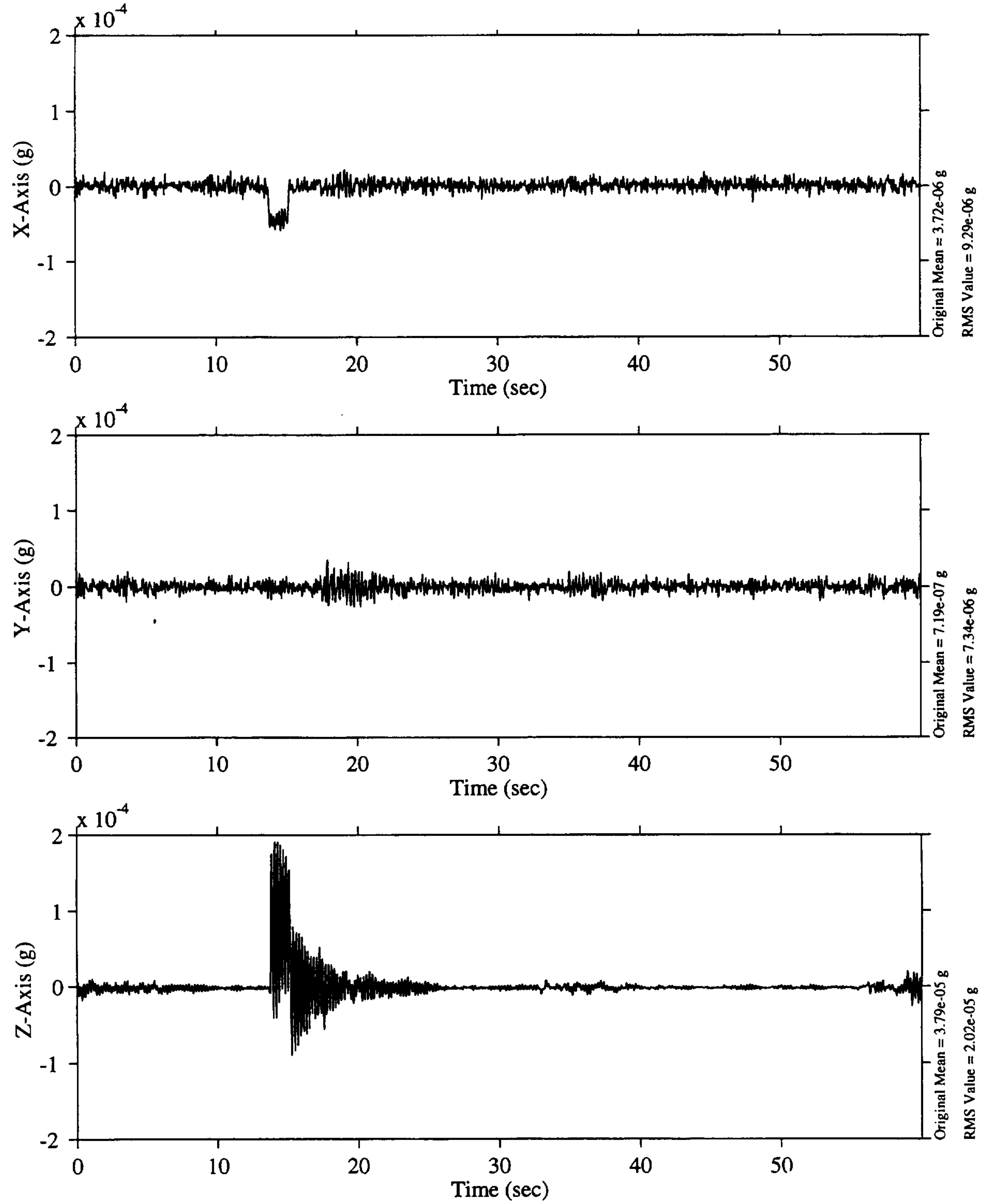

Figure 5. SAMS TSH A data collected on Atlantis prior to Mir docking. MET start 001/07:06. Simultaneous L5D and R5D VRCS firings start 13 seconds into plot.

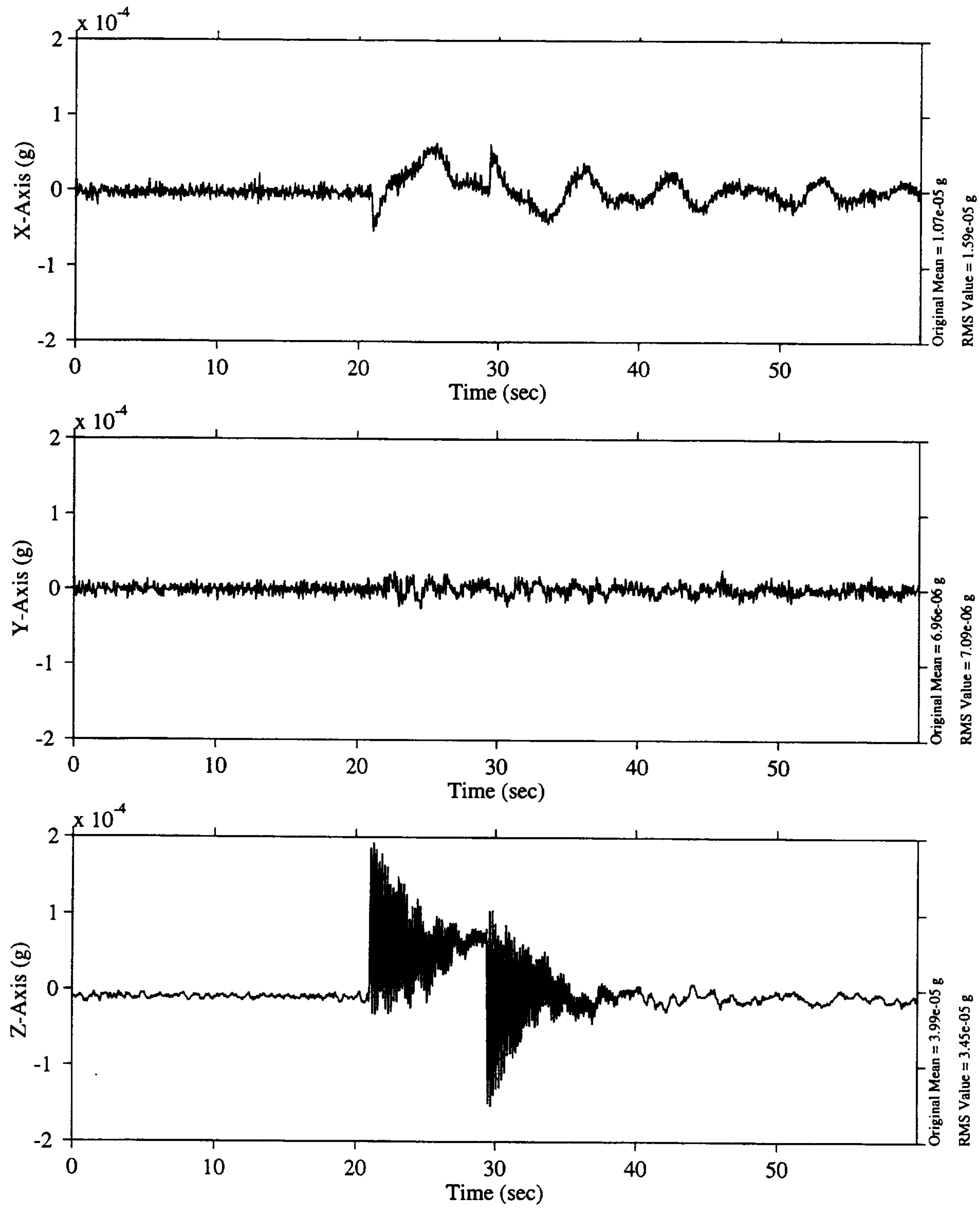

Figure 6. SAMS TSH A data collected on Atlantis while docked to Mir. MET start 005/11:03. Simultaneous L5D and R5D VRCS firings start at about 20 seconds into plot.

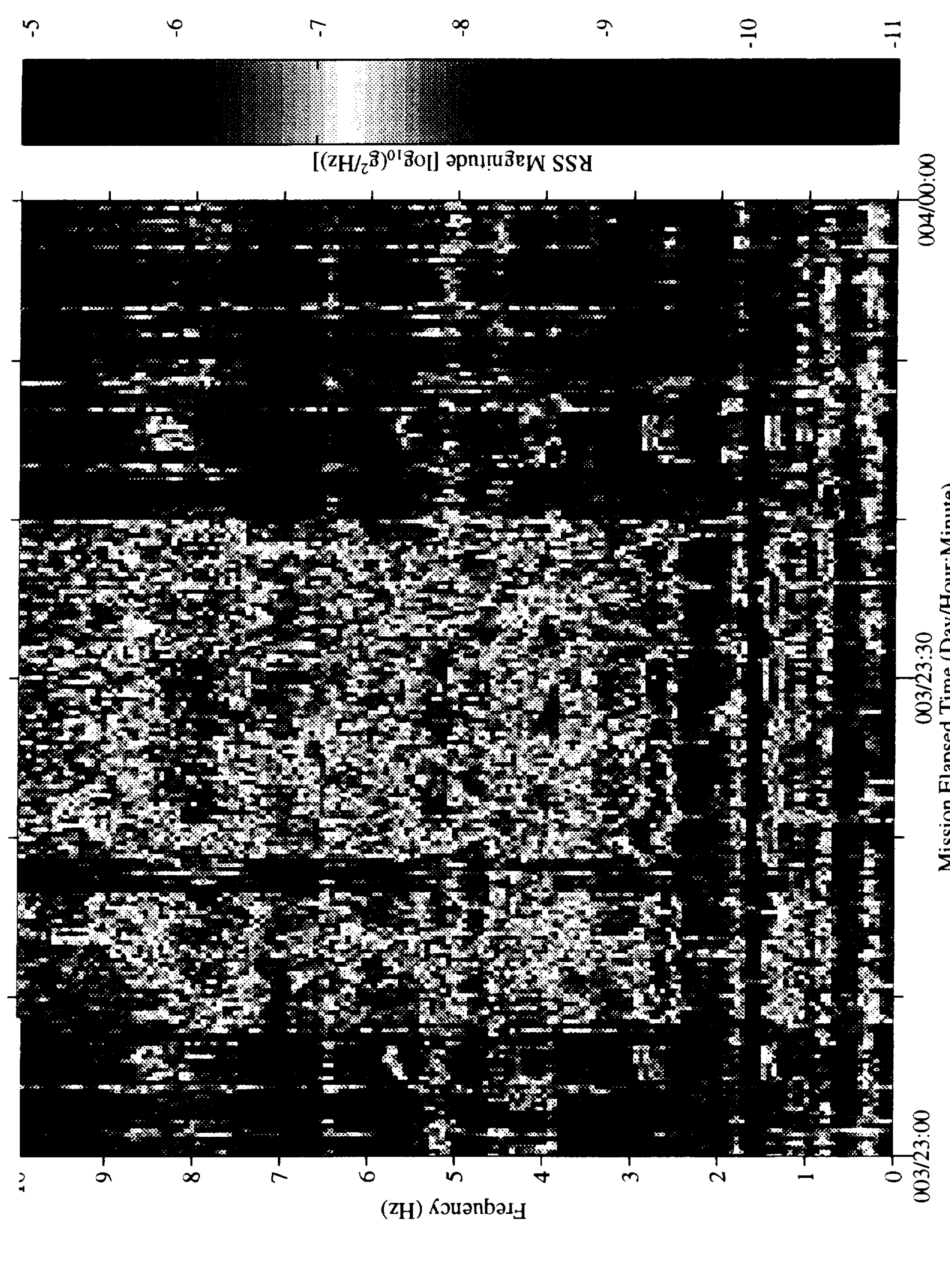

Figure 7. SAMS TSH C data collected on Atlantis during treadmill and resistance exercise in the Mir base module while Atlantis and Mir were docked. MET start 003/23:00. See text for details.

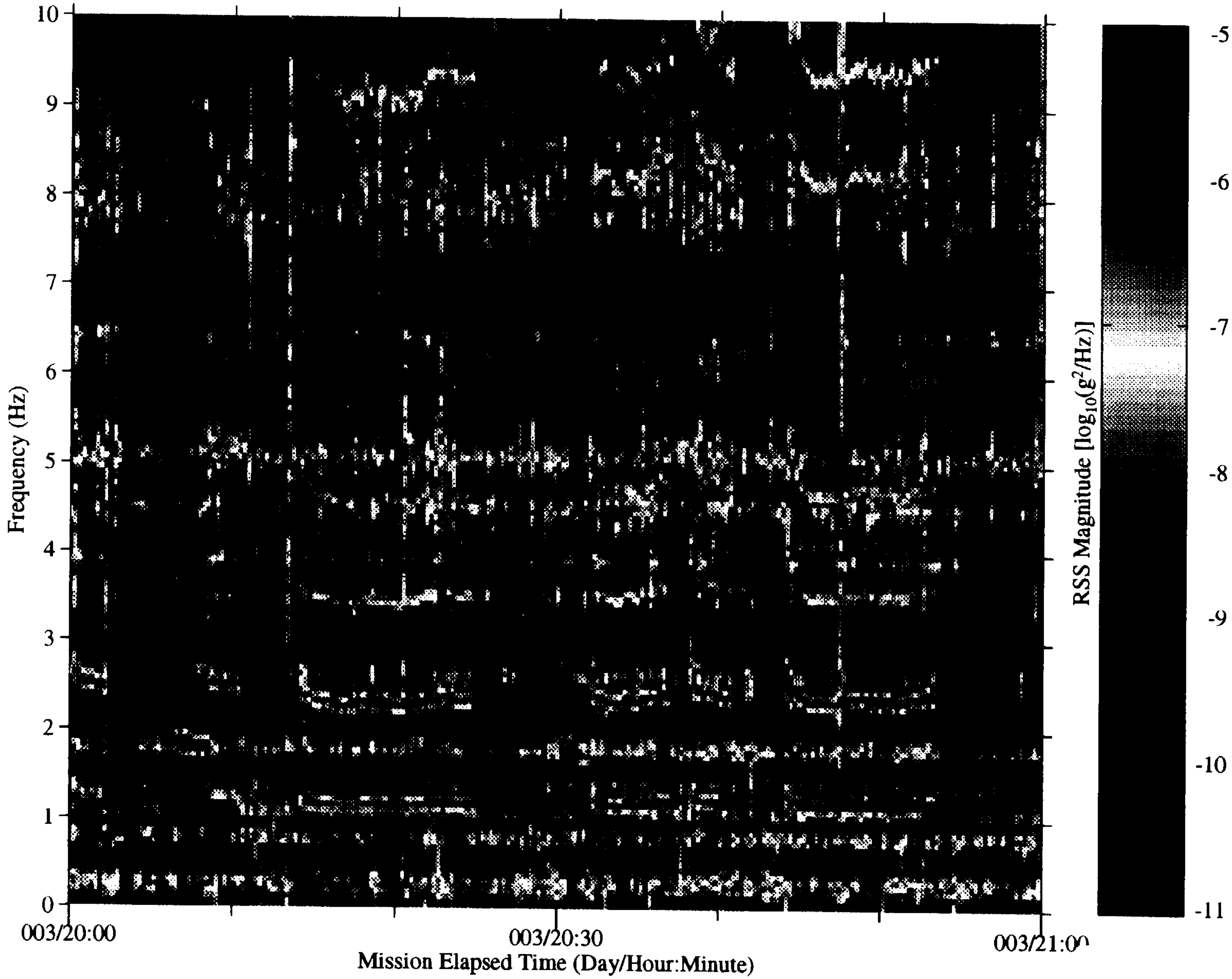

Figure 8. SAMS TSH C data collected on Atlantis during ergometer exercise in the Atlantis middeck while Atlantis and Mir were docked. MET start 003/20:00. See text for details.

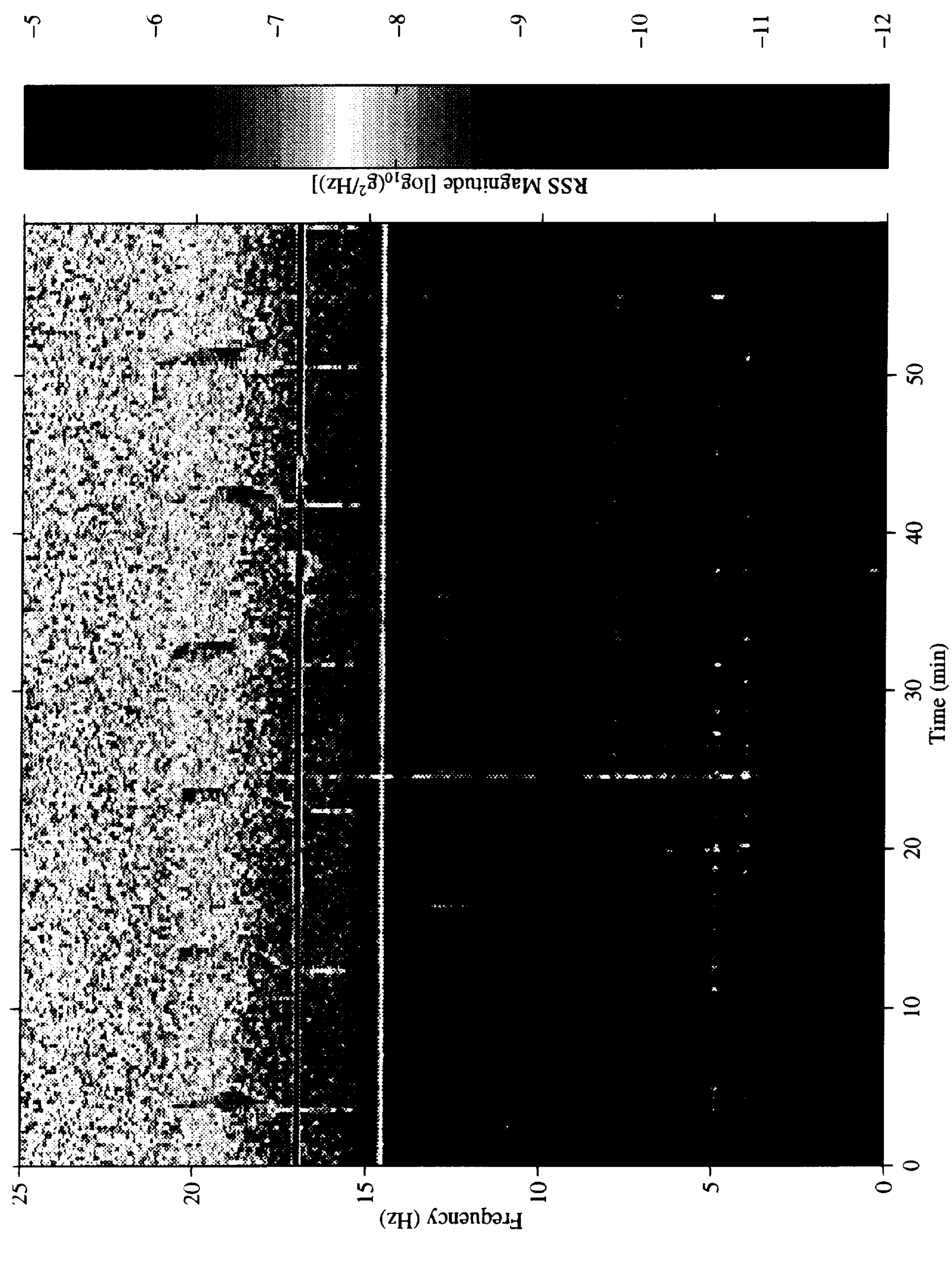

Figure 9. SAMS TSH C data collected on Atlantis during a crew sleep period prior to Mir docking. MET start 002/08:00. Note vibrations related to EORF compressor around 19 Hz.

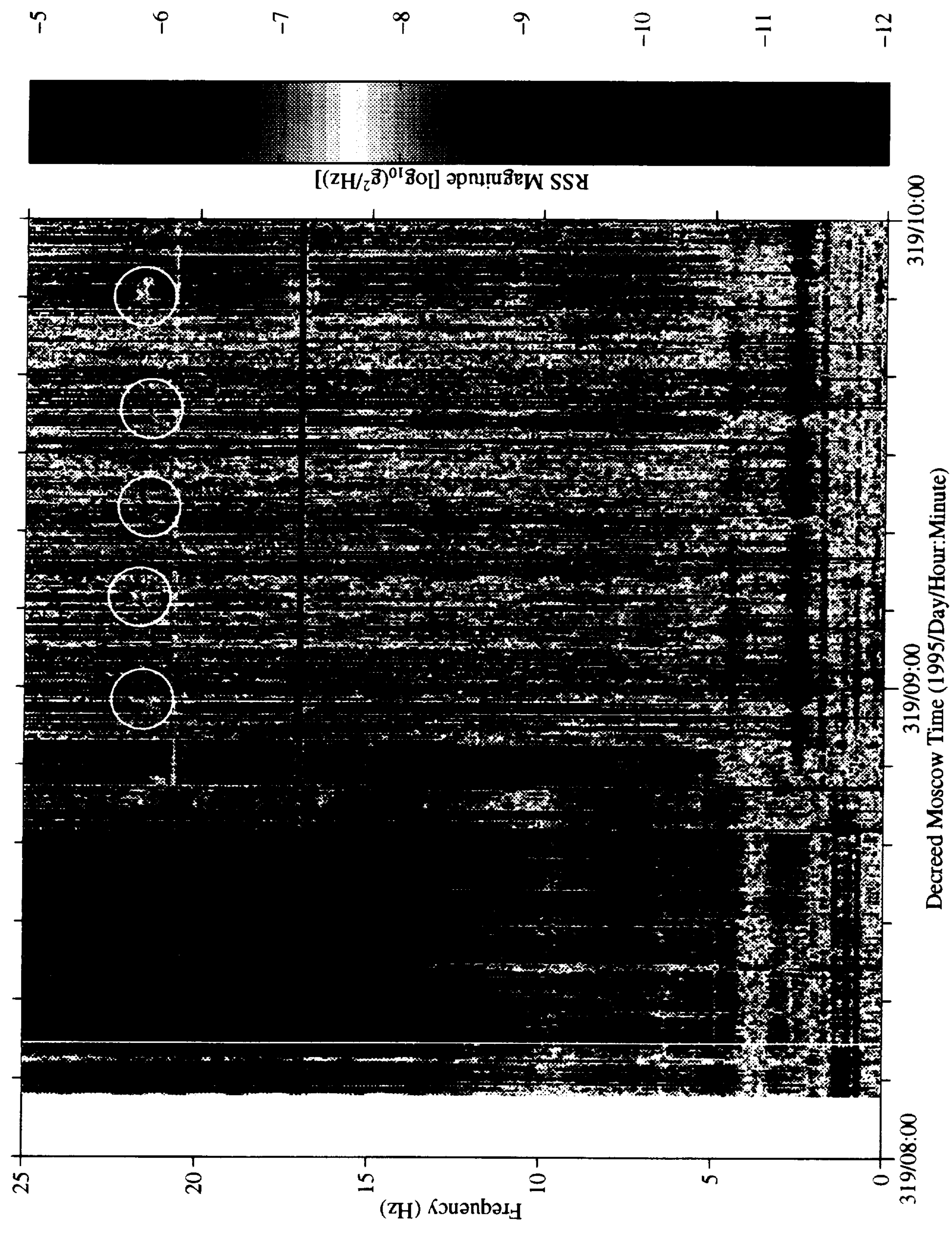

Figure 10. SAMS TSH A data collected on Mir while Atlantis was docked to Mir on the STS-74 mission. Note recurring signal (circled) caused by EORF on Atlantis and 17 Hz signal of Orbiter Ku-band antenna.

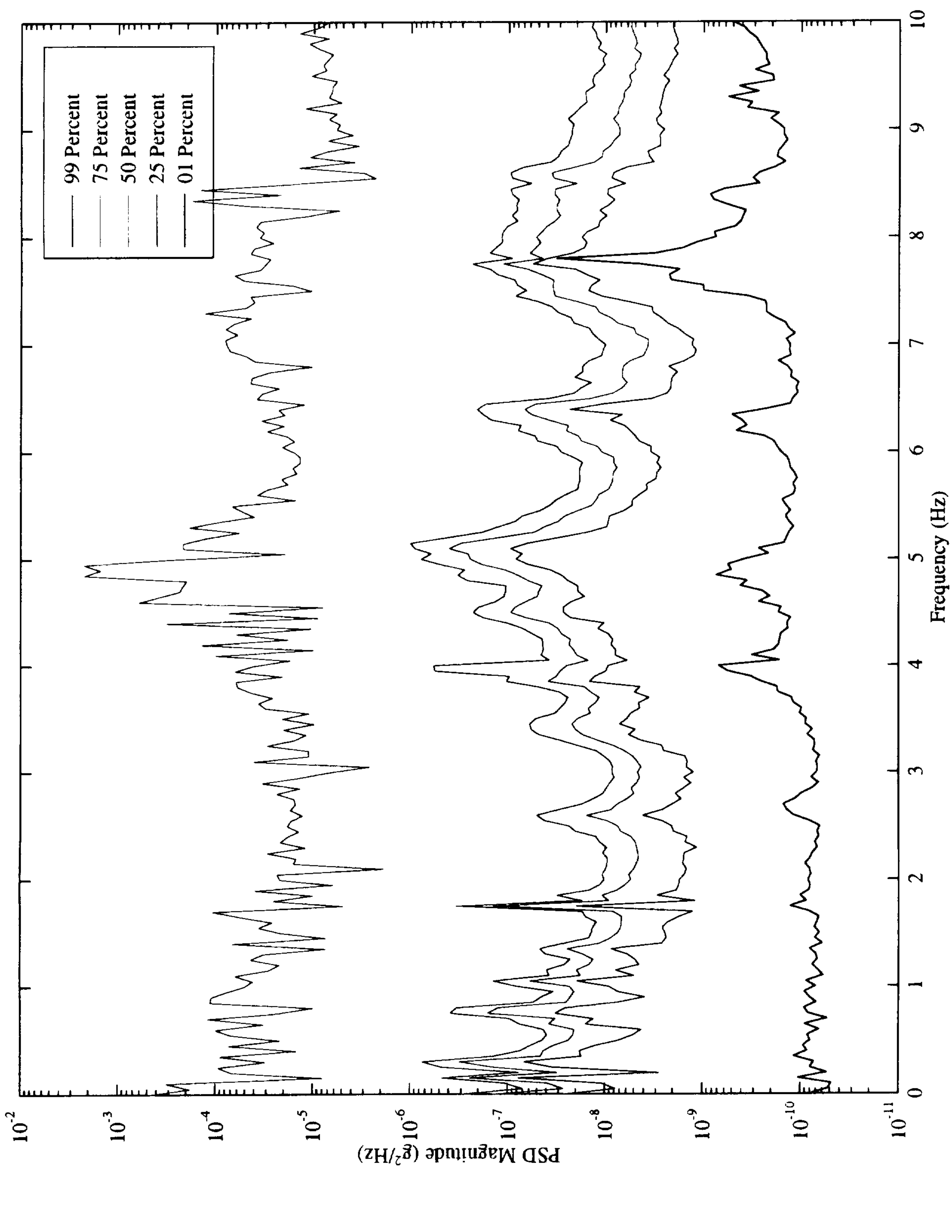

Figure 11. All SAMS TSH C data collected on Atlantis during STS-79. Analysis applied to data gives an indication of average acceleration levels during the mission.

Appendix A: Accessing Acceleration Data via the Internet

SAMS and OARE data are available over the internet from the NASA LeRC file server "beech.lerc.nasa.gov". Previously, SAMS data were made available on CD-ROM, but distribution of data from current (and future) missions will be primarily through this internet file server.

SAMS data files are arranged in a standard tree-like structure. Data are first separated based upon mission. Then, data are further subdivided based upon some portion of the mission, head, year (if applicable), day, and finally type of data file (acceleration, temperature, or gain). Effective November 1, 1996, there has been a minor reorganization of the beech.lerc.nasa.gov file server. There are now two locations for SAMS data: a directory called SAMS-SHUTTLE and a directory called SAMS-MIR. Under the SAMS-SHUTTLE directory, the data are segregated by mission. Under the SAMS-MIR directory, the data are segregated by year. The following figure illustrates this structure.

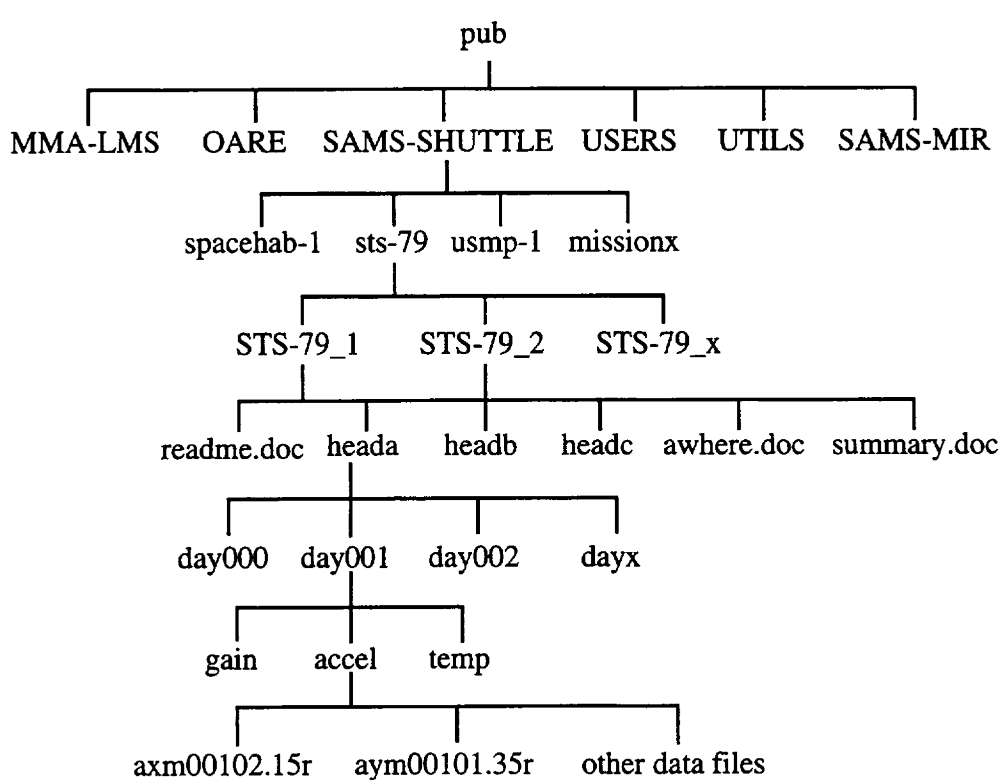

The SAMS data files (located at the bottom of the tree structure) are named based upon the contents of the file. For example, a file named "axm00102.15r" would contain head A data for the x-axis for day 001, hour 02, file 1 of 5. The readme.doc files give a complete explanation of the file naming convention.

OARE data files are also arranged in a tree-like structure, but with different branches. The data are first divided based upon mission, and then are divided based upon type of data. The OARE tree structure looks like this:

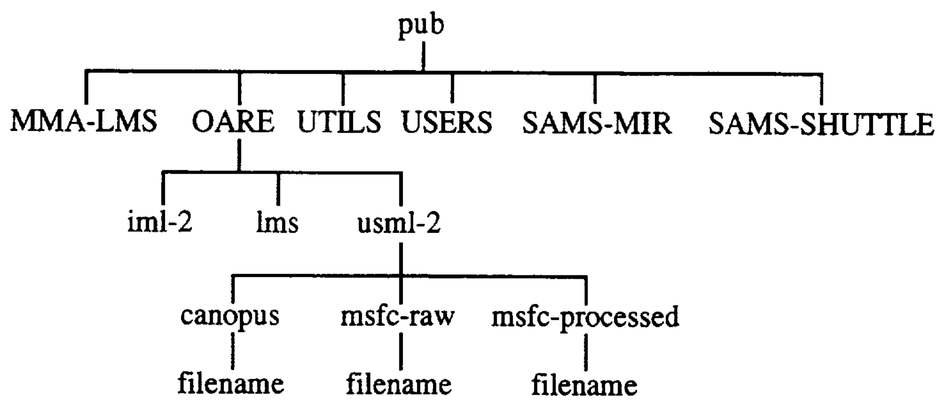

Files under the canopus directory are trimmean filter data, computed by Canopus Systems, Inc. Files under the msfc-raw directory contain the telemetry data files provided to PIMS by the Marshall Space Flight Center Payload Operations Control Center data reduction group. Files under the msfc-processed directory are raw files containing binary floating point values, listing the MET (in hours), and the x, y, and z axis acceleration in micro-g's. Selected MMA data files are located in the MMA-LMS subdirectory. See the readme files for complete data descriptions.

Data access tools for different computer platforms (MS-DOS, Macintosh, SunOS, and MS-Windows) are available in the /pub/UTILS directory.

The NASA LeRC beech file server can be accessed via anonymous File Transfer Protocol (ftp), as follows:

1) Open an ftp connection to "beech.lerc.nasa.gov"
2) Login as userid "anonymous"
3) Enter your e-mail address as the password
4) Change directory to pub
5) List the files and directories in the pub directory
6) Change directories to the area of interest
7) Change directories to the mission of interest

8) Enable binary file transfers
9) Use the data file structures (described above) to locate the desired files
10) Transfer the desired files

If you encounter difficulty in accessing the data using the file server, please send an electronic mail message to "pims@lerc.nasa.gov". Please describe the nature of the difficulty and also give a description of the hardware and software you are using to access the file server. If you are interested in requesting specific data analysis or information from the PIMS team, also send e-mail to pims@lerc.nasa.gov or call the PIMS Project Manager, Duc Truong at (216) 433-8394.

Appendix B: SAMS Time Histories and Color Spectrograms

The Principal Investigator Microgravity Services (PIMS) group has further processed SAMS data from STS-79, Head C to produce the plots shown here. Three representations of the data are presented here: ten second interval average, ten second interval RMS, and PSD magnitude versus frequency versus time (spectrogram) plots. These calculations are presented in 6 hour plots, with the corresponding average and RMS plots on one page, and the spectrogram on the facing page.

The ten-second interval average plots give an indication of net accelerations which last for a period of 10 seconds or more. Shorter duration, high amplitude accelerations may be seen with this type of plot, however their exact timing and magnitude cannot be extracted. The ten-second interval RMS plots give a measure of the oscillatory content in the acceleration data. Plots of this type may be used to identify times when oscillatory and/or transient deviations from the background acceleration levels occurred.

Color spectrograms are used to show how the microgravity environment varies in intensity with respect to both the time and frequency domains. These spectrograms are provided as an overview of the frequency characteristics of the SAMS data during the mission. Each spectrogram is a composite of 6 hour's worth of data. The time resolution used to compute the spectrograms seen here is 65.536 seconds. This corresponds to a frequency resolution of 0.0153 Hz.

These data were collected at 125 samples per second, and a 25 Hz low pass filter was applied to the data by the SAMS unit prior to digitization. Prior to plot production, the raw SAMS data were compensated for gain changes, and then demeaned. Demeaning was accomplished by analyzing individual sections with a nominal length of 30 minutes. Users who are interested in further details for either of these operations are encouraged to contact the PIMS group.

Interval Average and Root Mean Square Calculations

The interval average plots were produced by calculating the average of ten second intervals of data for each axis. This operation is described as:

$$x_{avg_k} = \frac{1}{M}\sum_{i=1}^{M} x_{(k-1)M+i} ,$$

where x represents the x, y, or z axis data, M is the number of points analyzed in an interval, and k refers to the kth interval analyzed.

The resulting data streams (x_{avg_k}, y_{avg_k}, z_{avg_k}) are then combined by a vector-magnitude operation.

This computation is expressed mathematically as: $accel_{avg_k} = \sqrt{x^2_{avg_k} + y^2_{avg_k} + z^2_{avg_k}}$.

The interval RMS plots were produced by taking the root-mean-square of ten second intervals of data for each axis and forming a vector magnitude of the resulting data stream.

The interval RMS operation is expressed mathematically as: $x_{RMS_k} = \sqrt{\frac{1}{M}\sum_{i=1}^{M}\left(x_{(k-1)M+i}\right)^2}$.

The same definitions apply for x, M, and k as in the interval average computation. The resulting data streams are combined by a vector-magnitude operation.

Power Spectral Density versus Frequency versus Time Calculations

In order to produce the spectrogram image, Power Spectral Densities were computed for successive time intervals (the length of the interval is equal to the time resolution). For the PSD computation, a Hanning window was applied. In order to combine all three axes into a single plot to show an overall level, a Vector-Magnitude (VM) operation was performed. Stated mathematically:

$$VM_k = \sqrt{PSD^2_{x_k} + PSD^2_{y_k} + PSD^2_{z_k}}.$$

By imaging the base 10 logarithm ($\log_{10}$) magnitude as a color and stacking successive PSDs from left to right, variations of acceleration magnitude and frequency are shown as a function of time. Colors are assigned to discrete magnitude ranges, so that there are 64 colors assigned to the entire range of magnitudes shown.

The colorbar limits are chosen in order to maximize the data value and visibility in a given set of spectrogram plots. Data which fall outside of these limits will be imaged as either the highest or lowest magnitude, depending on which side they have saturated. For this report, less than 1% of the total points lie below the lower limit, and less than 1% of the total points lie above the upper limit. If an area of interest seems to be saturated, care should be taken in that the actual values may lie above or below the color mapping shown on the plot.

Due to the nature of spectrograms, care should be taken to not merely read a color's numeric value as being the "amount" of acceleration that is present at a given frequency. In order to get this type of information, the PSDs must be integrated between two frequencies. These frequencies (lower and upper) form the "band" of interest. The result of this integration is the g_{RMS} acceleration level in the $[f_{lower}, f_{upper}]$ band. The PIMS group is able to provide this type of analysis on a per-request basis.

Plot gaps (if any exist) are shown by either white or dark blue areas on the page. Care should be taken to not mistake a plot gap (represented by a blue vertical band) with a quiet period. If a plot gap exists for an entire plot (or series of successive plots), a comment is placed on the page to let the user know there is a gap in the data. These "no data available" comments will not show exact times for which the data are not available, but will only indicate missing plots.

Contacting PIMS

To request additional analysis or information, users are encouraged to send an e-mail to pims@lerc.nasa.gov, or FAX a request to (216) 433-8545.

Figure 1a: STS–79, Head C (fc=25 Hz), Ten Second Interval Average

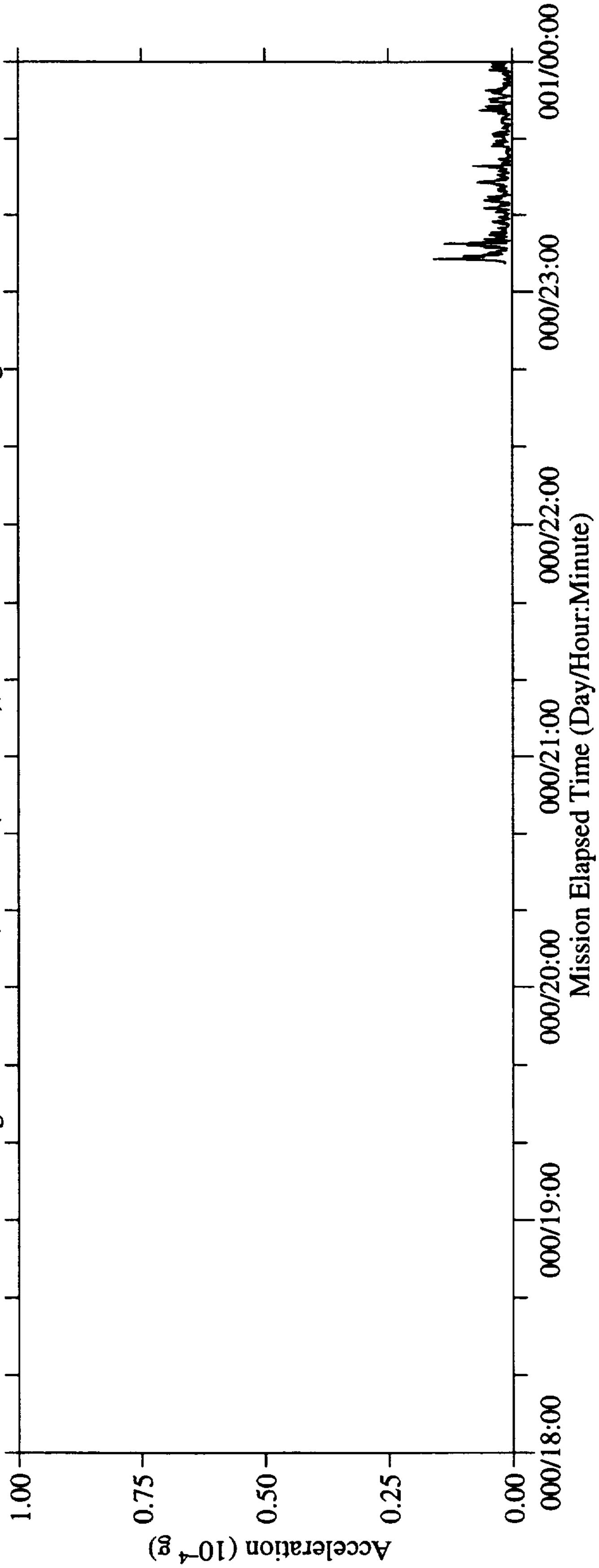

Figure 1b: STS–79, Head C (fc=25 Hz), Ten Second Interval RMS

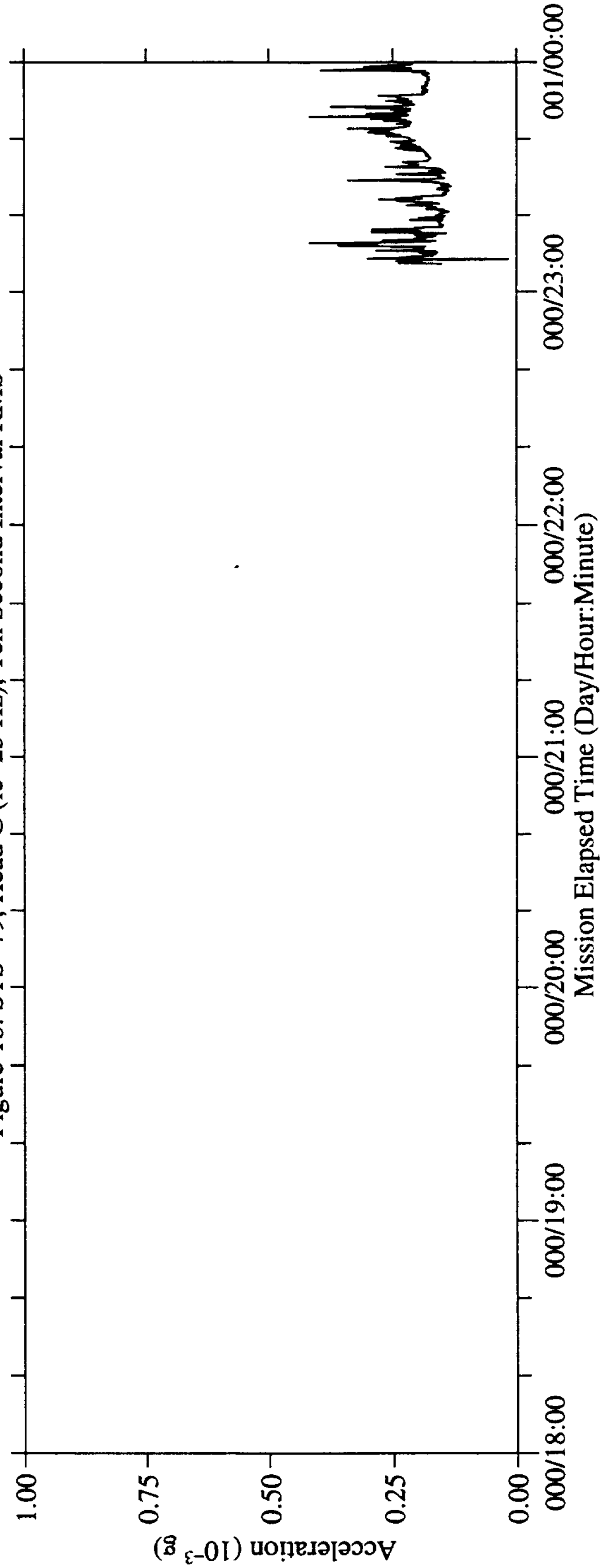

Figure 2: STS-79, Head C (fc=25 Hz)

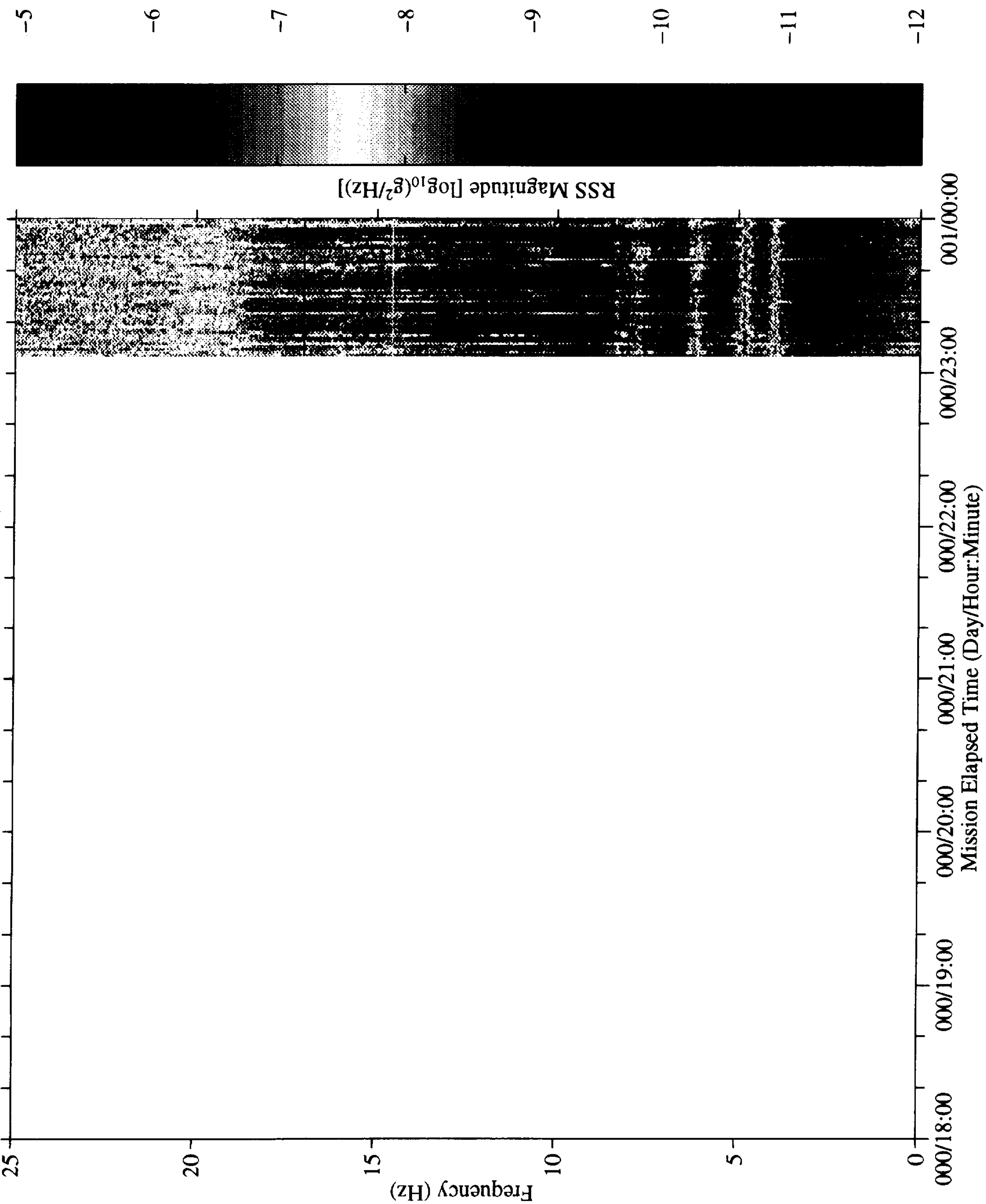

Figure 3a: STS–79, Head C (fc=25 Hz), Ten Second Interval Average

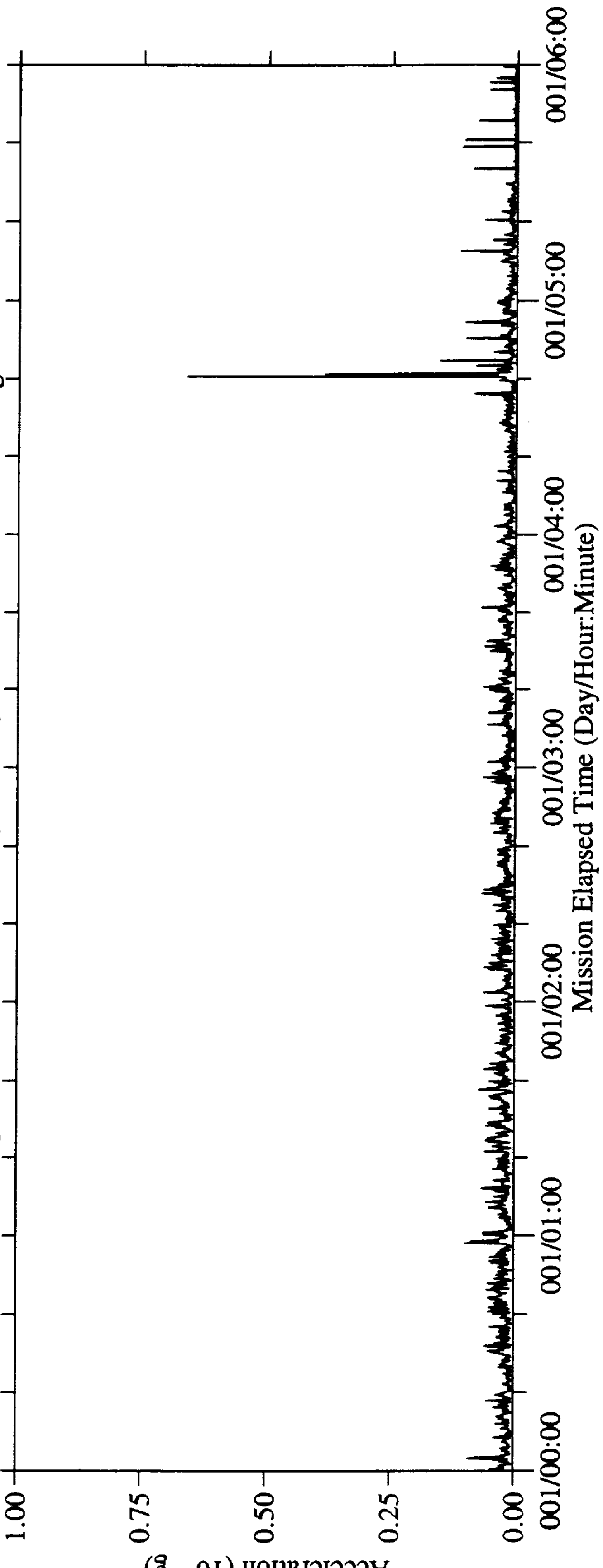

Figure 3b: STS–79, Head C (fc=25 Hz), Ten Second Interval RMS

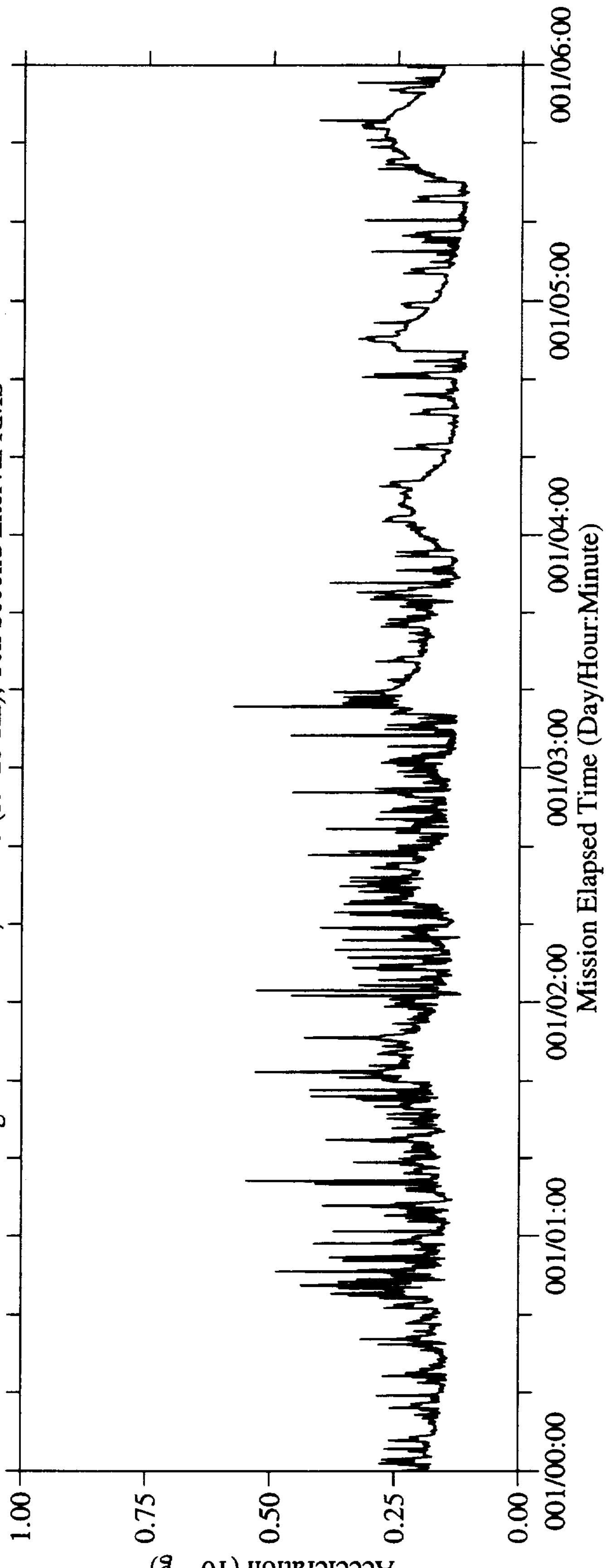

Figure 4: STS–79, Head C (fc=25 Hz)

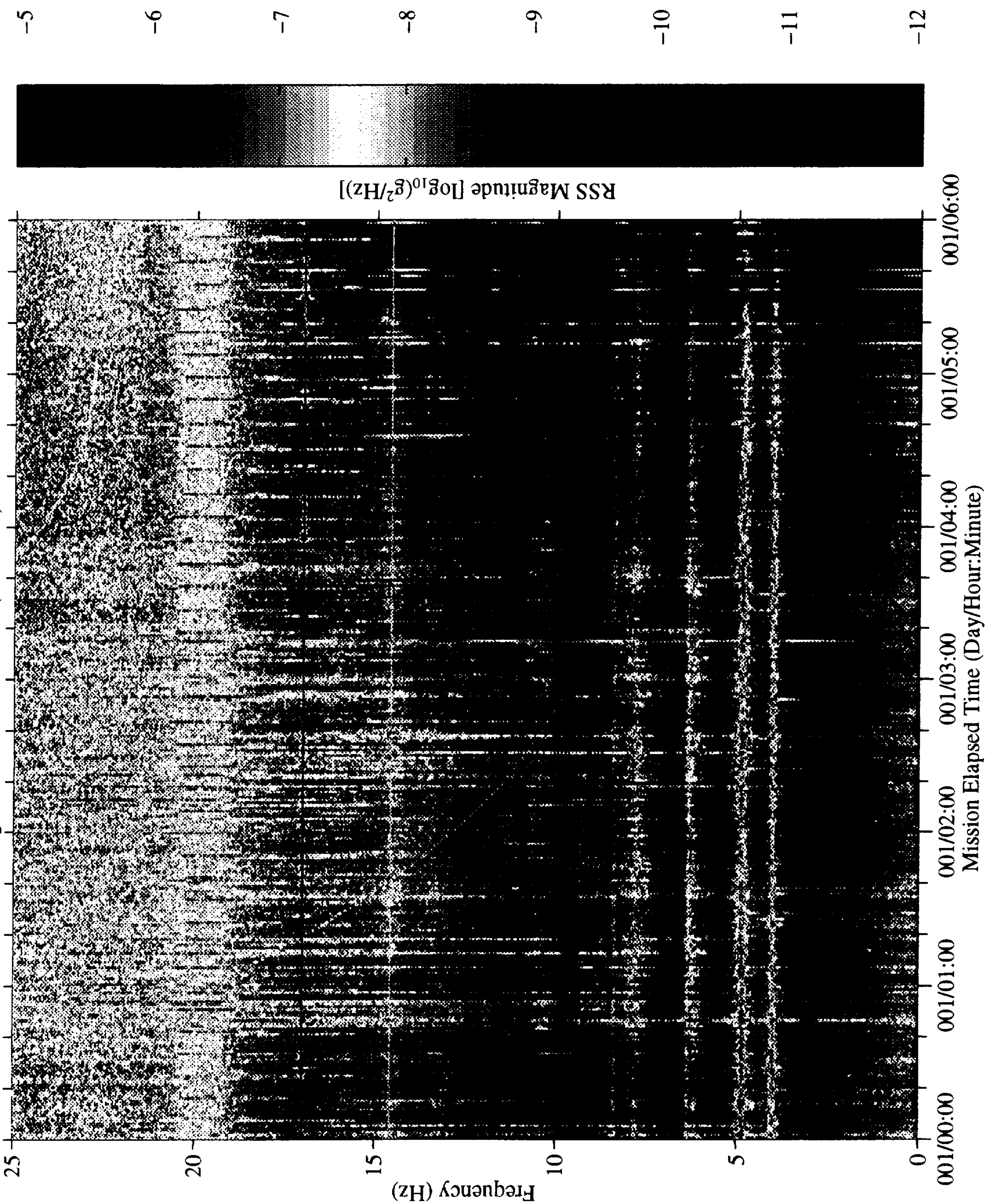

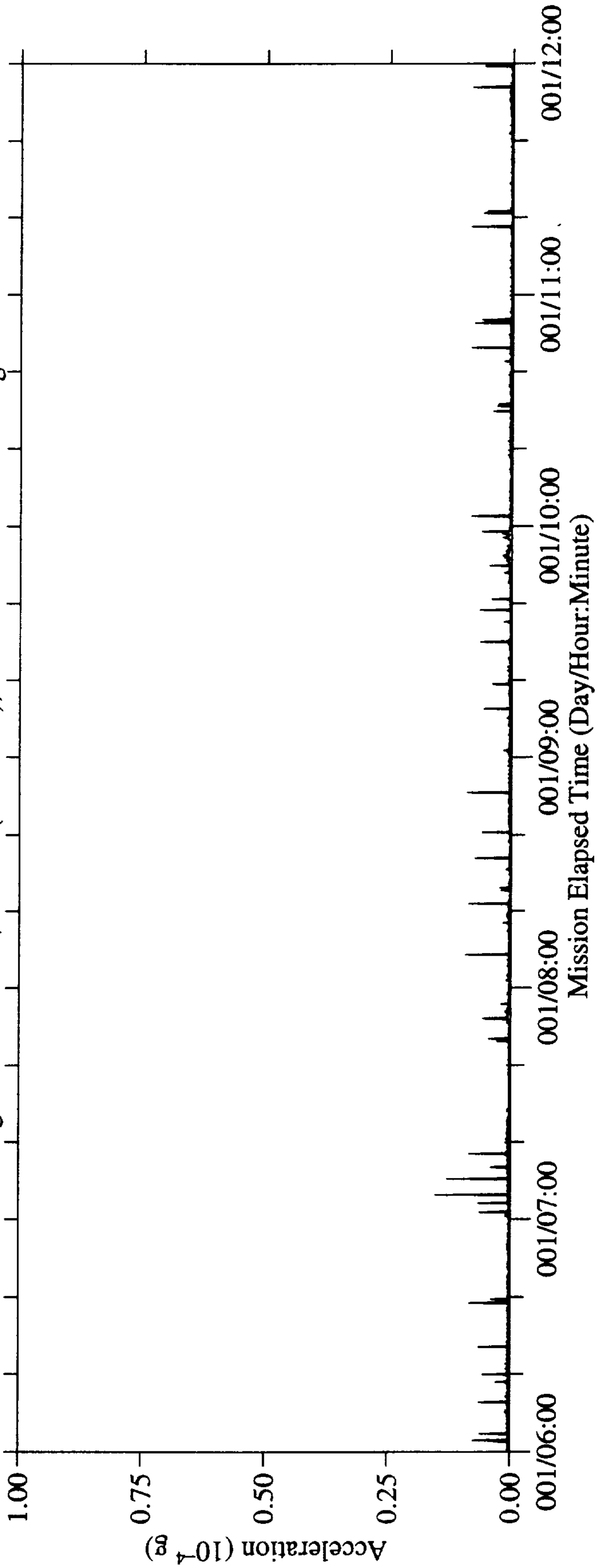

Figure 5a: STS–79, Head C (fc=25 Hz), Ten Second Interval Average

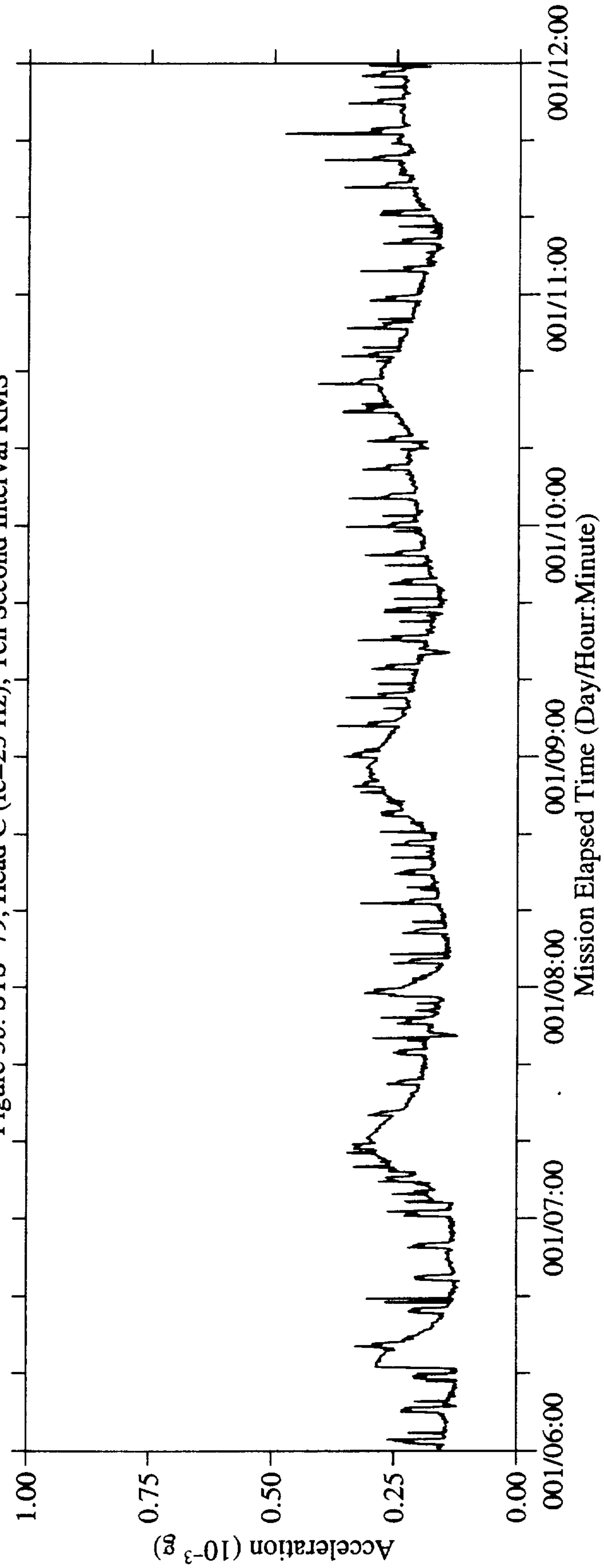

Figure 5b: STS–79, Head C (fc=25 Hz), Ten Second Interval RMS

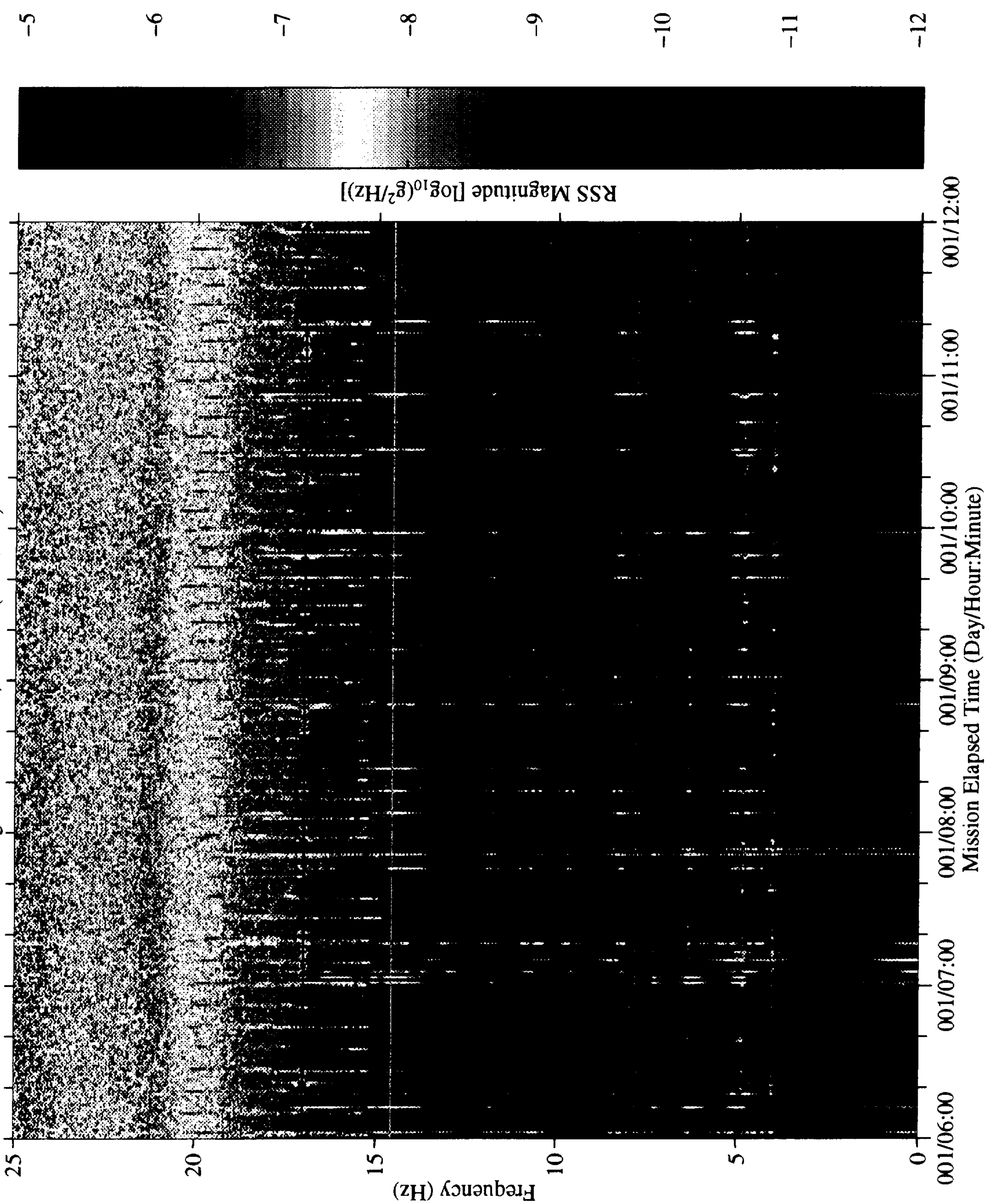

Figure 6: STS-79, Head C (fc=25 Hz)

Figure 7a: STS-79, Head C (fc=25 Hz), Ten Second Interval Average

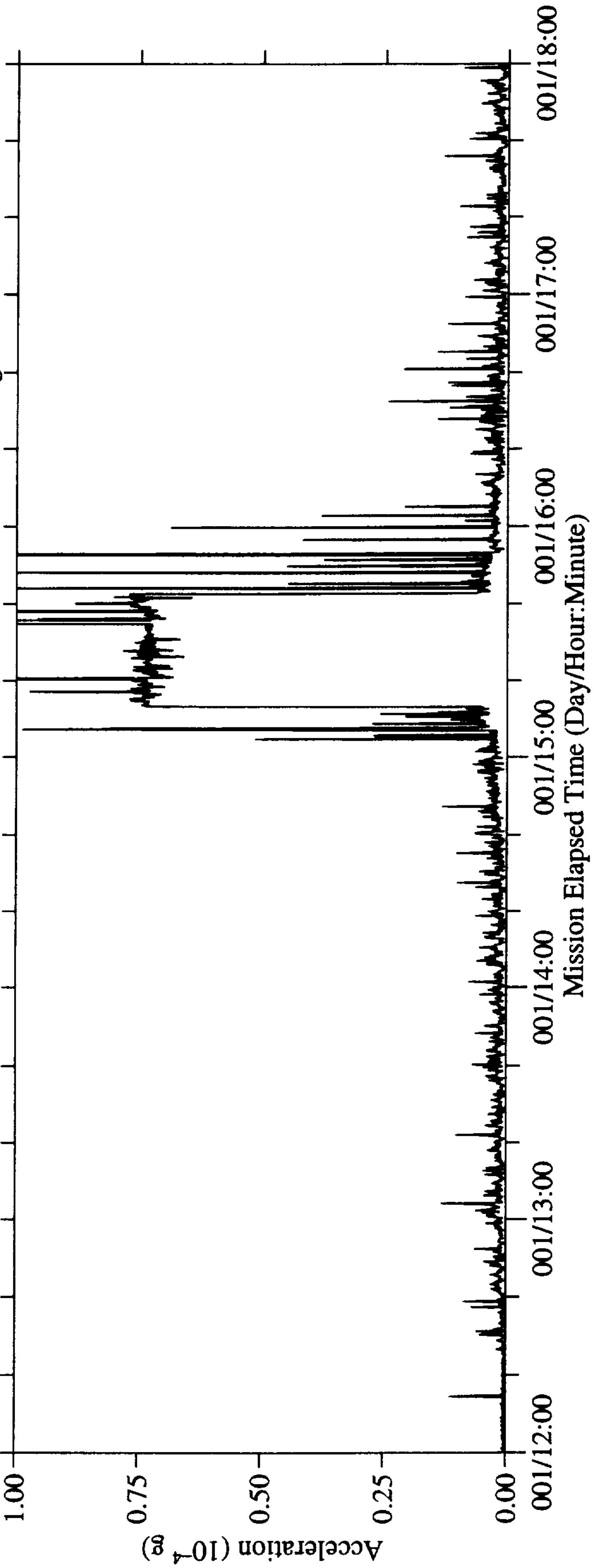

Figure 7b: STS-79, Head C (fc=25 Hz), Ten Second Interval RMS

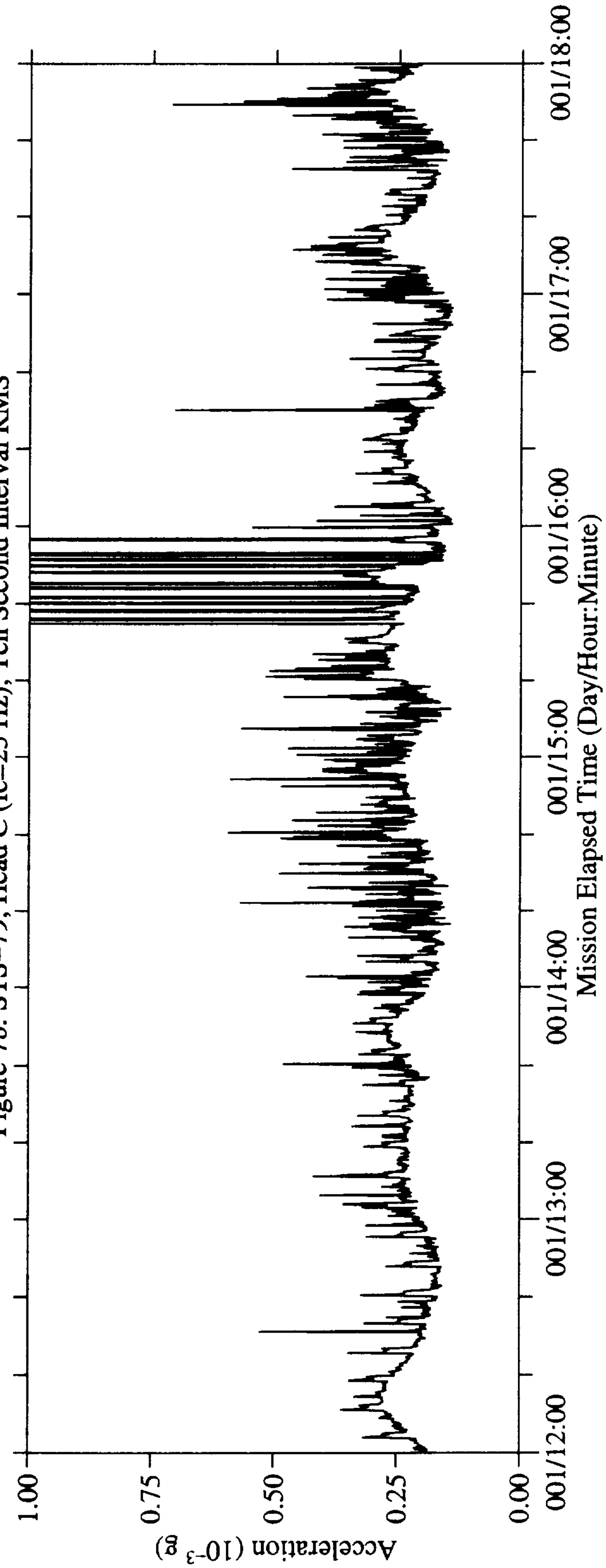

Figure 8: STS–79, Head C (fc=25 Hz)

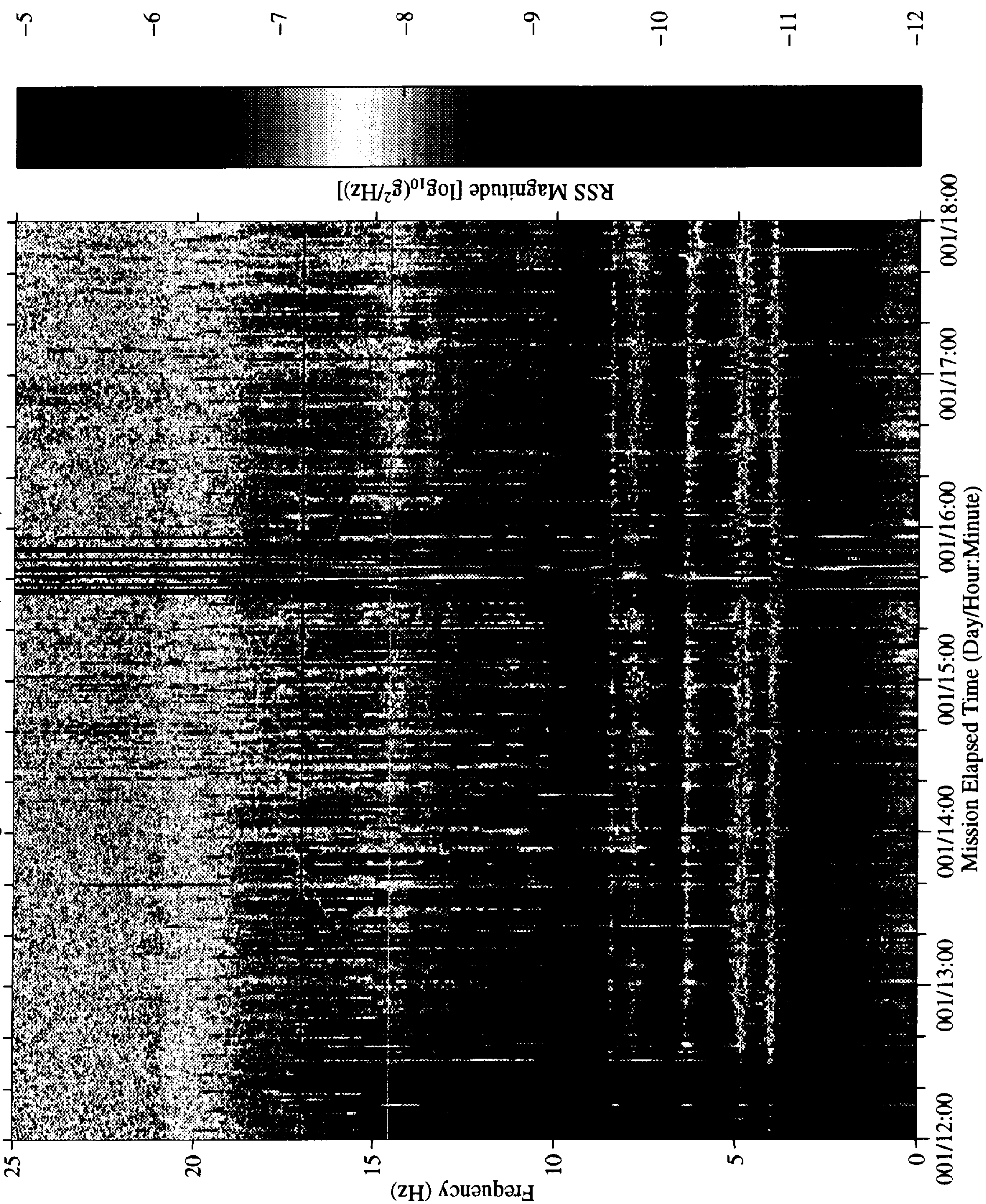

Figure 9a: STS–79, Head C (fc=25 Hz), Ten Second Interval Average

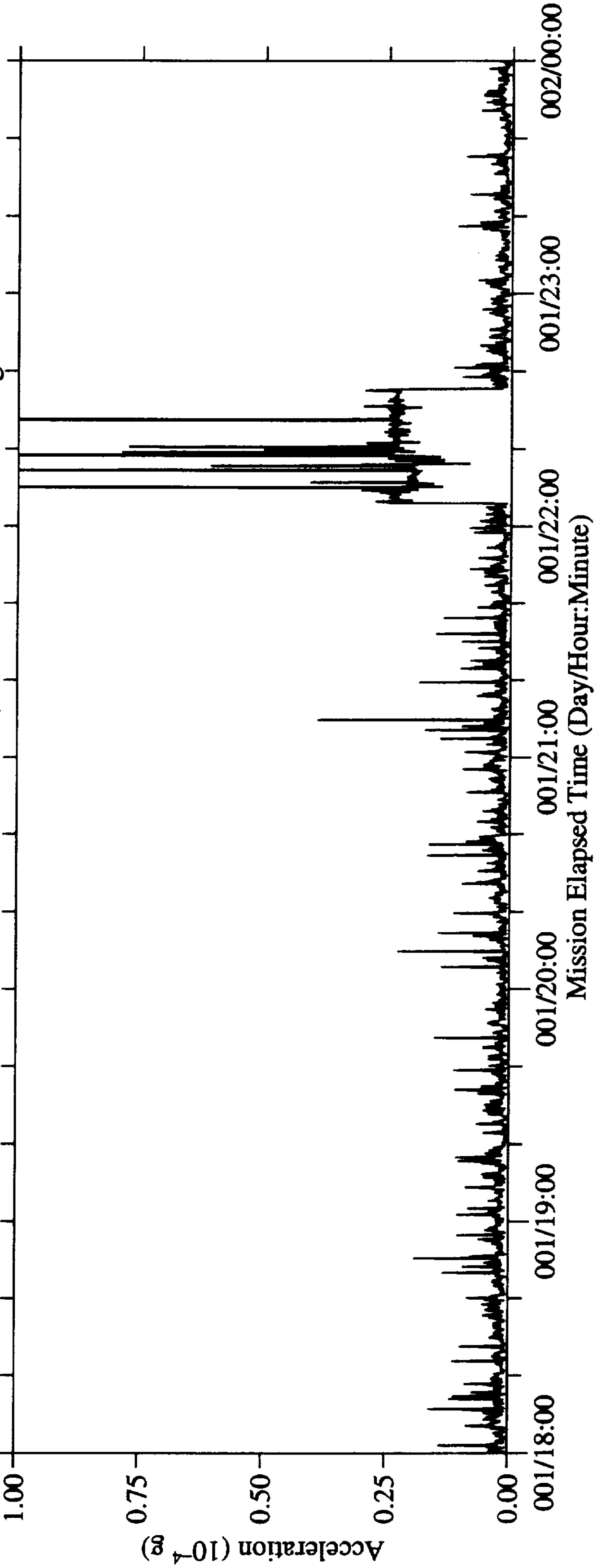

Figure 9b: STS–79, Head C (fc=25 Hz), Ten Second Interval RMS

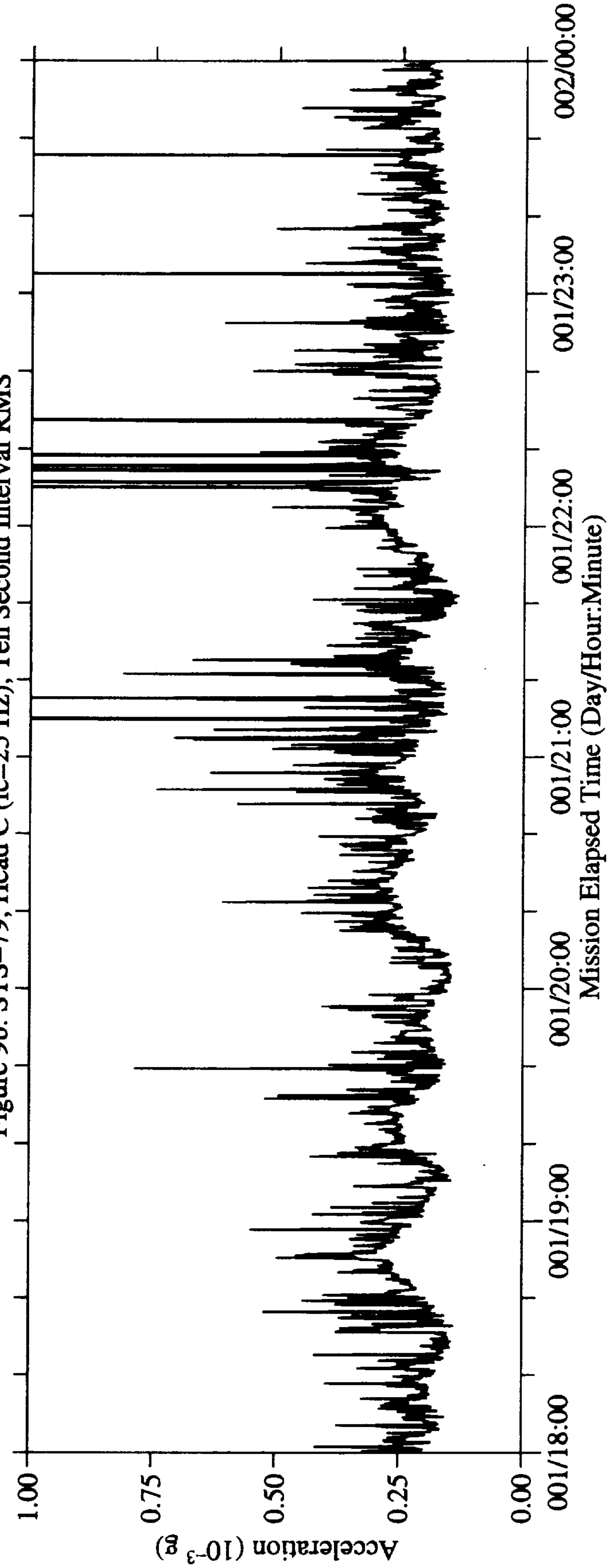

Figure 10: STS–79, Head C (fc=25 Hz)

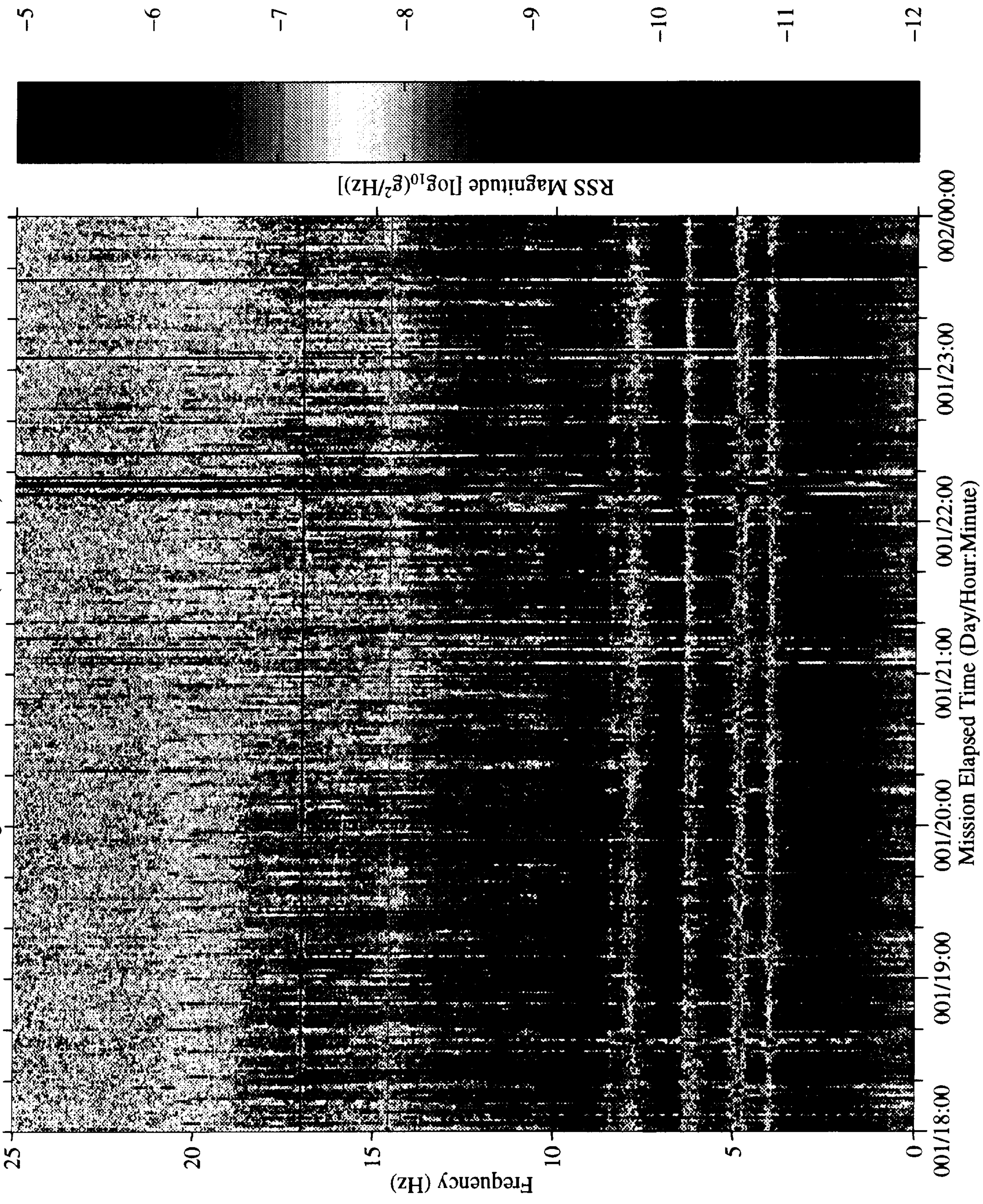

Figure 11a: STS–79, Head C (fc=25 Hz), Ten Second Interval Average

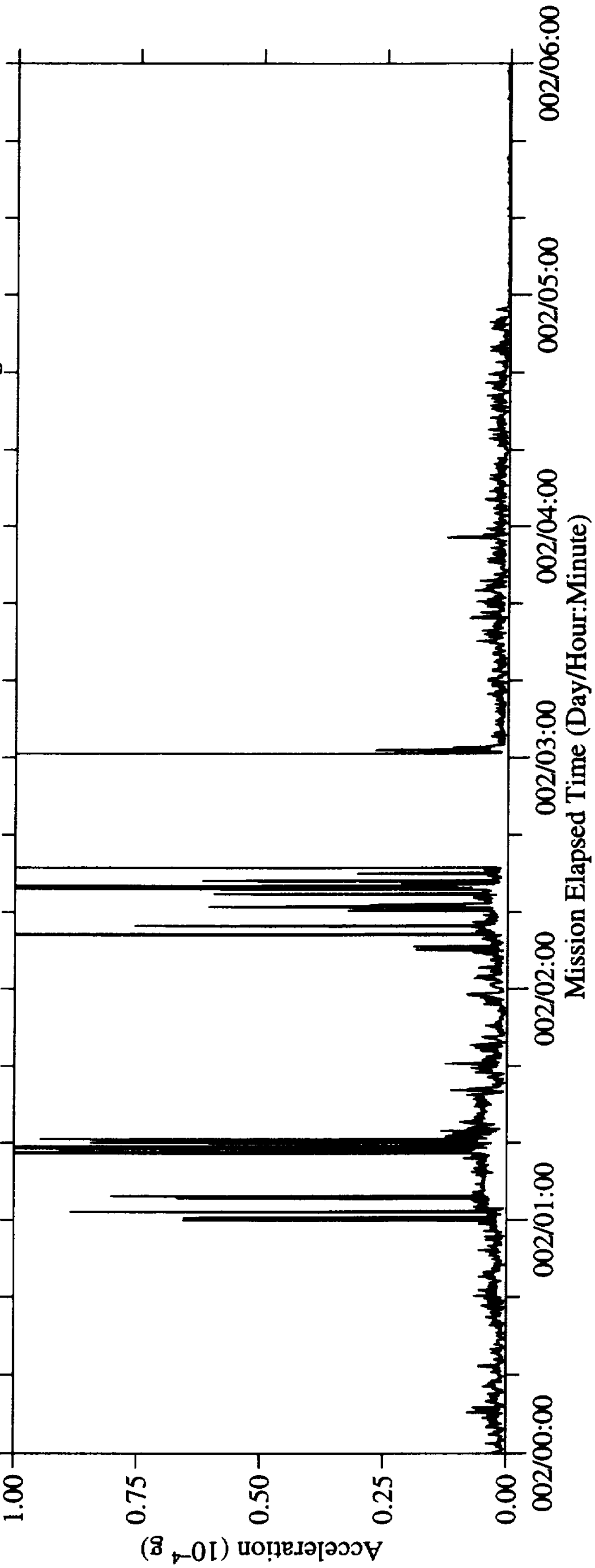

Figure 11b: STS–79, Head C (fc=25 Hz), Ten Second Interval RMS

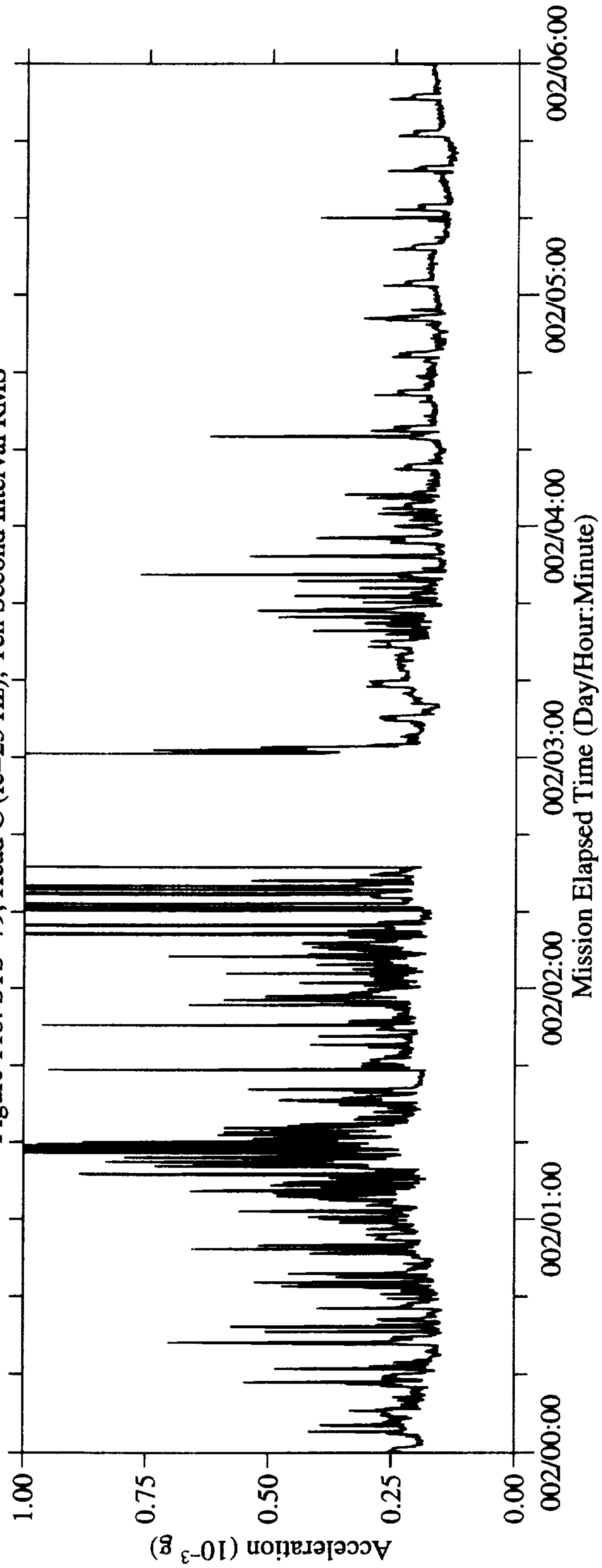

Figure 12: STS-79, Head C (fc=25 Hz)

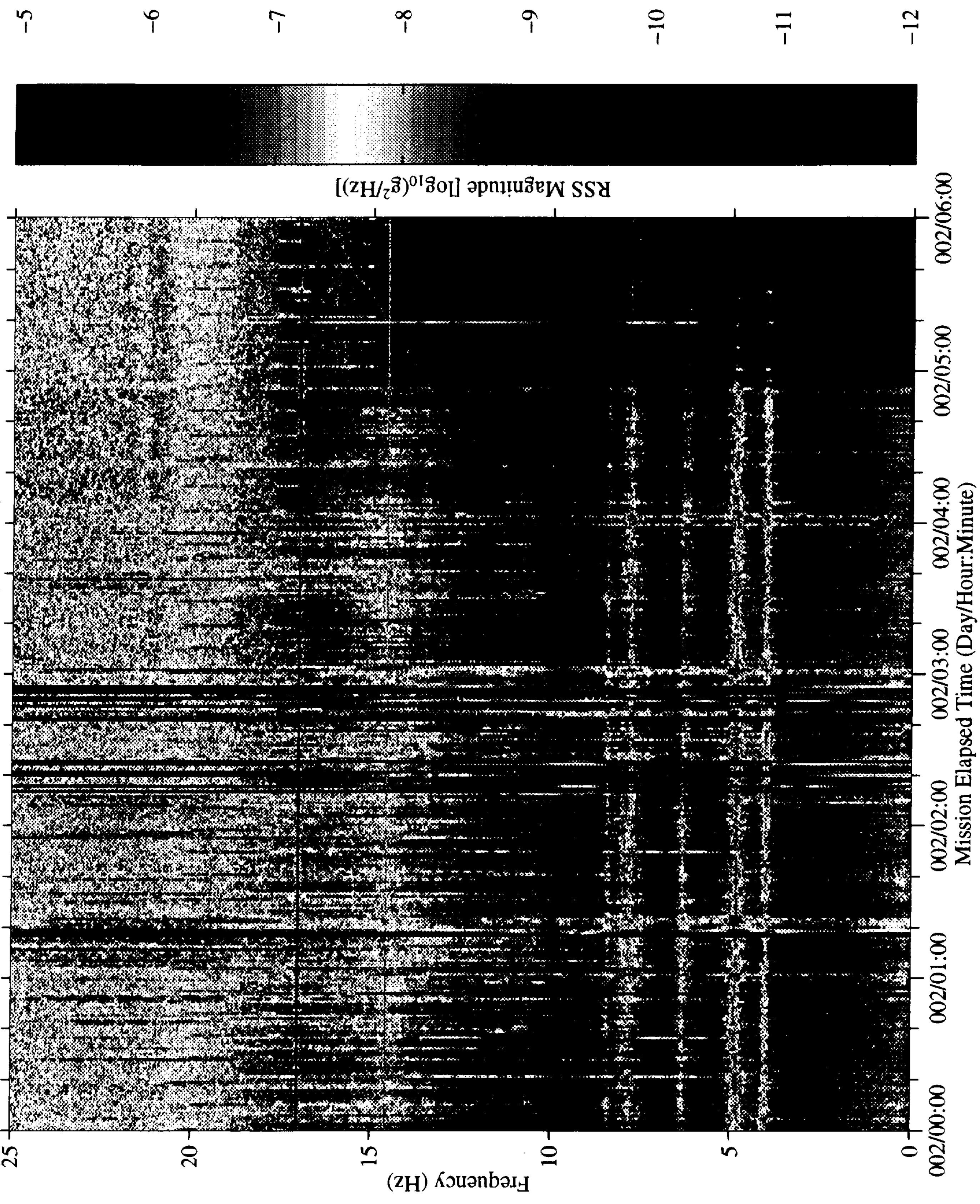

Figure 13a: STS–79, Head C (fc=25 Hz), Ten Second Interval Average

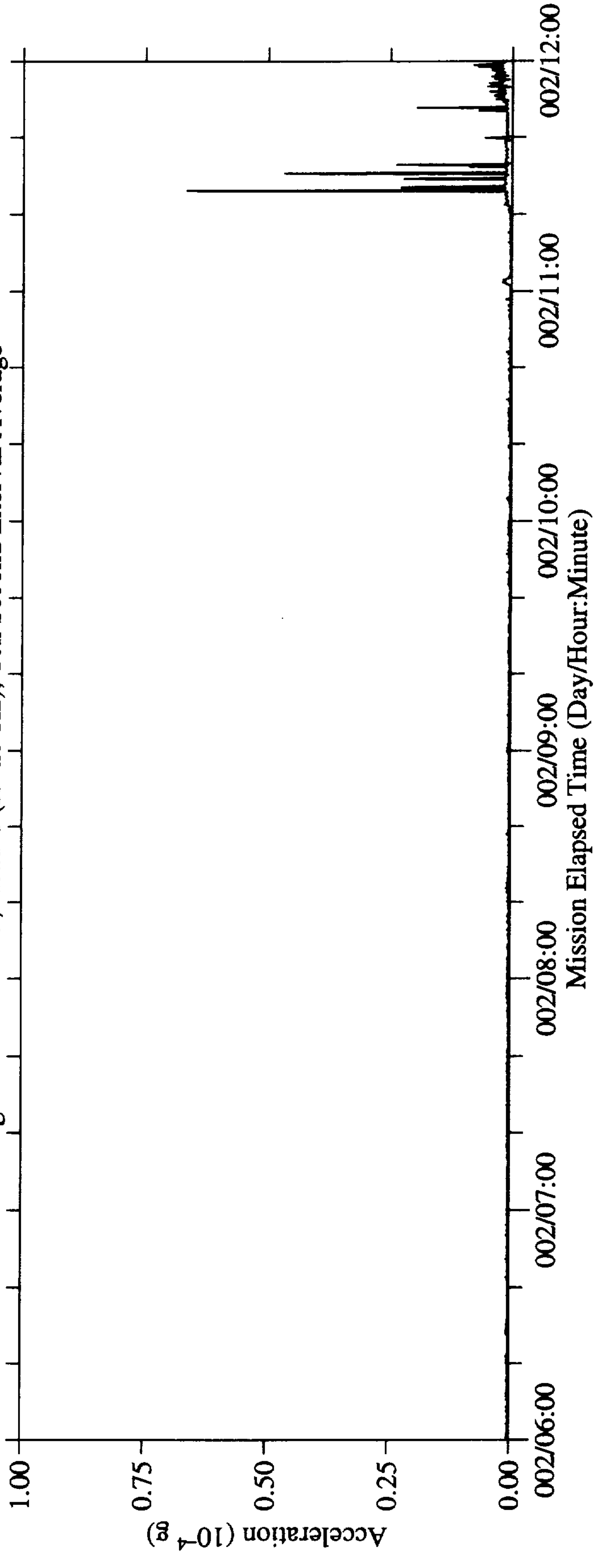

Figure 13b: STS–79, Head C (fc=25 Hz), Ten Second Interval RMS

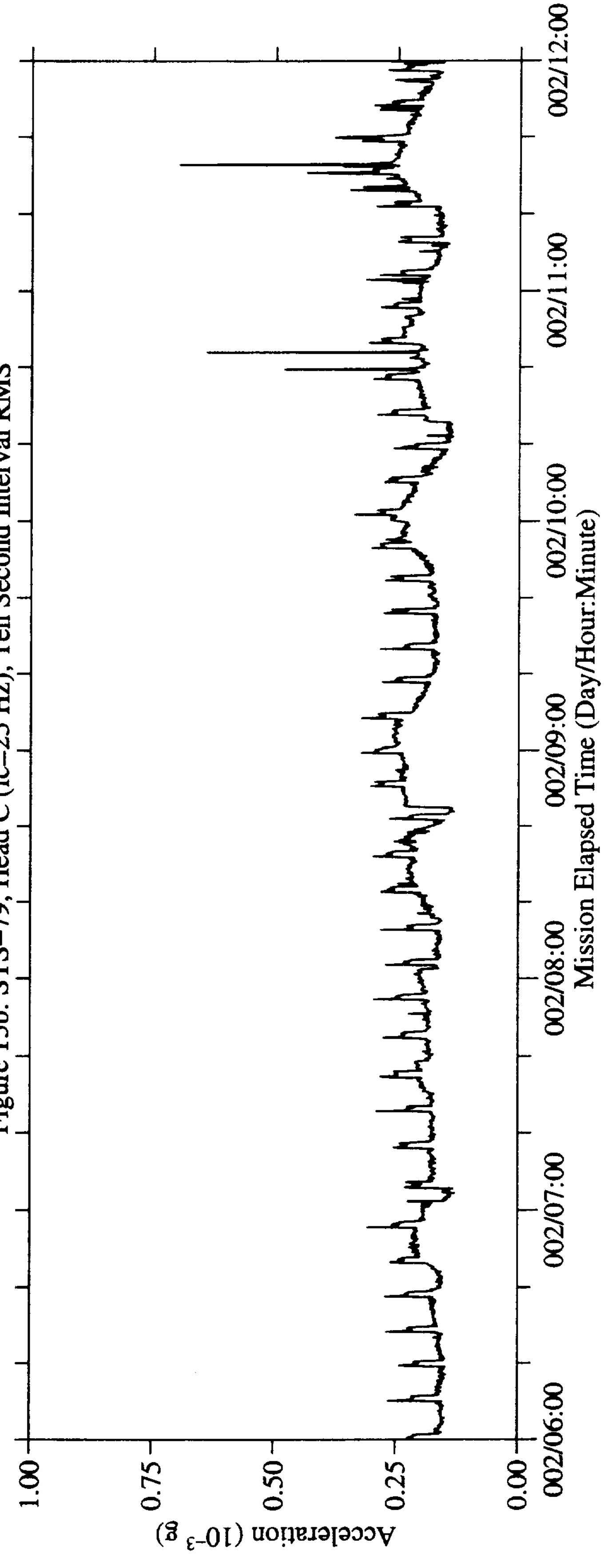

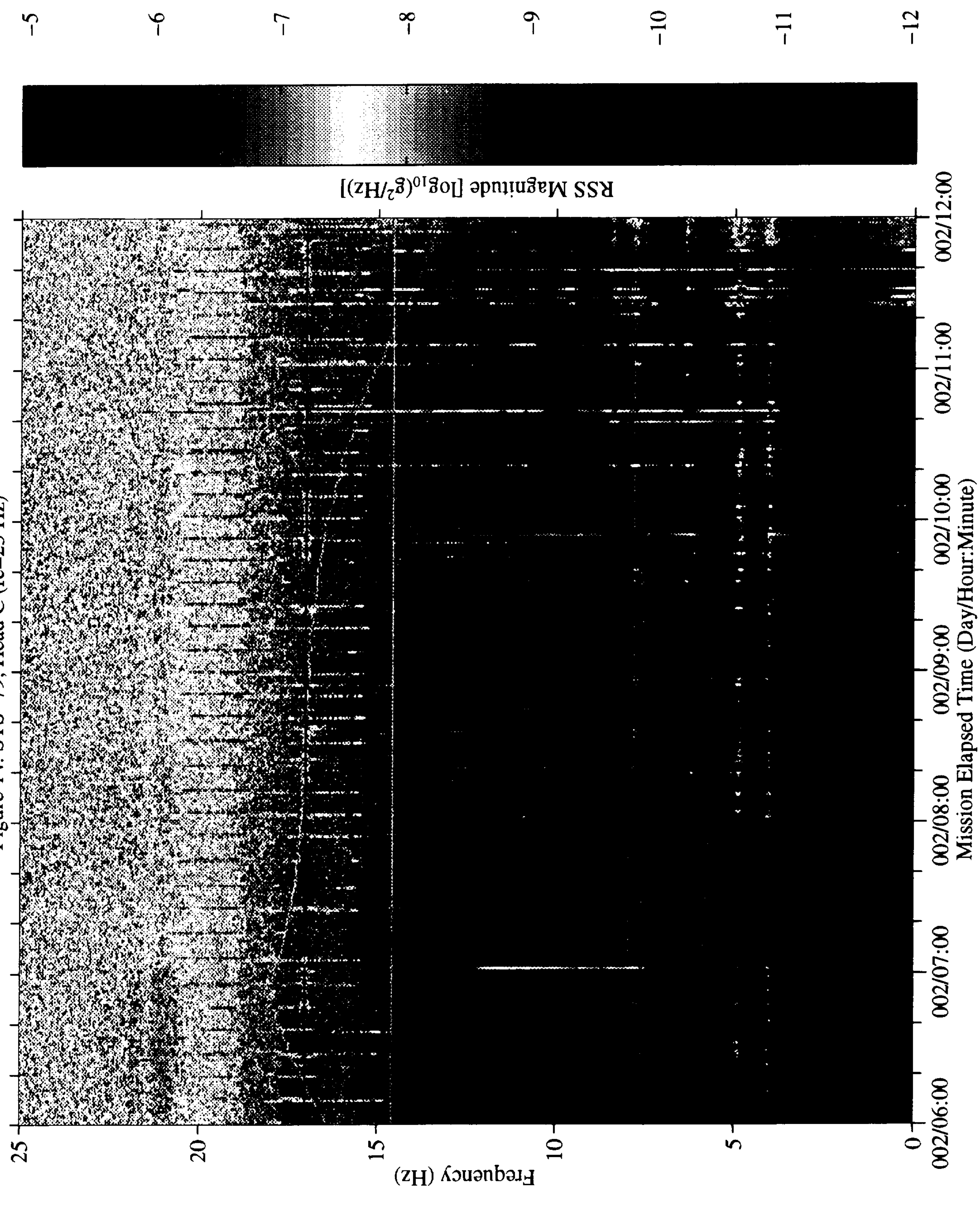

Figure 14: STS–79, Head C (fc=25 Hz)

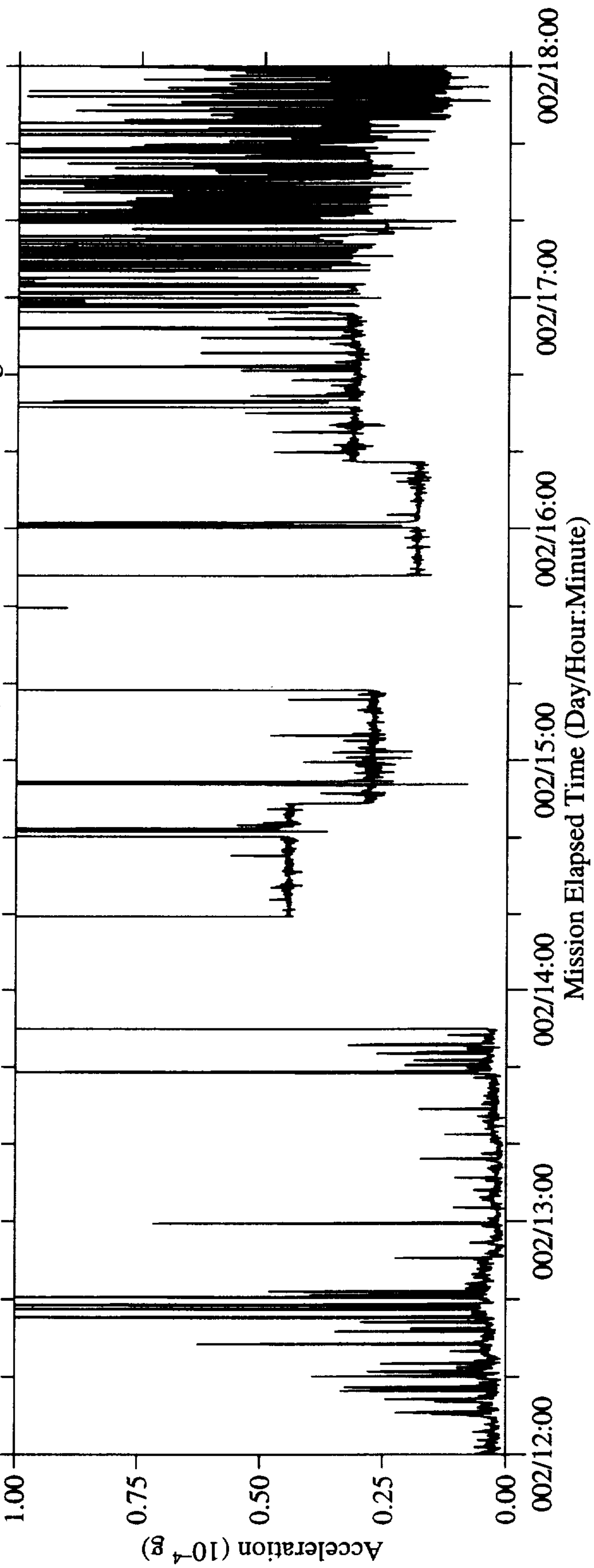

Figure 15a: STS–79, Head C (fc=25 Hz), Ten Second Interval Average

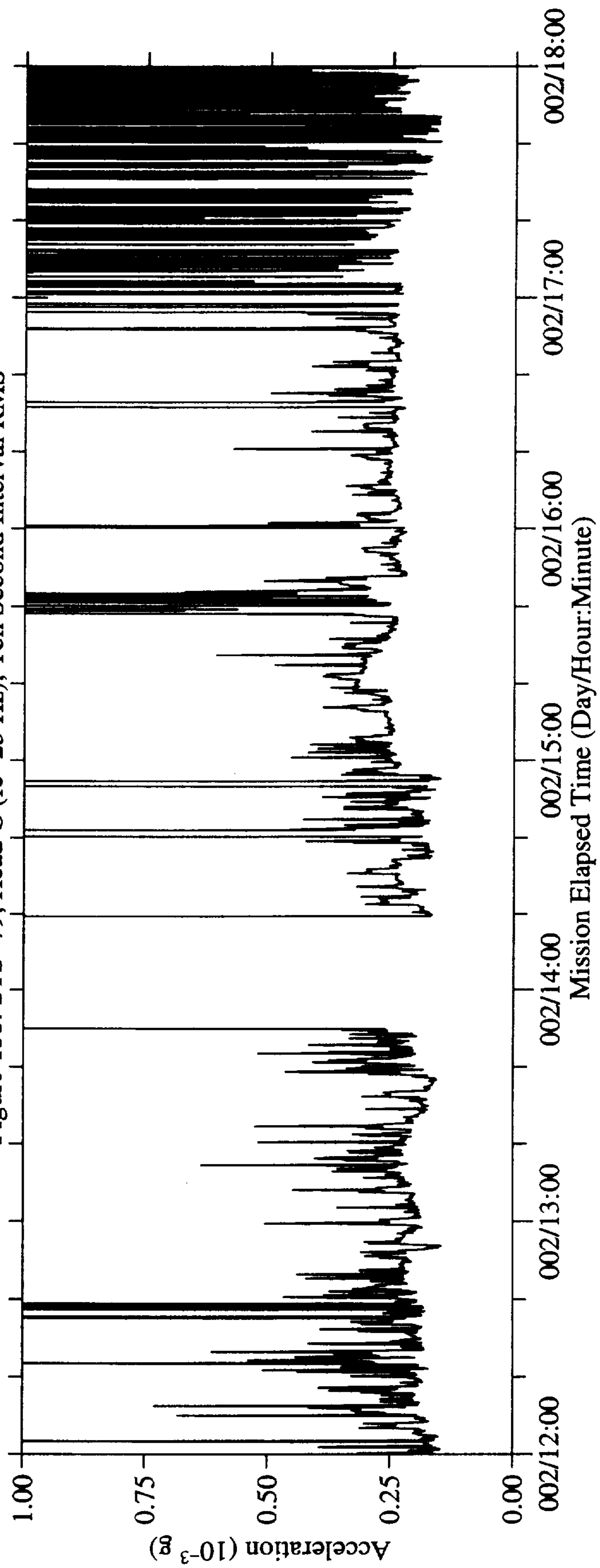

Figure 15b: STS–79, Head C (fc=25 Hz), Ten Second Interval RMS

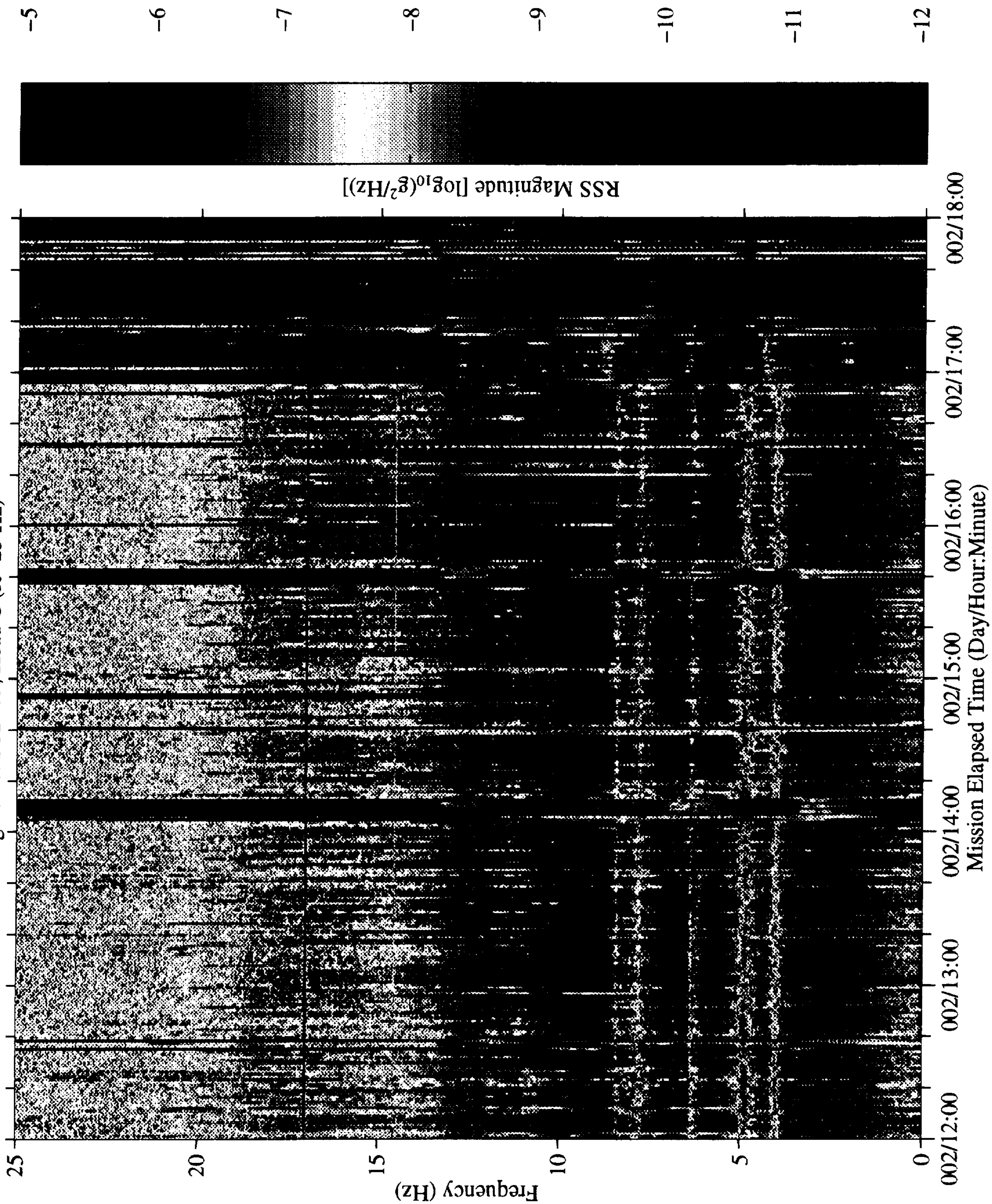

Figure 16: STS–79, Head C (fc=25 Hz)

Figure 17a: STS-79, Head C (fc=25 Hz), Ten Second Interval Average

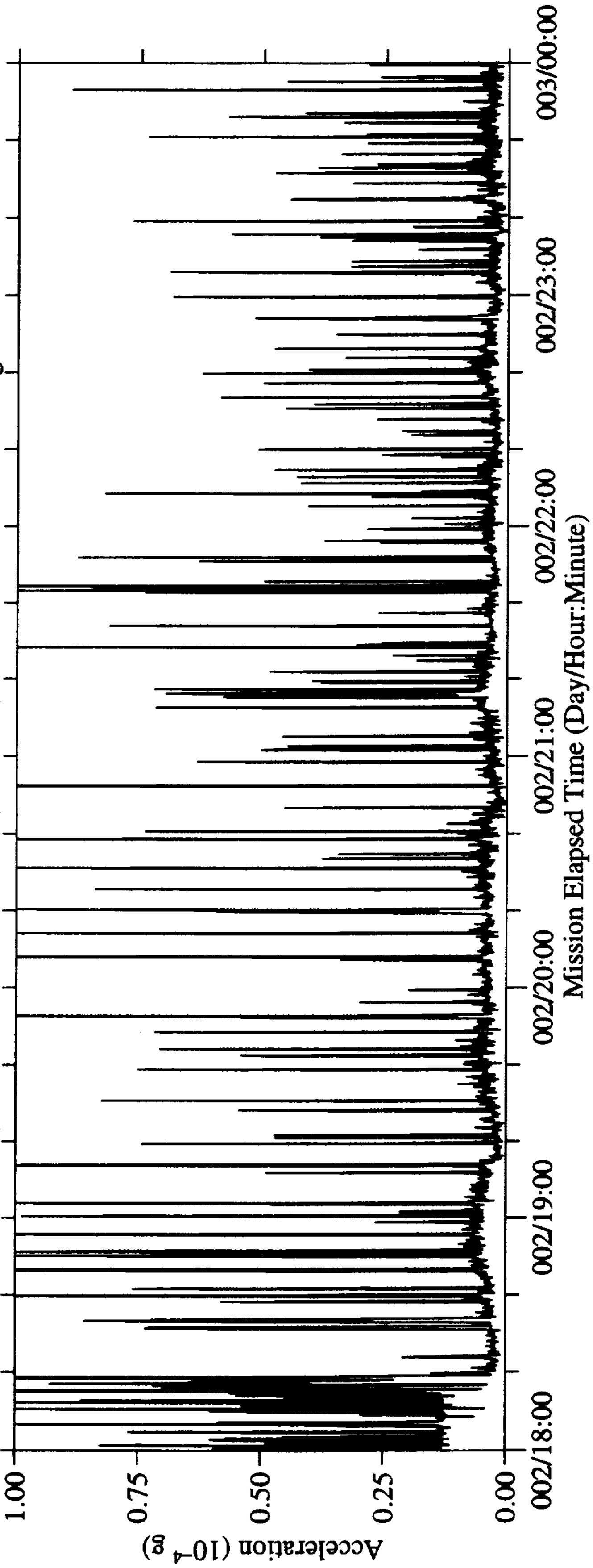

Figure 17b: STS-79, Head C (fc=25 Hz), Ten Second Interval RMS

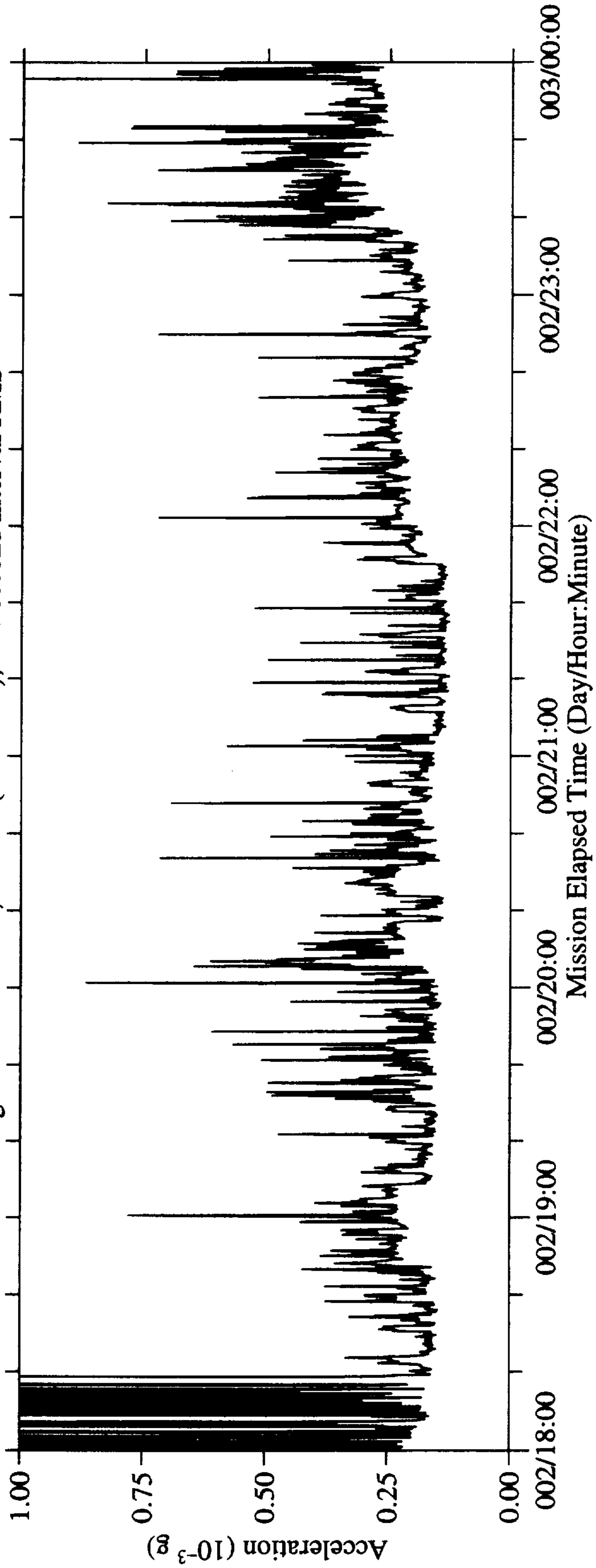

Figure 18: STS-79, Head C (fc=25 Hz)

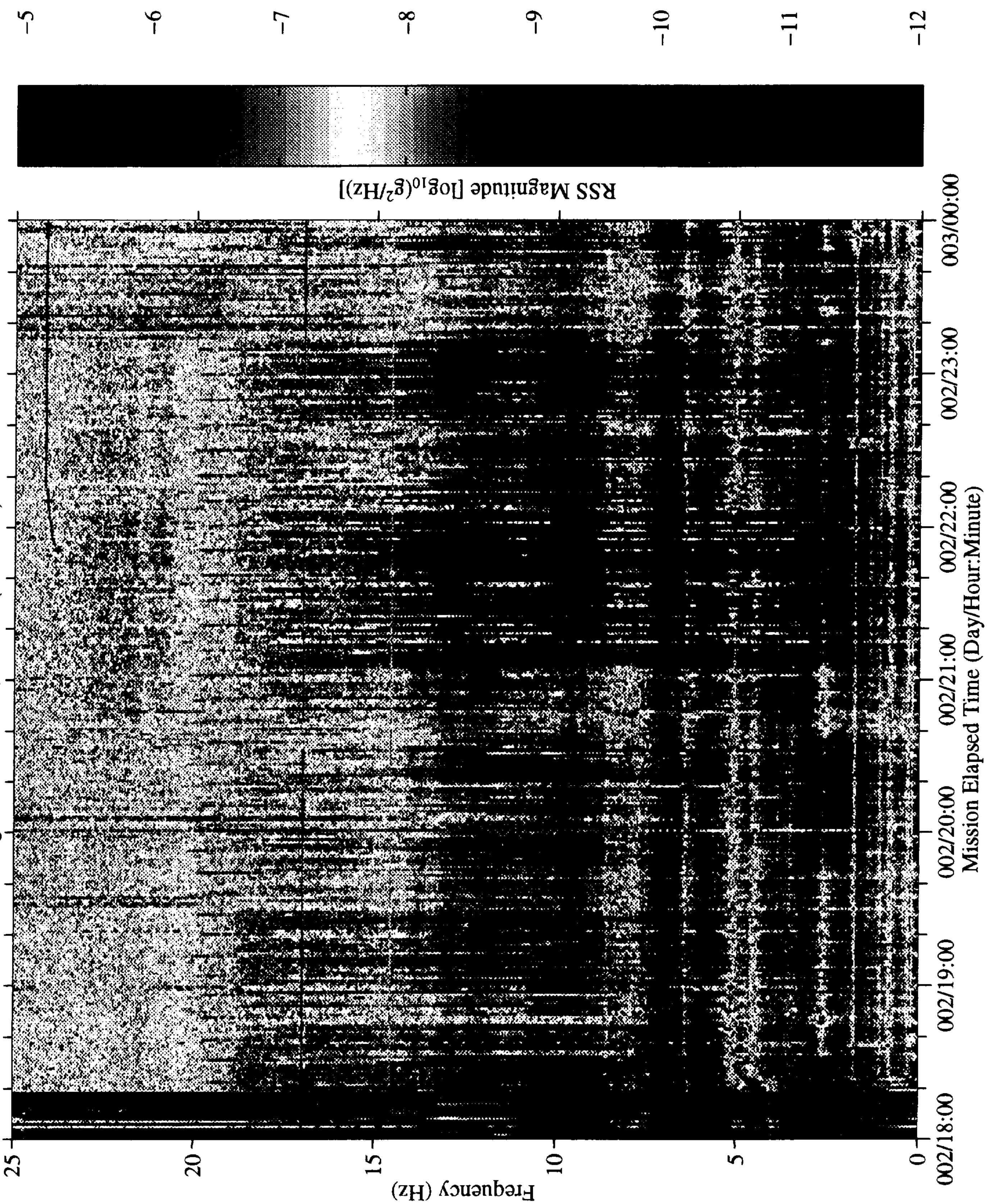

Figure 19a: STS-79, Head C (fc=25 Hz), Ten Second Interval Average

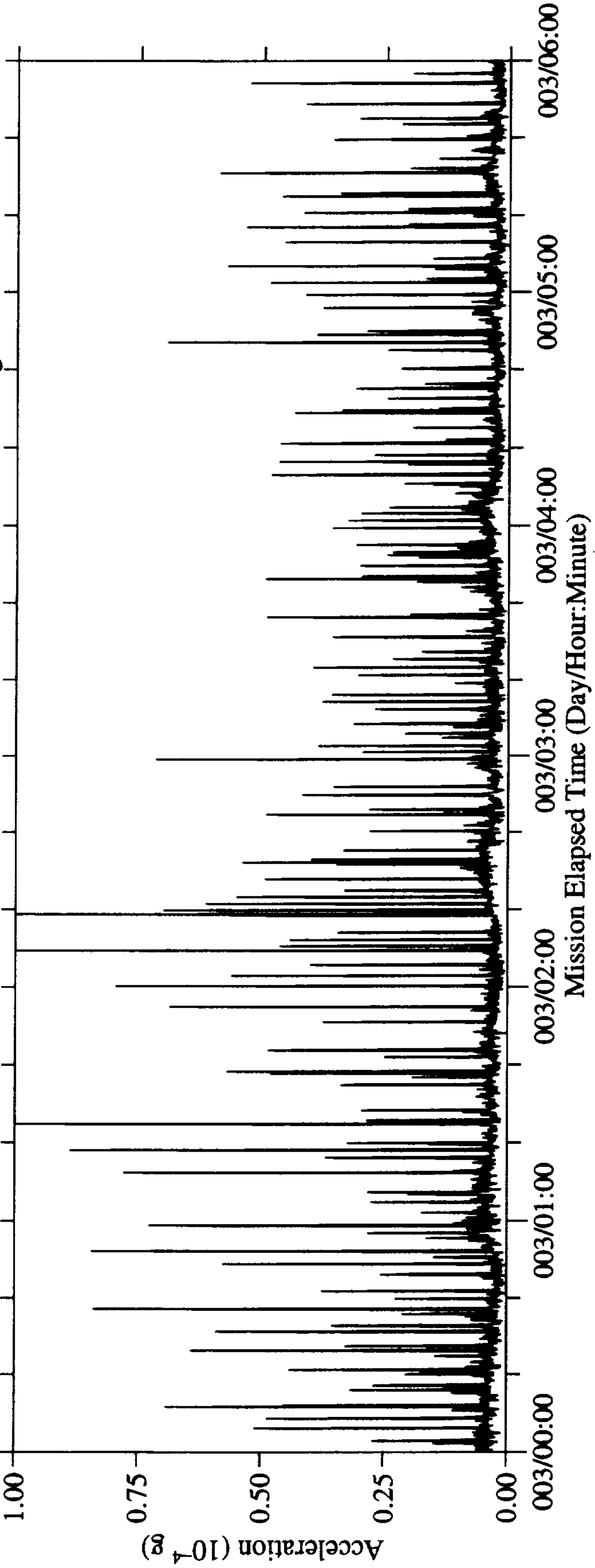

Figure 19b: STS-79, Head C (fc=25 Hz), Ten Second Interval RMS

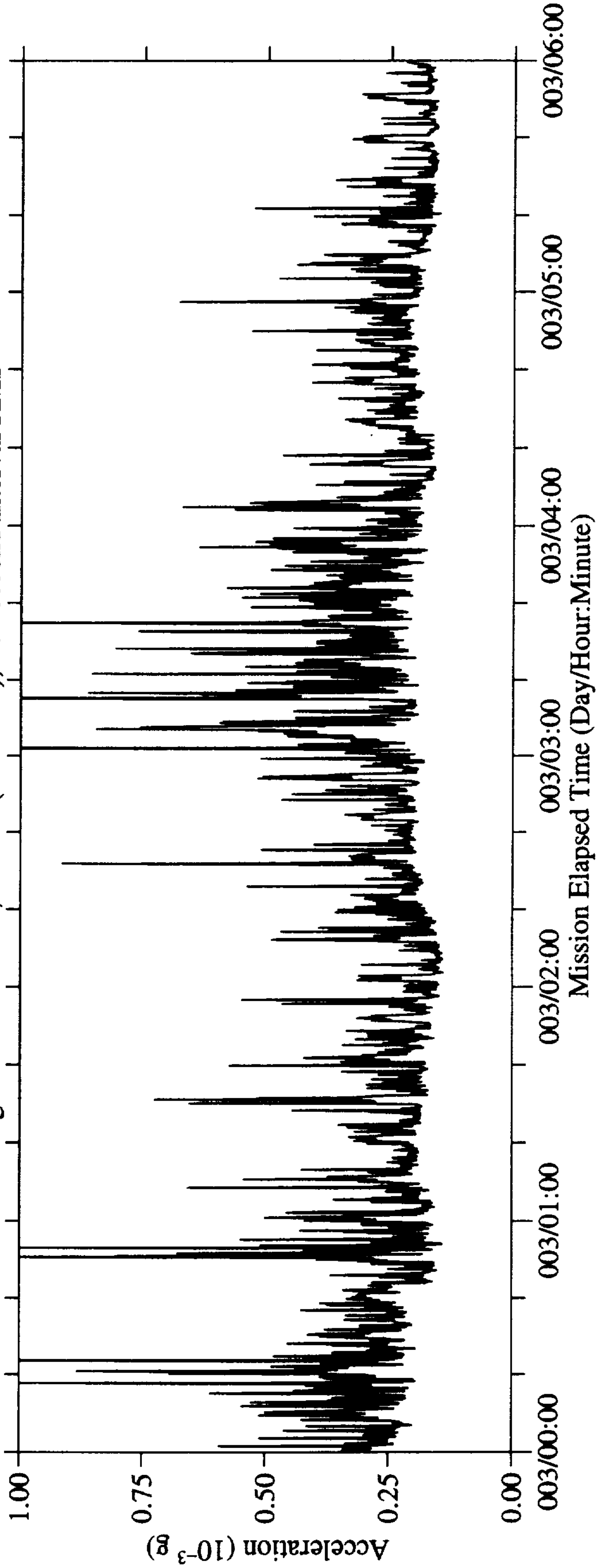

Figure 20: STS-79, Head C (fc=25 Hz)

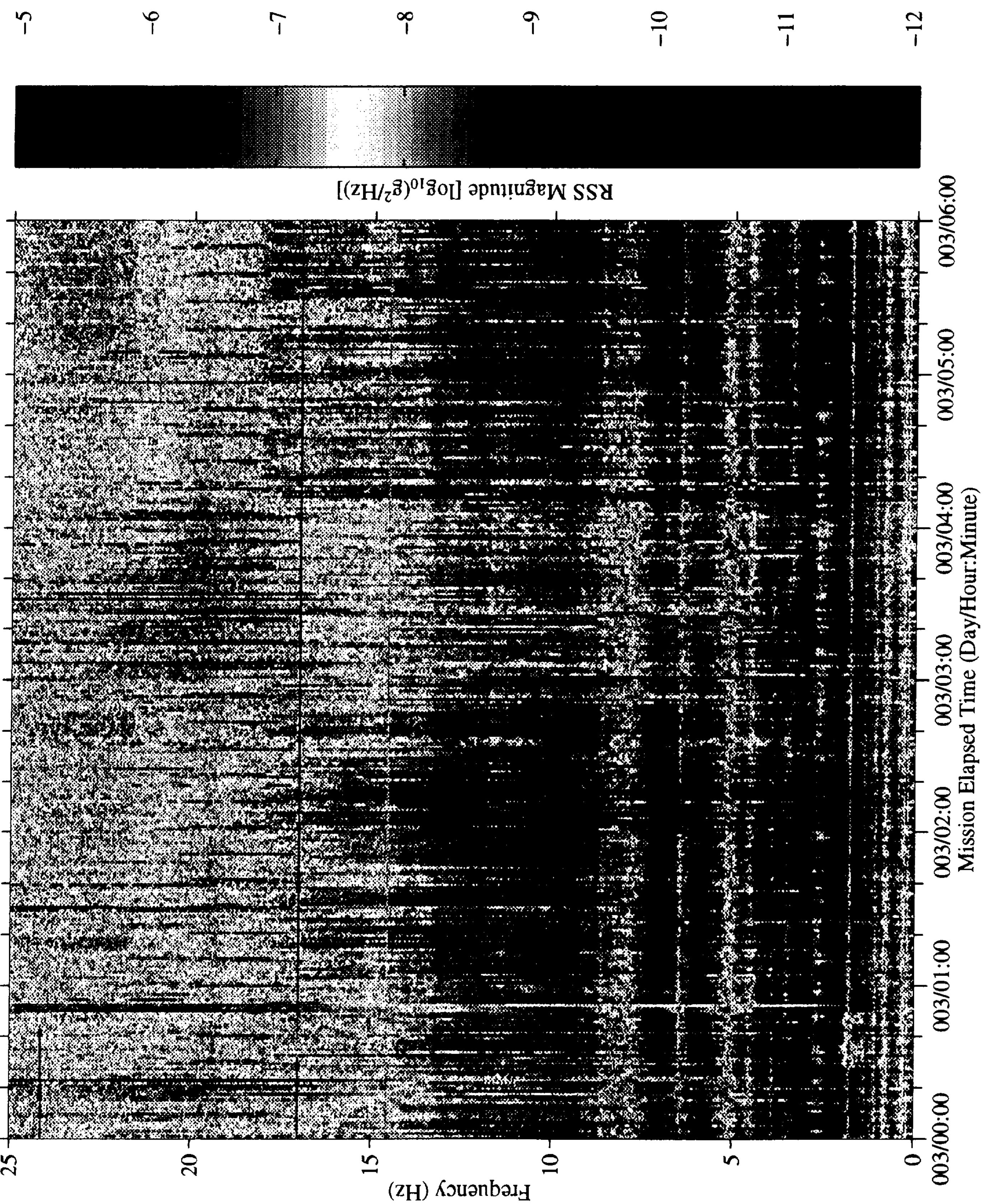

Figure 21a: STS-79, Head C (fc=25 Hz), Ten Second Interval Average

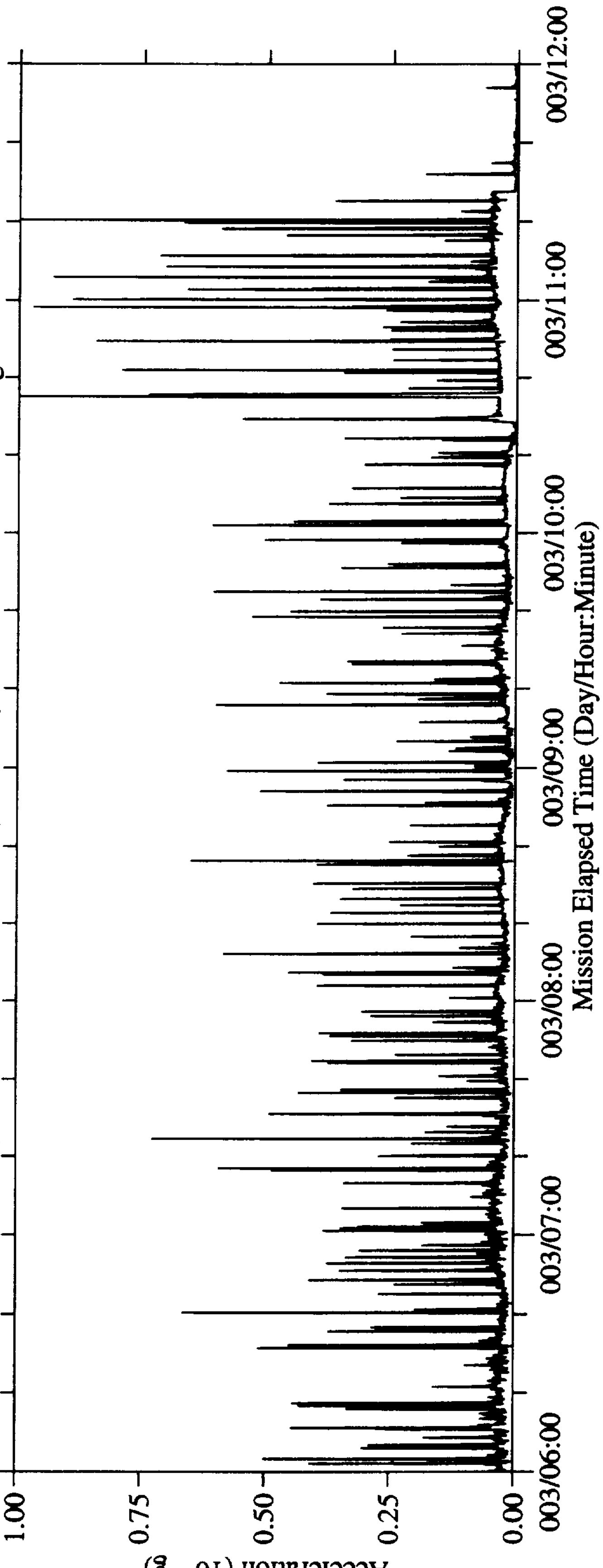

Figure 21b: STS-79, Head C (fc=25 Hz), Ten Second Interval RMS

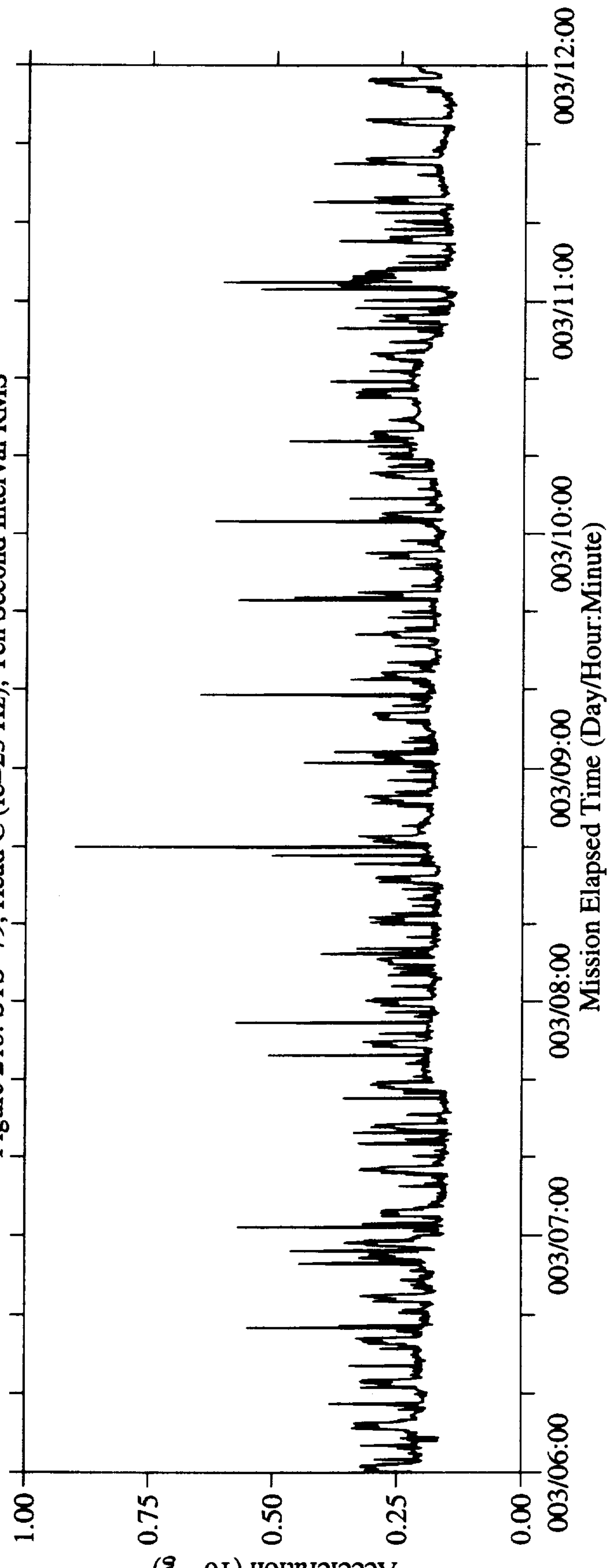

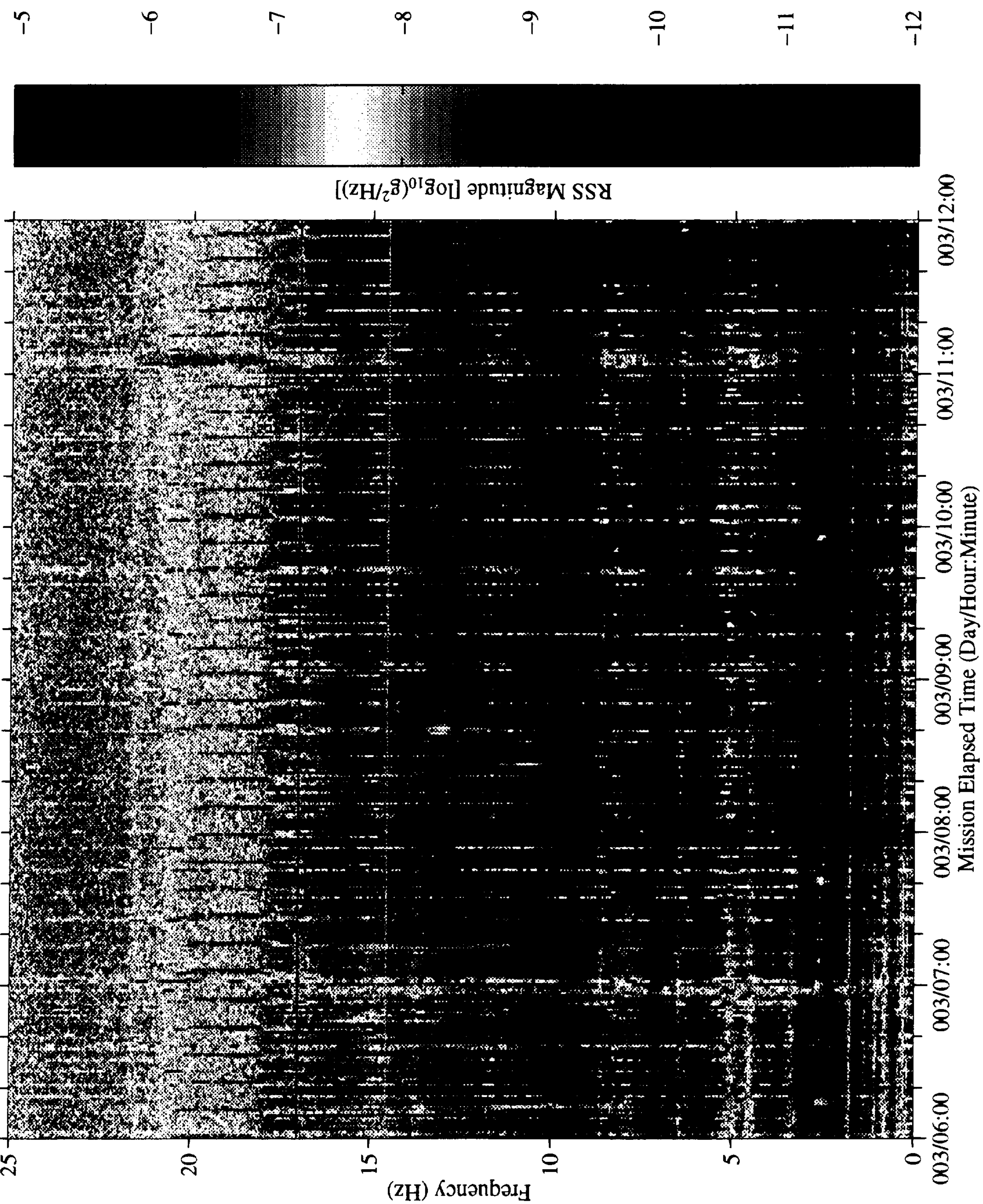

Figure 22: STS–79, Head C (fc=25 Hz)

Figure 23a: STS-79, Head C (fc=25 Hz), Ten Second Interval Average

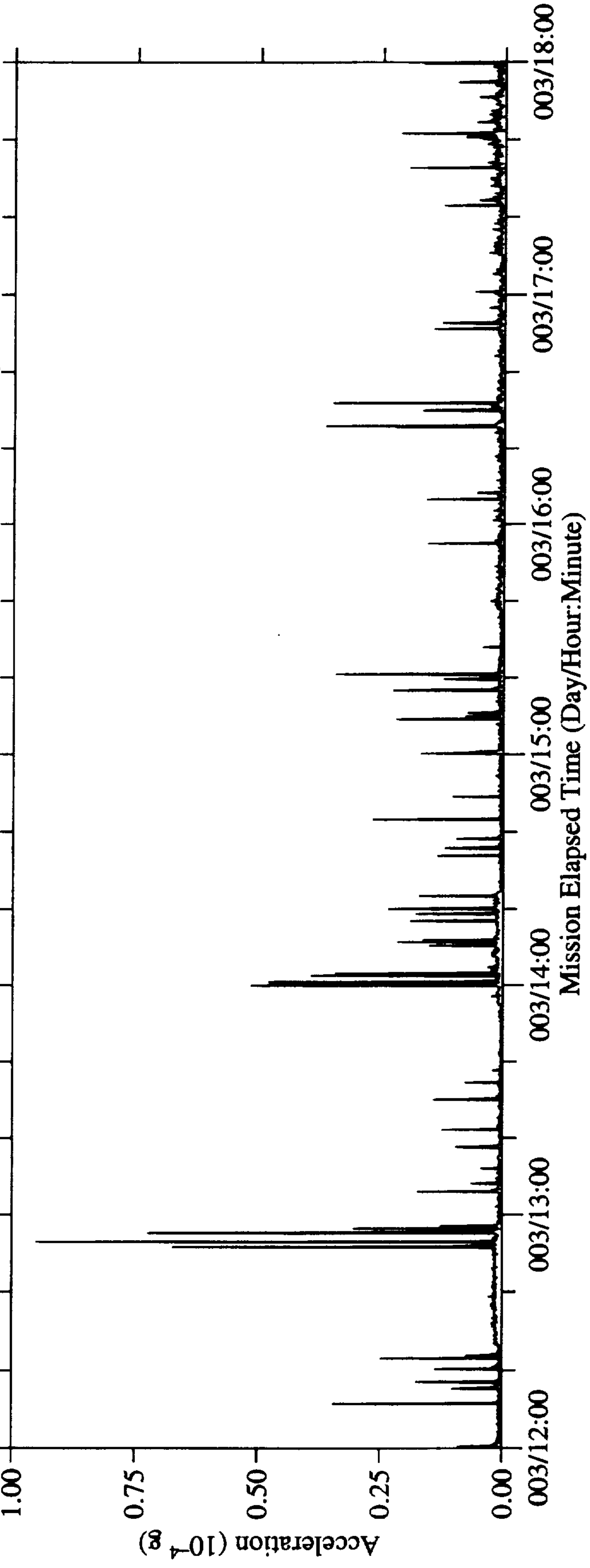

Figure 23b: STS-79, Head C (fc=25 Hz), Ten Second Interval RMS

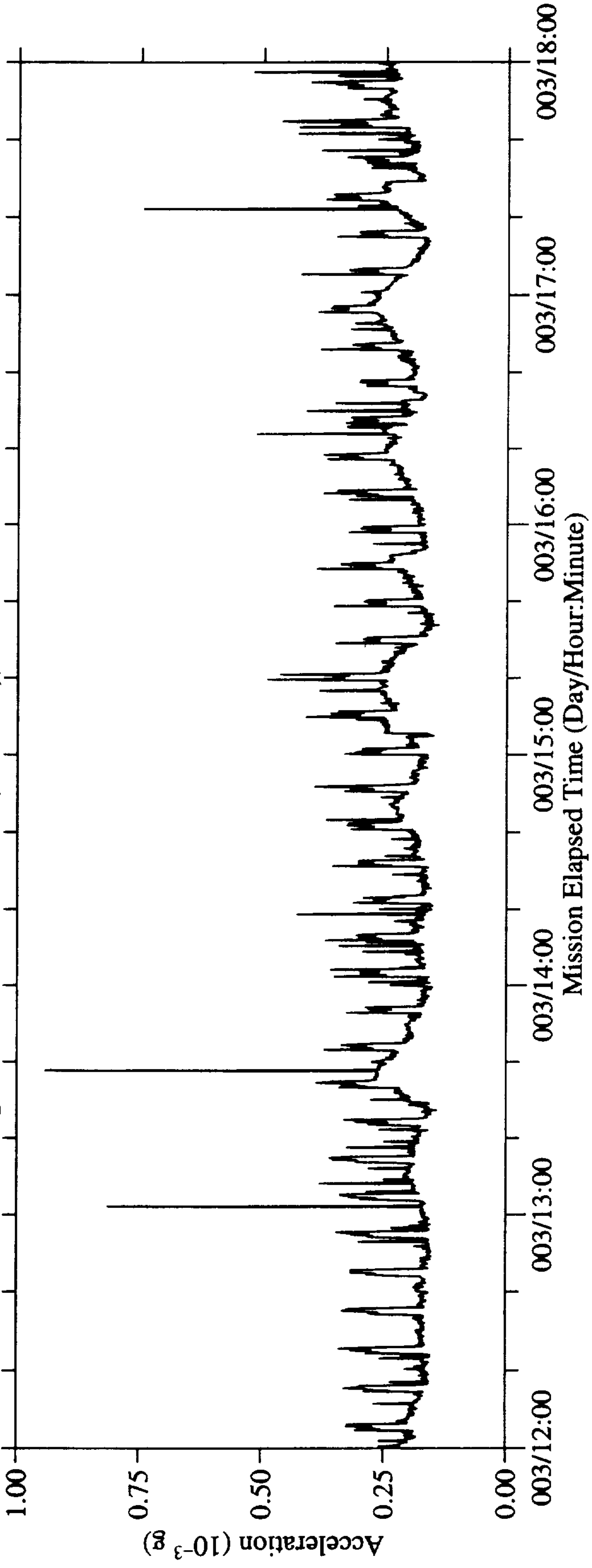

Figure 24: STS–79, Head C (fc=25 Hz)

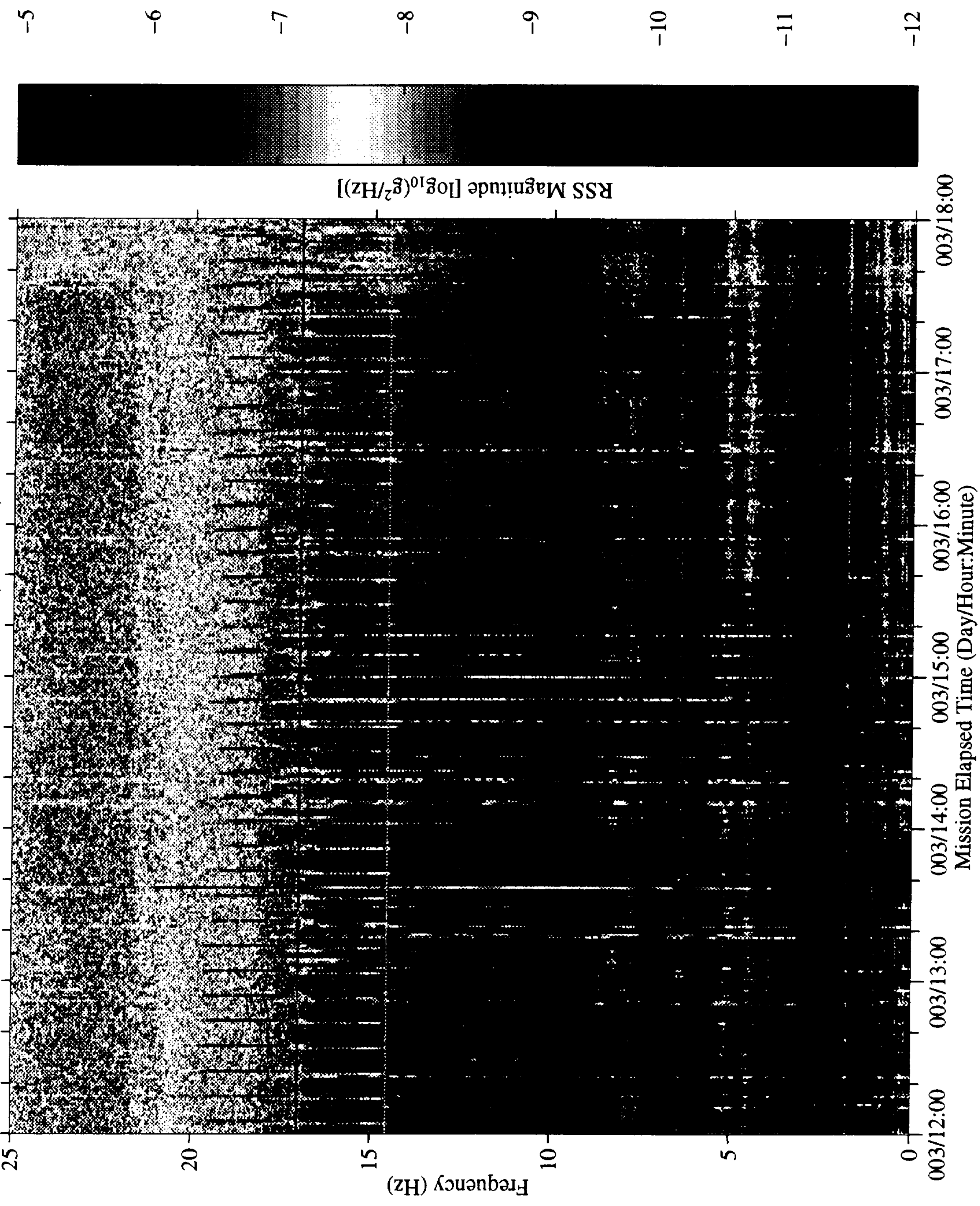

Figure 25a: STS–79, Head C (fc=25 Hz), Ten Second Interval Average

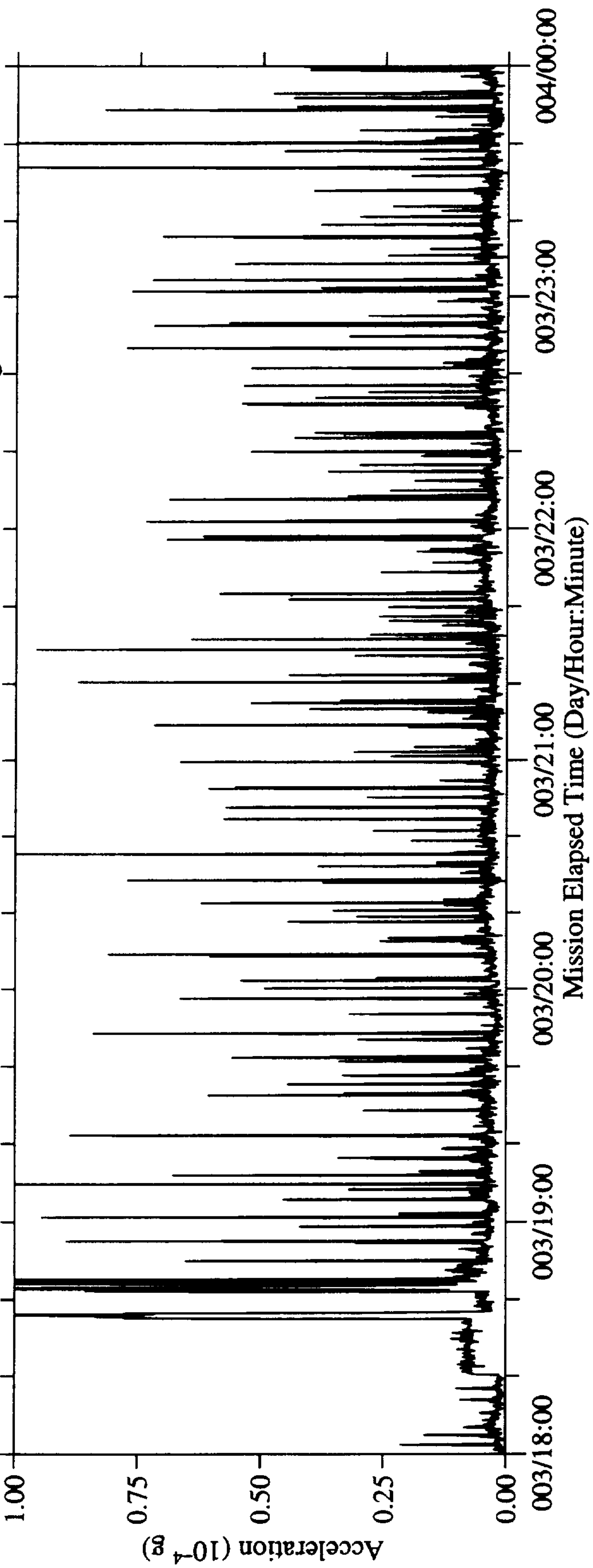

Figure 25b: STS–79, Head C (fc=25 Hz), Ten Second Interval RMS

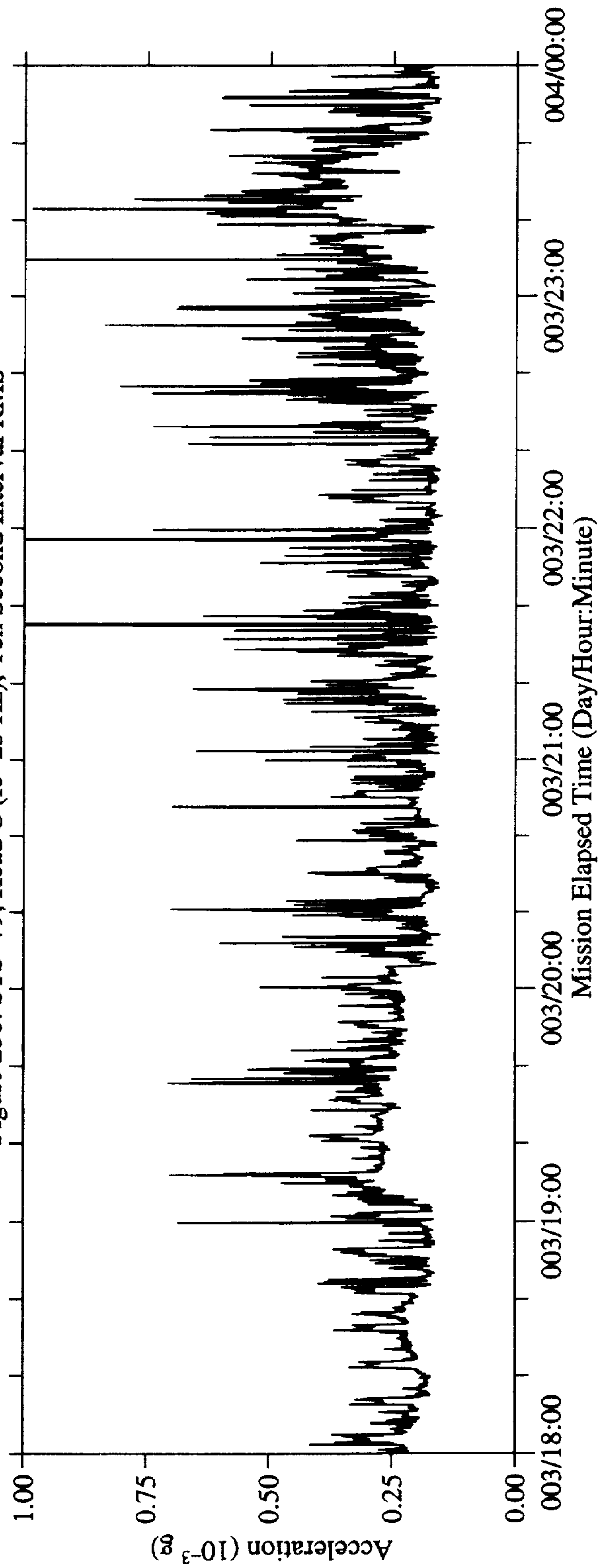

Figure 26: STS–79, Head C (fc=25 Hz)

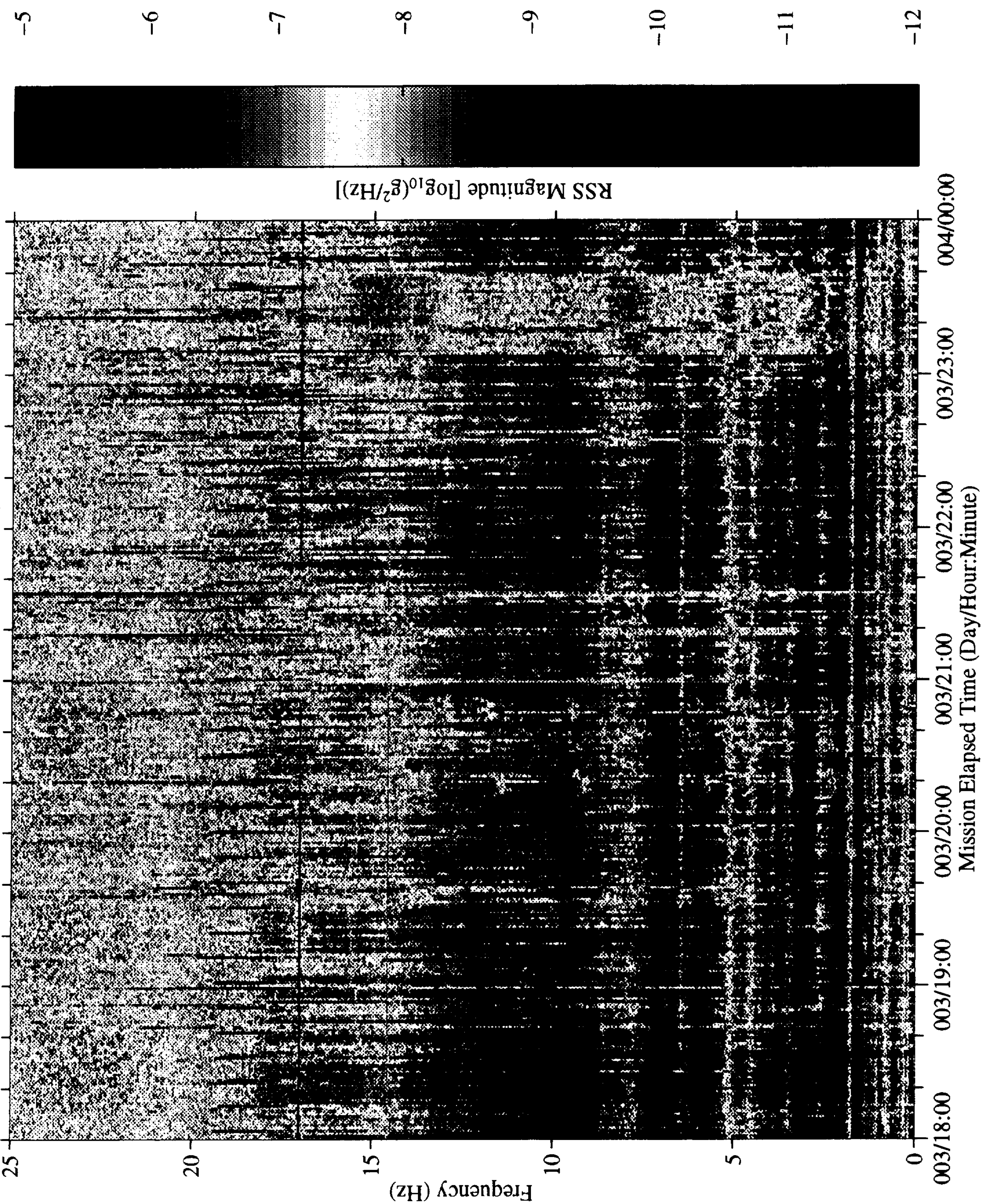

Figure 27a: STS−79, Head C (fc=25 Hz), Ten Second Interval Average

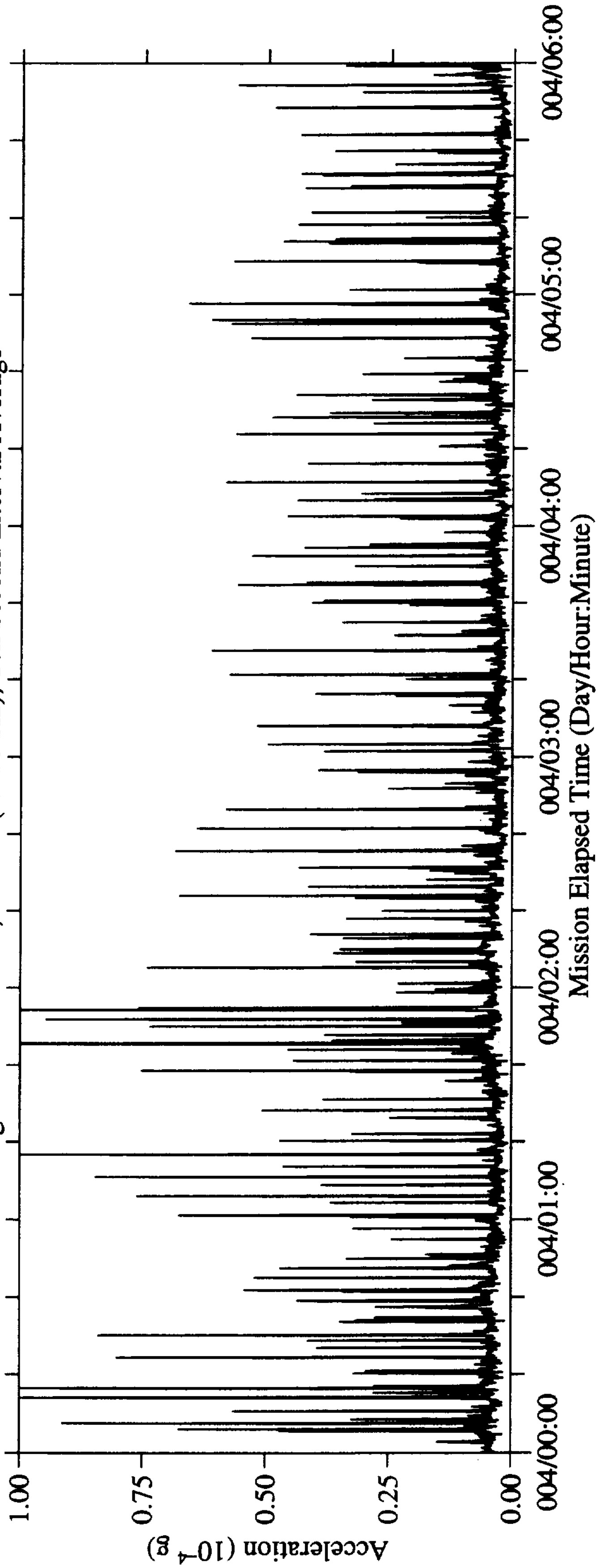

Figure 27b: STS−79, Head C (fc=25 Hz), Ten Second Interval RMS

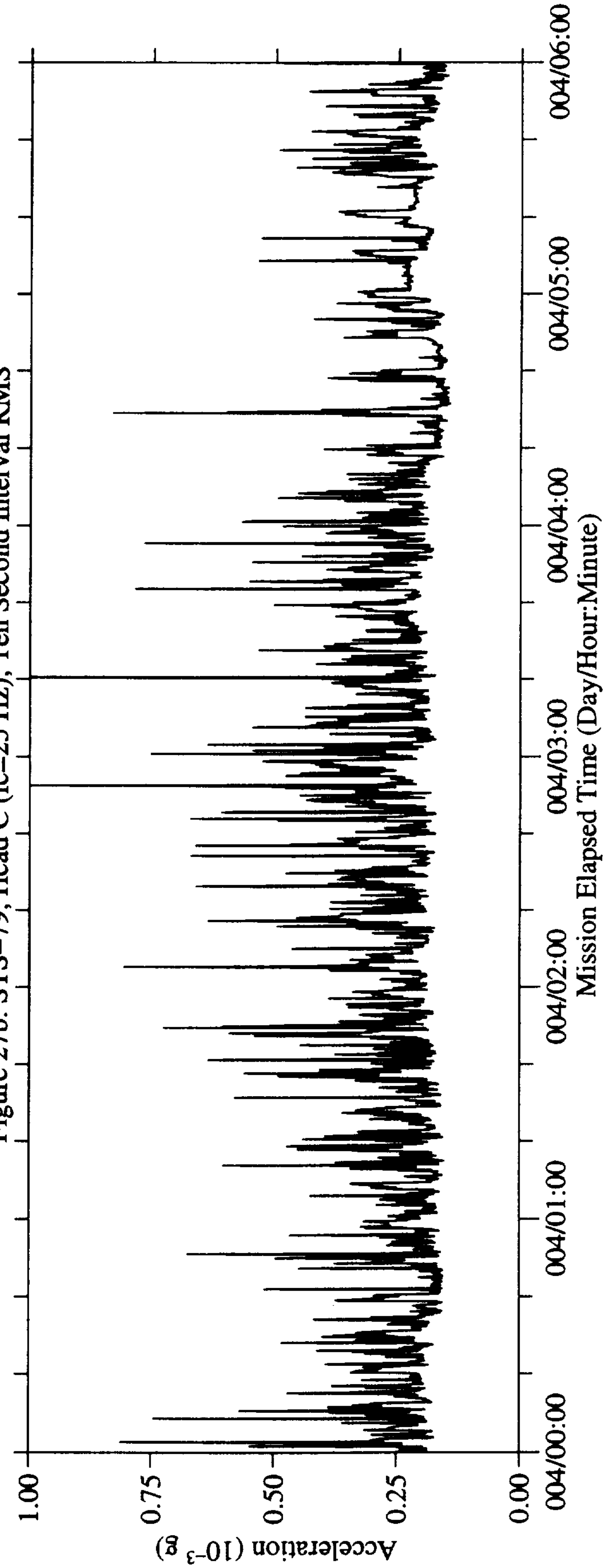

Figure 28: STS-79, Head C (fc=25 Hz)

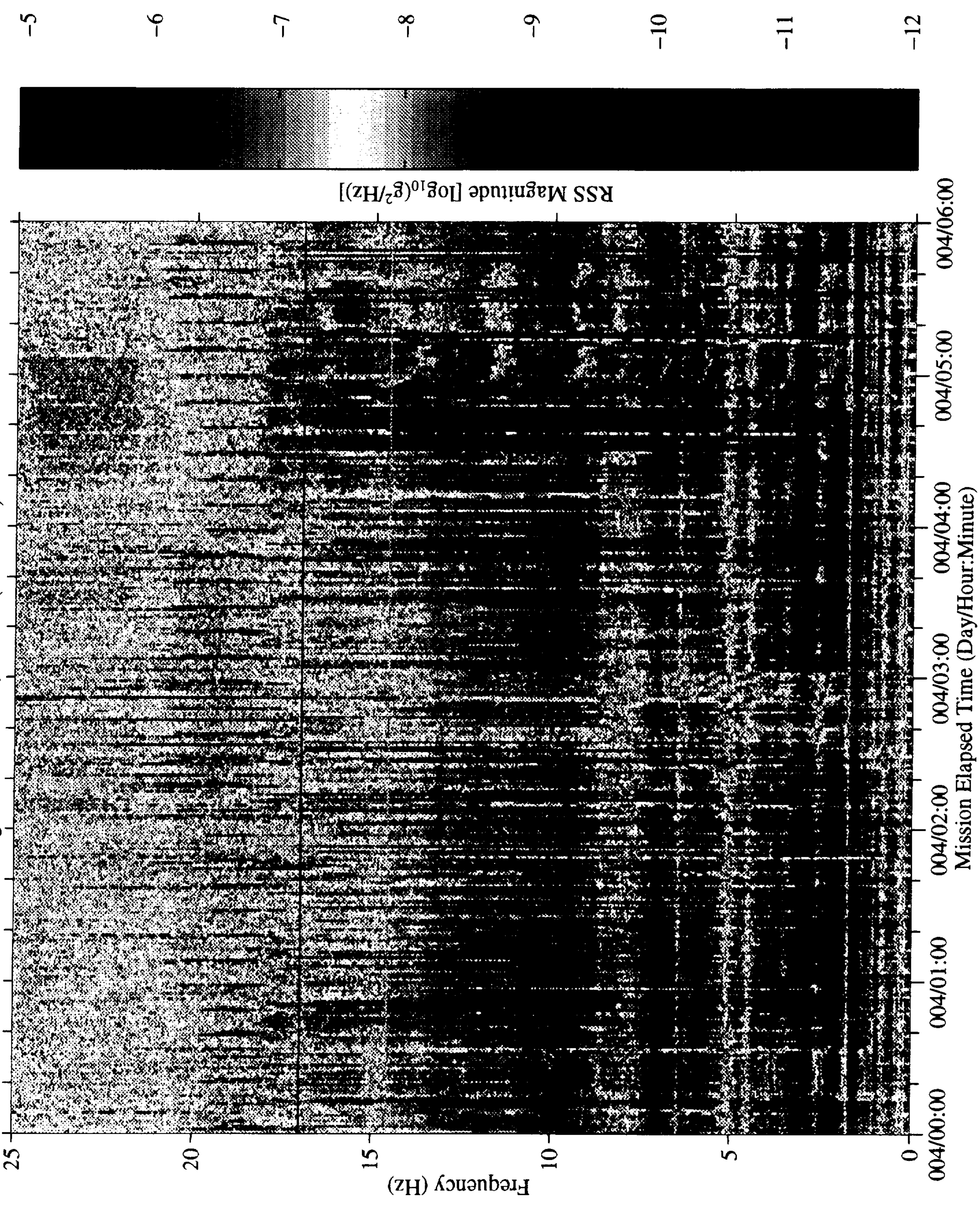

Figure 29a: STS–79, Head C (fc=25 Hz), Ten Second Interval Average

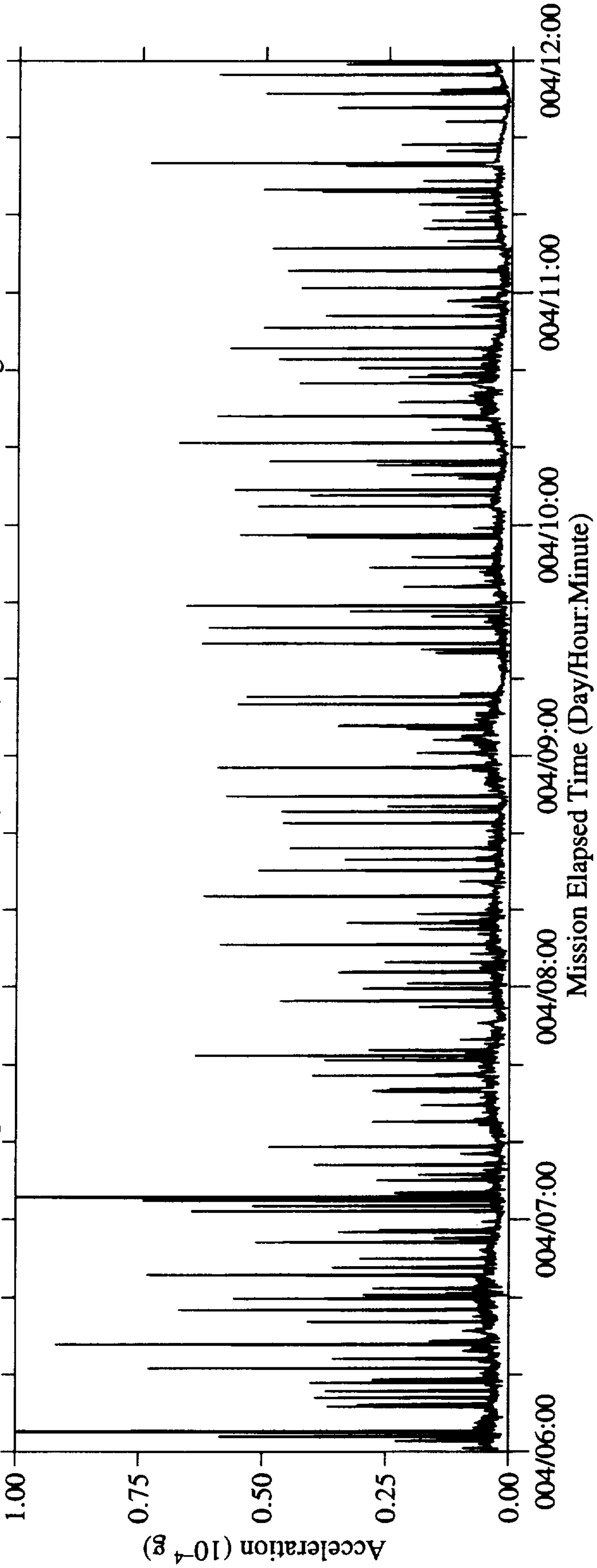

Figure 29b: STS–79, Head C (fc=25 Hz), Ten Second Interval RMS

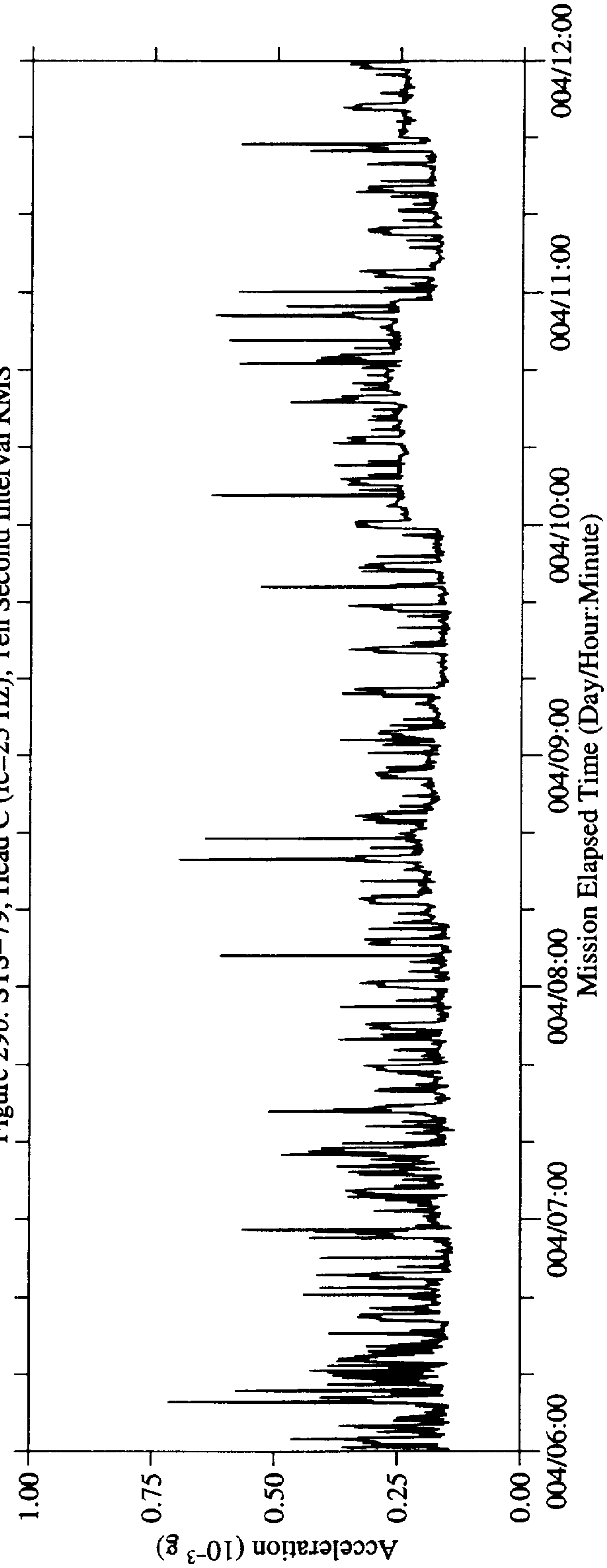

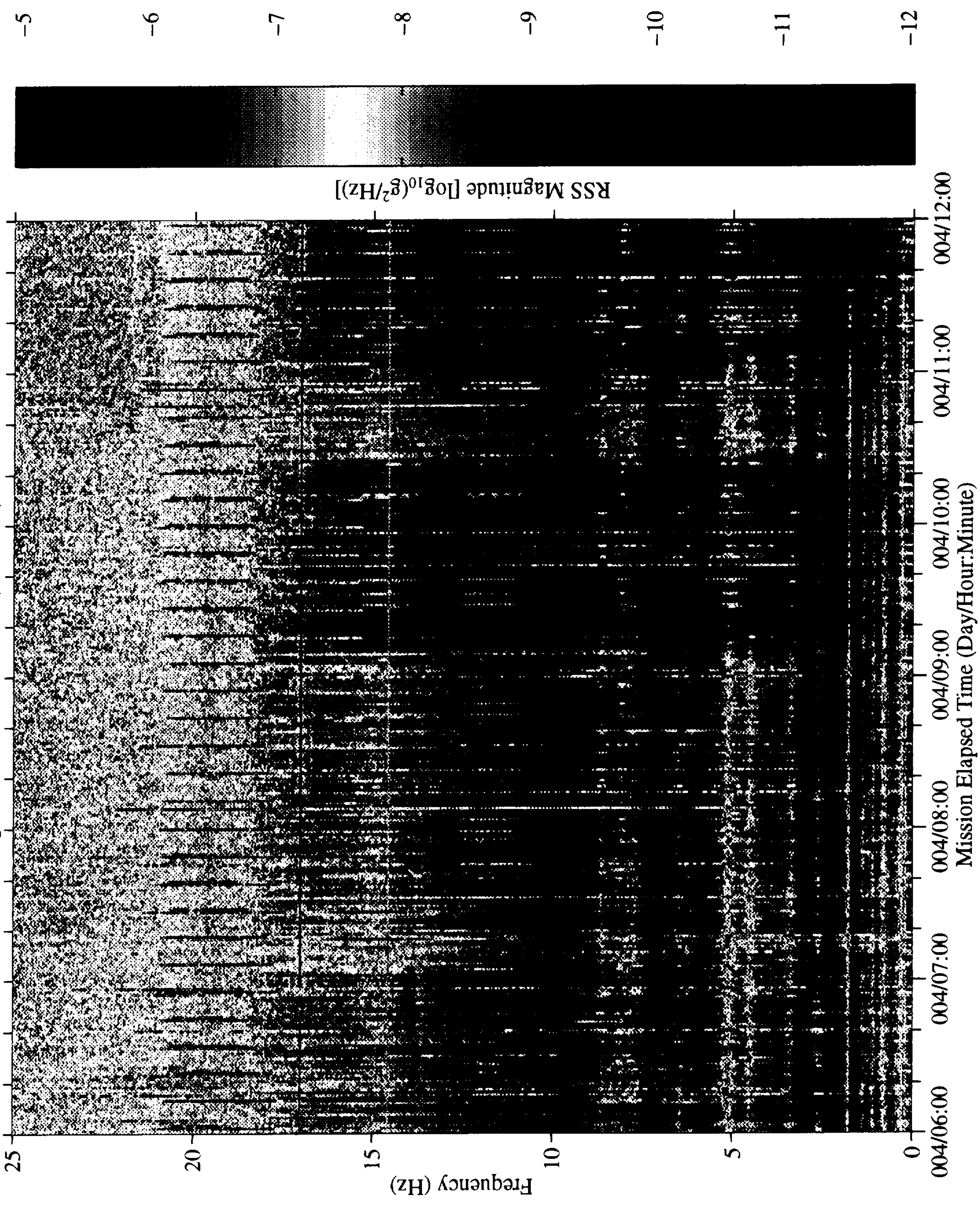

Figure 30: STS–79, Head C (fc=25 Hz)

Figure 31a: STS–79, Head C (fc=25 Hz), Ten Second Interval Average

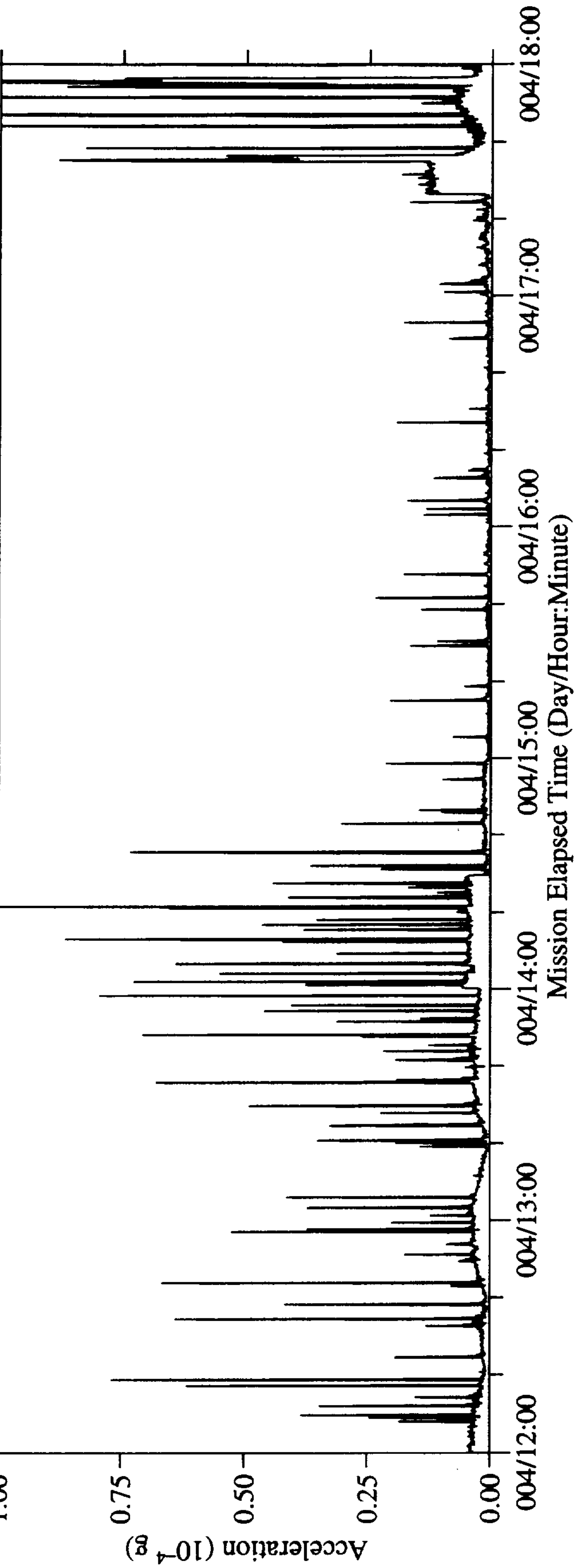

Figure 31b: STS–79, Head C (fc=25 Hz), Ten Second Interval RMS

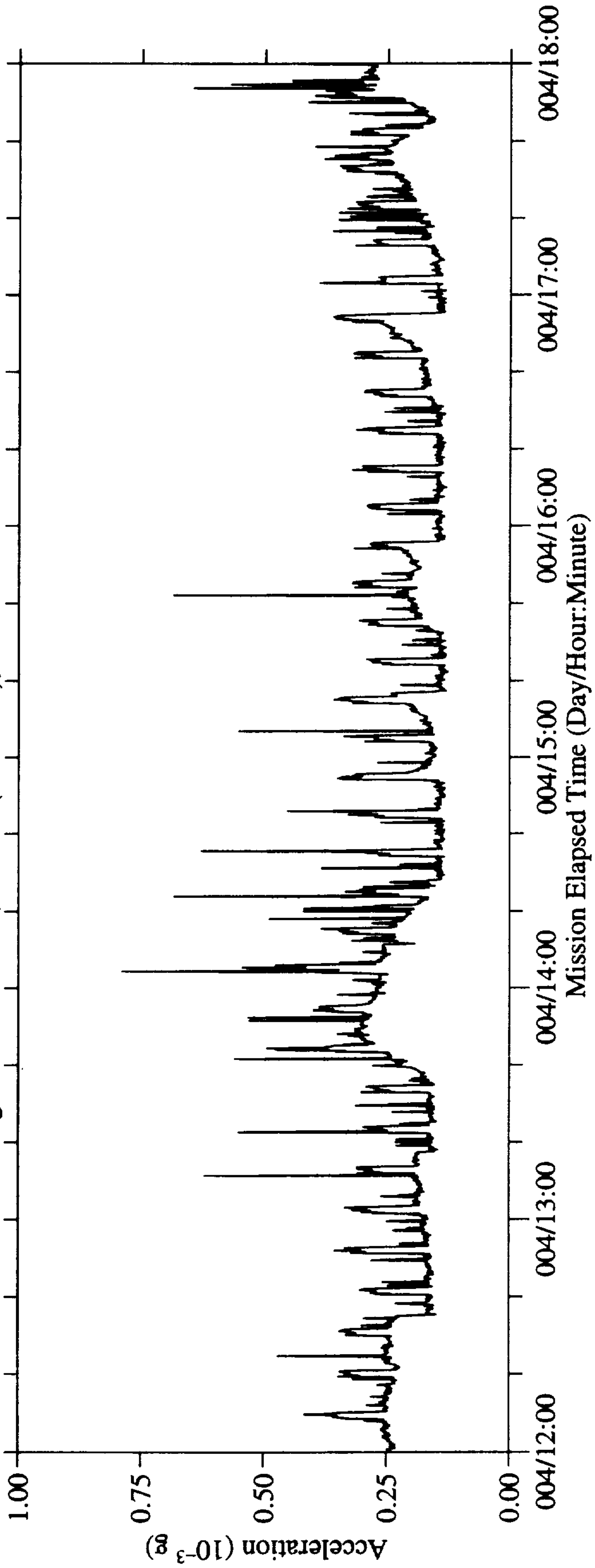

Figure 32: STS-79, Head C (fc=25 Hz)

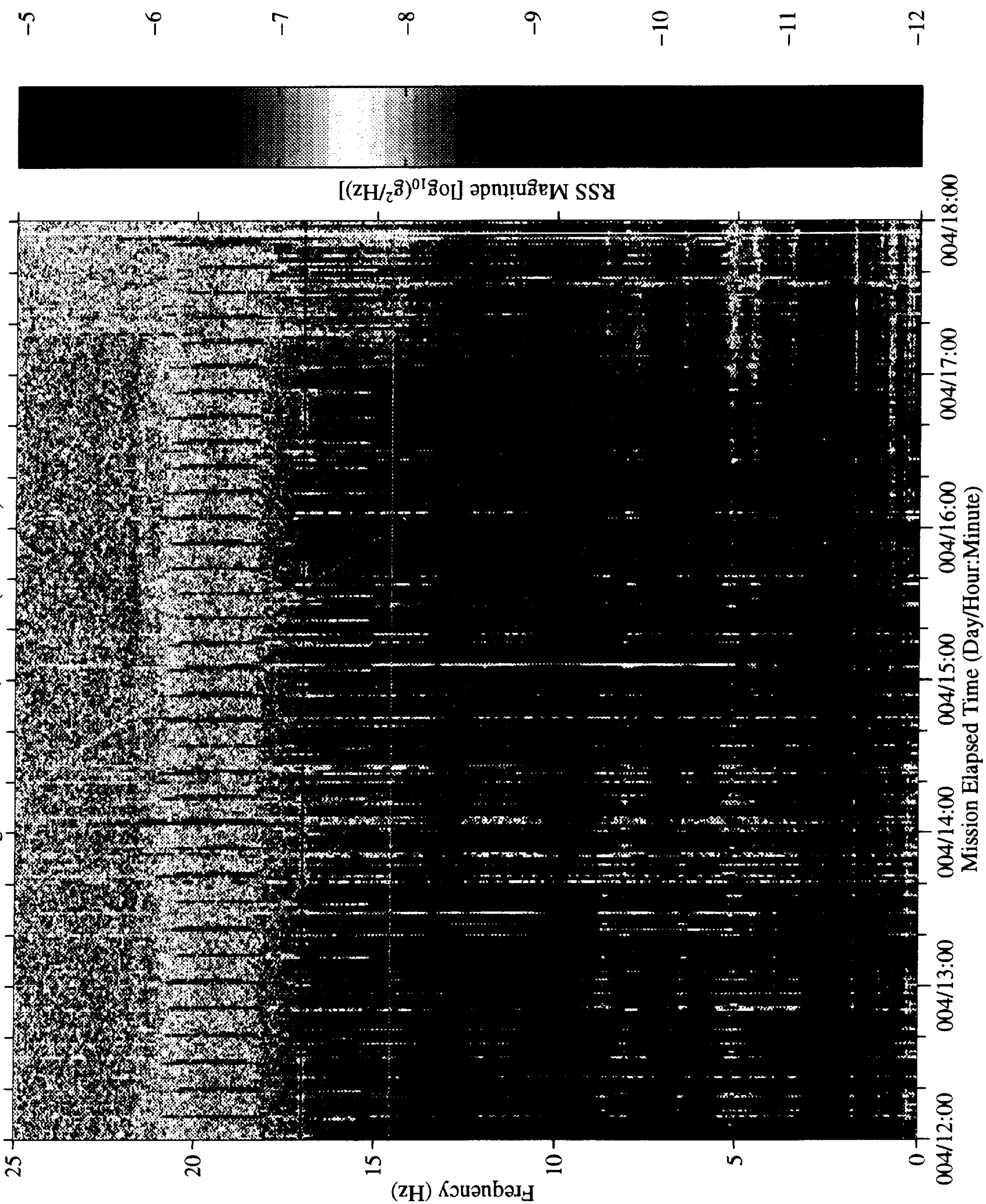

Figure 33a: STS–79, Head C (fc=25 Hz), Ten Second Interval Average

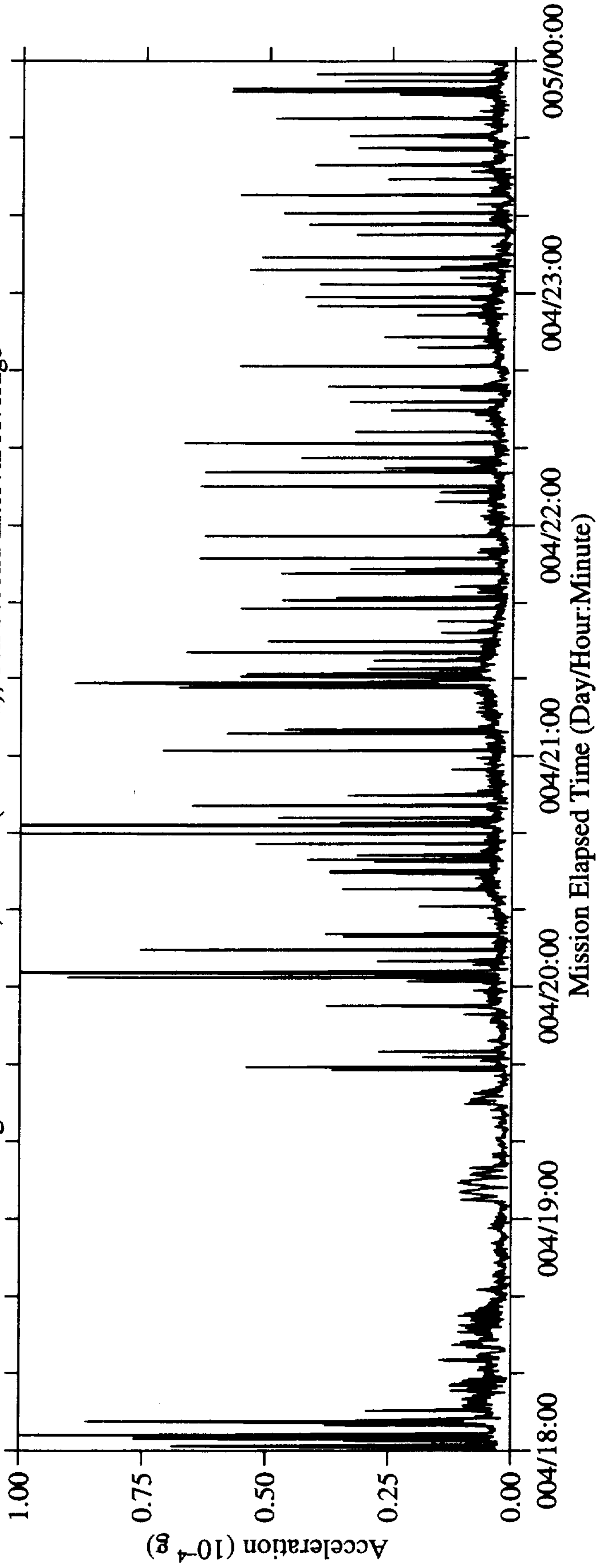

Figure 33b: STS–79, Head C (fc=25 Hz), Ten Second Interval RMS

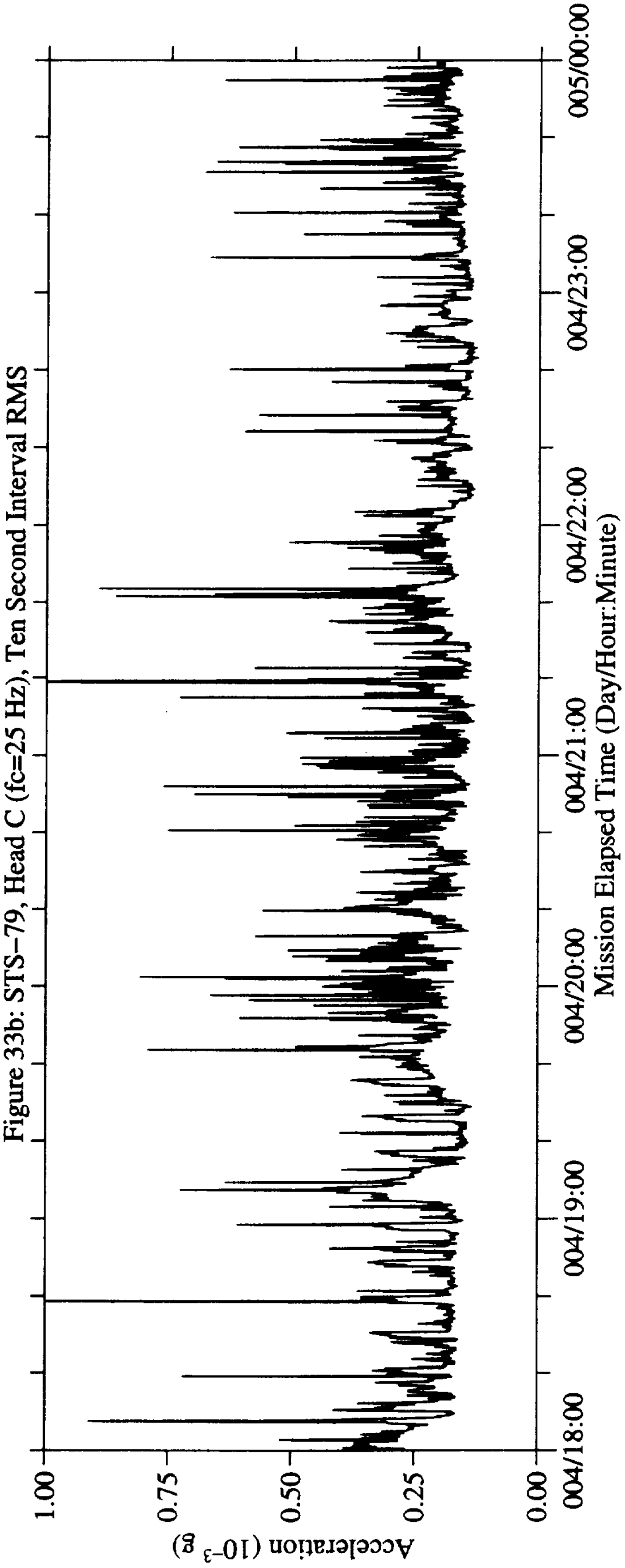

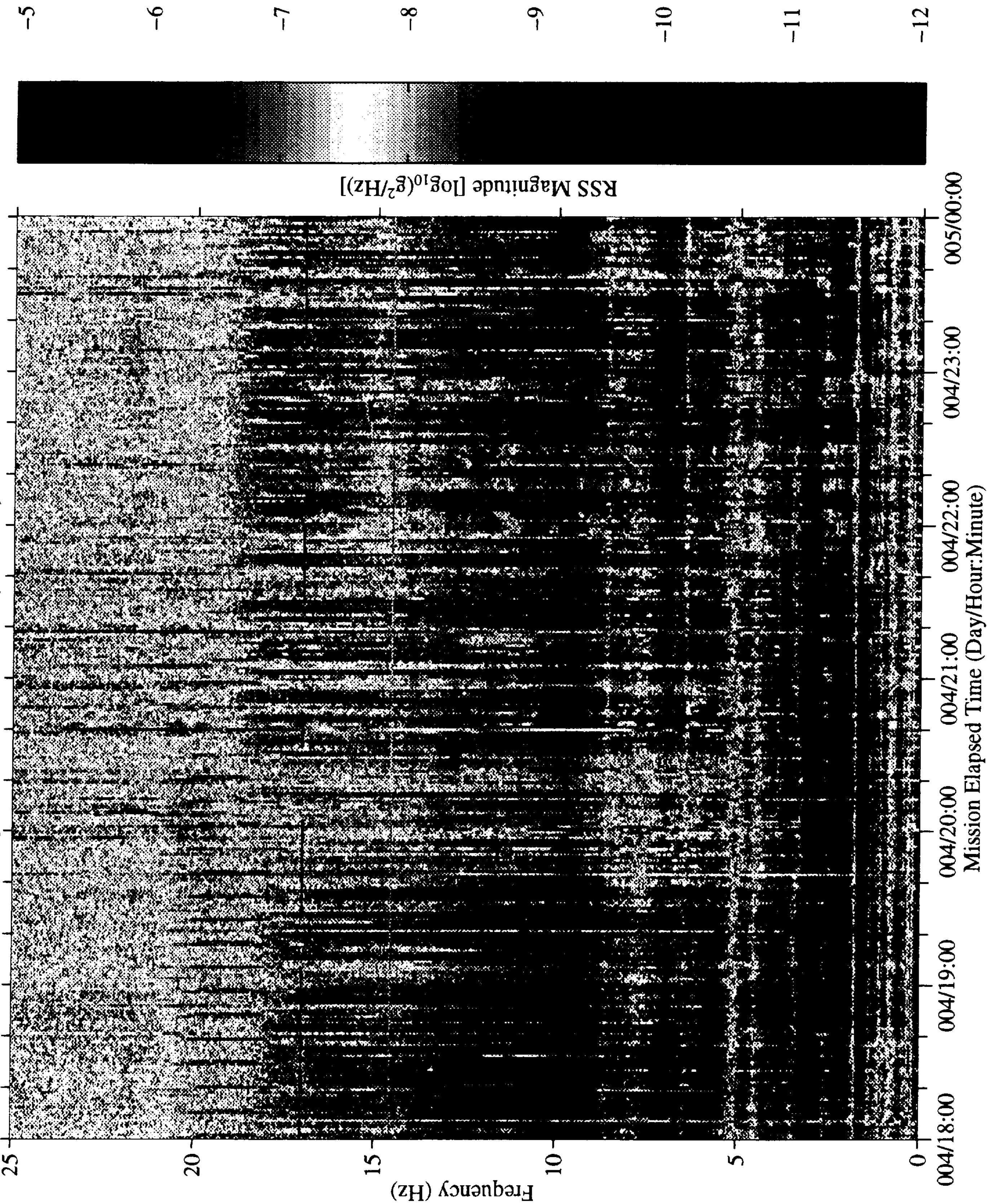

Figure 34: STS–79, Head C (fc=25 Hz)

Figure 35a: STS-79, Head C (fc=25 Hz), Ten Second Interval Average

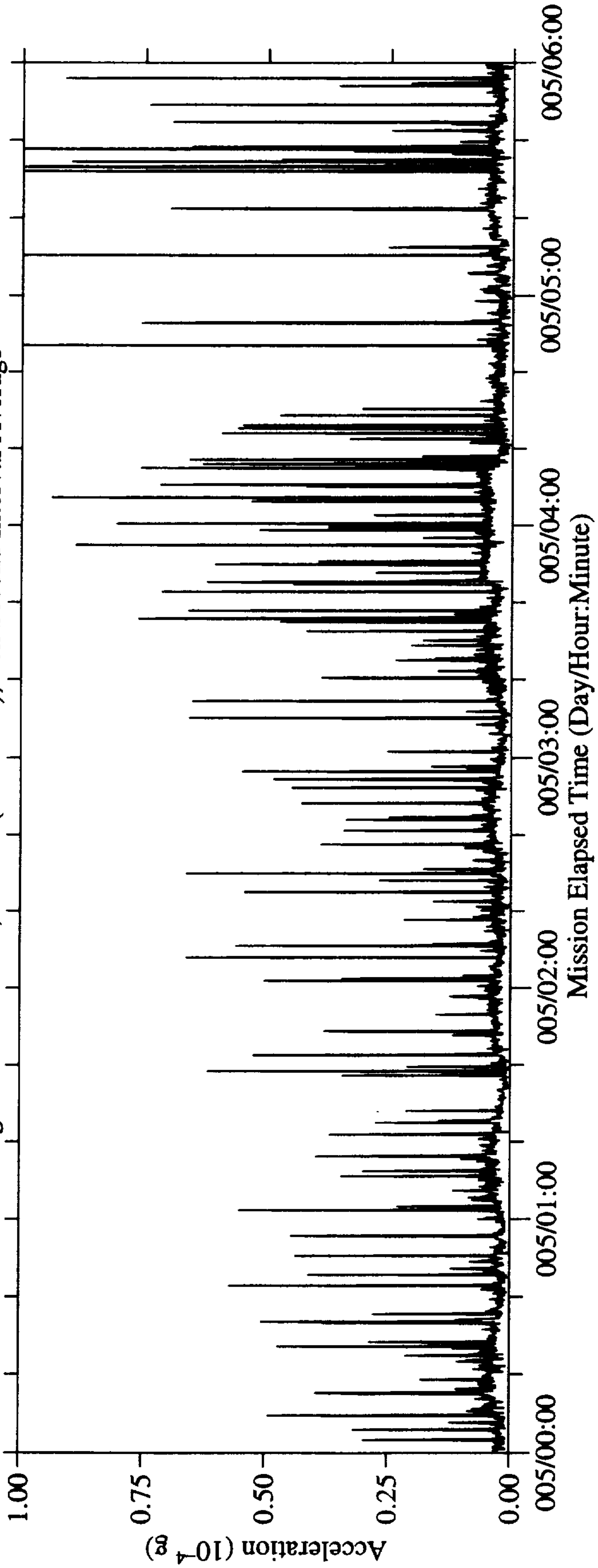

Figure 35b: STS-79, Head C (fc=25 Hz), Ten Second Interval RMS

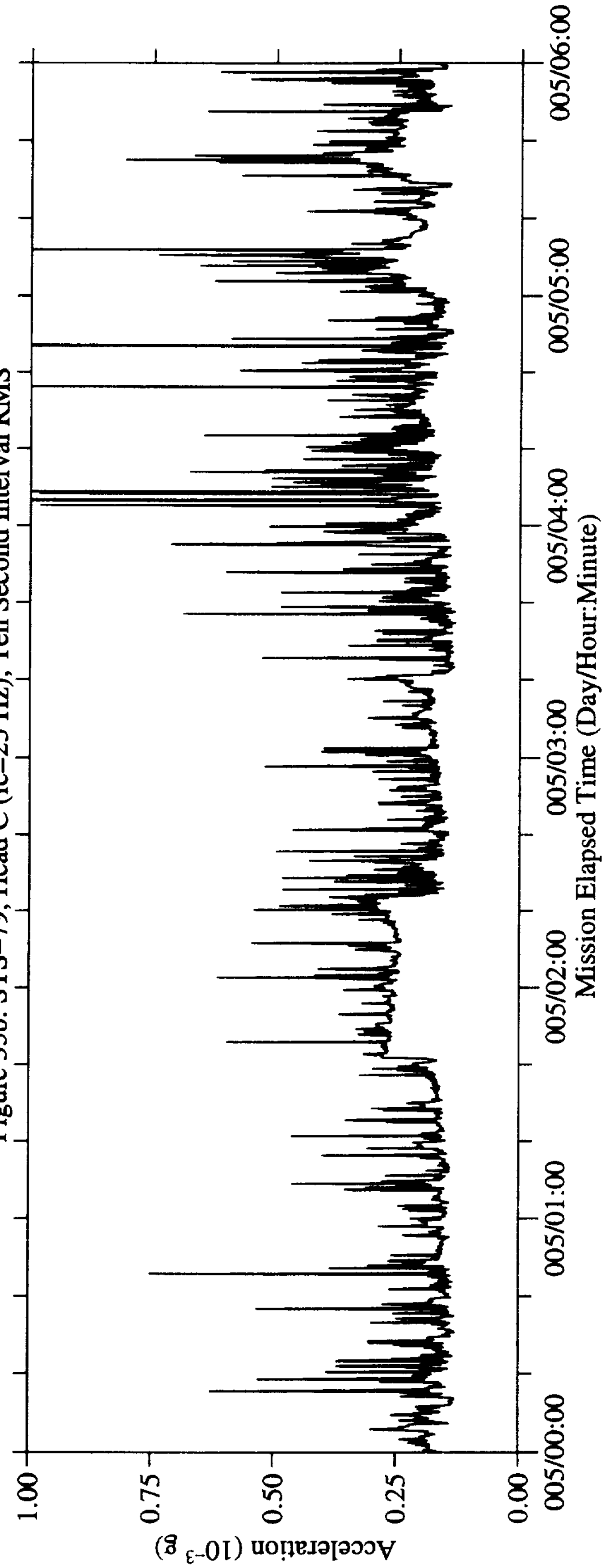

Figure 36: STS-79, Head C (fc=25 Hz)

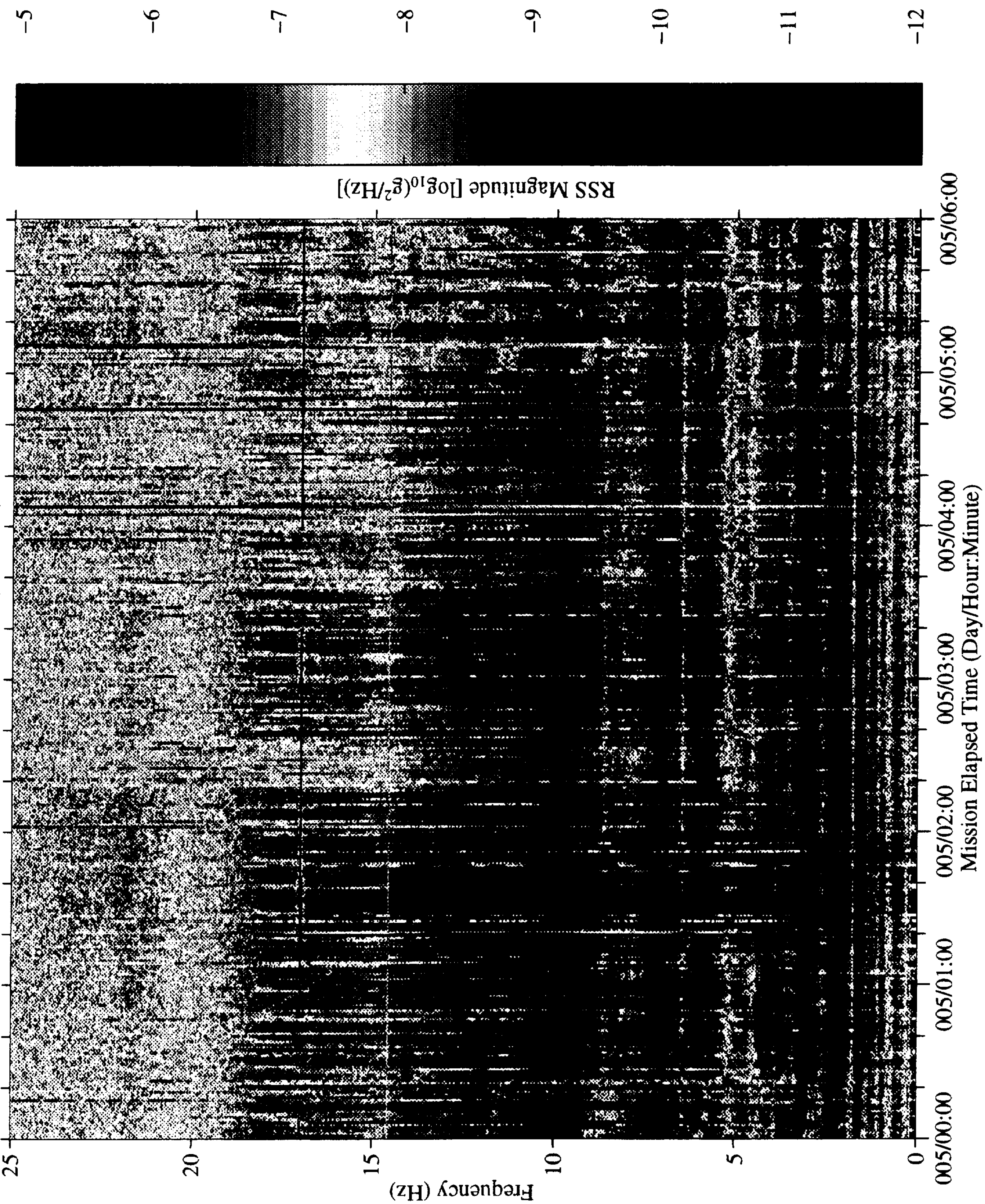

Figure 37a: STS-79, Head C (fc=25 Hz), Ten Second Interval Average

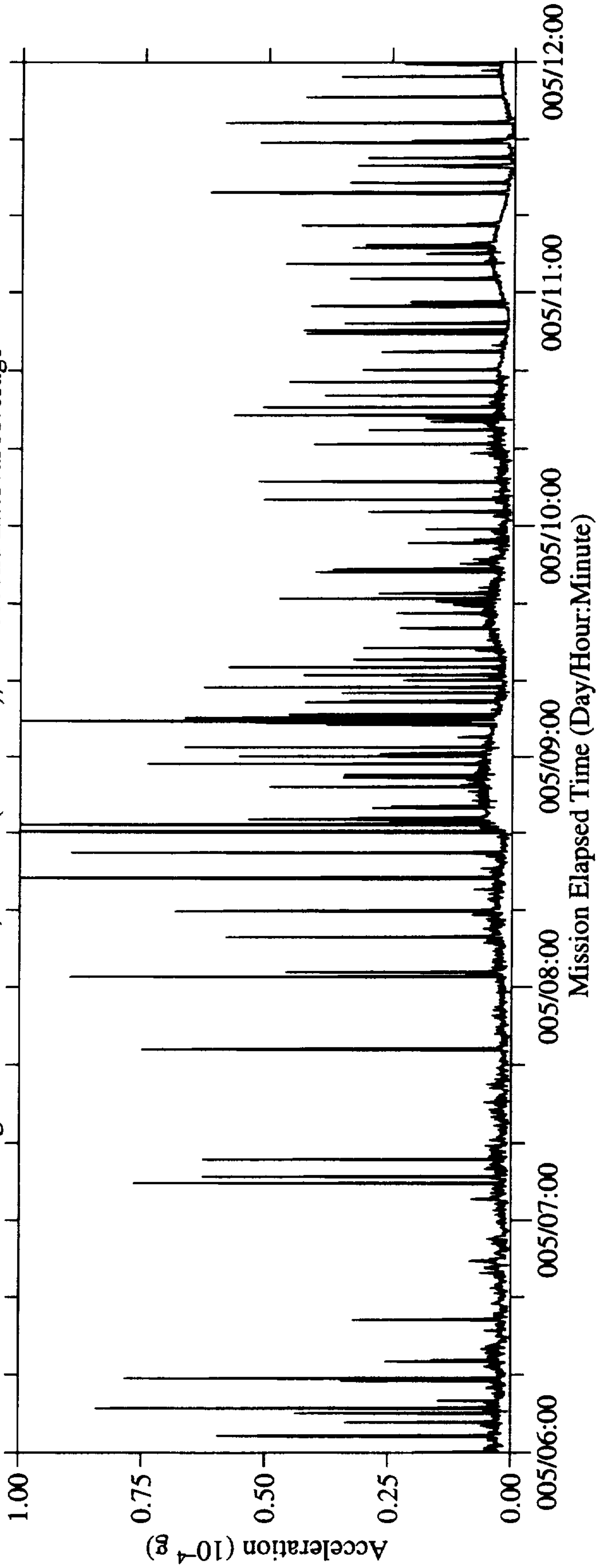

Figure 37b: STS-79, Head C (fc=25 Hz), Ten Second Interval RMS

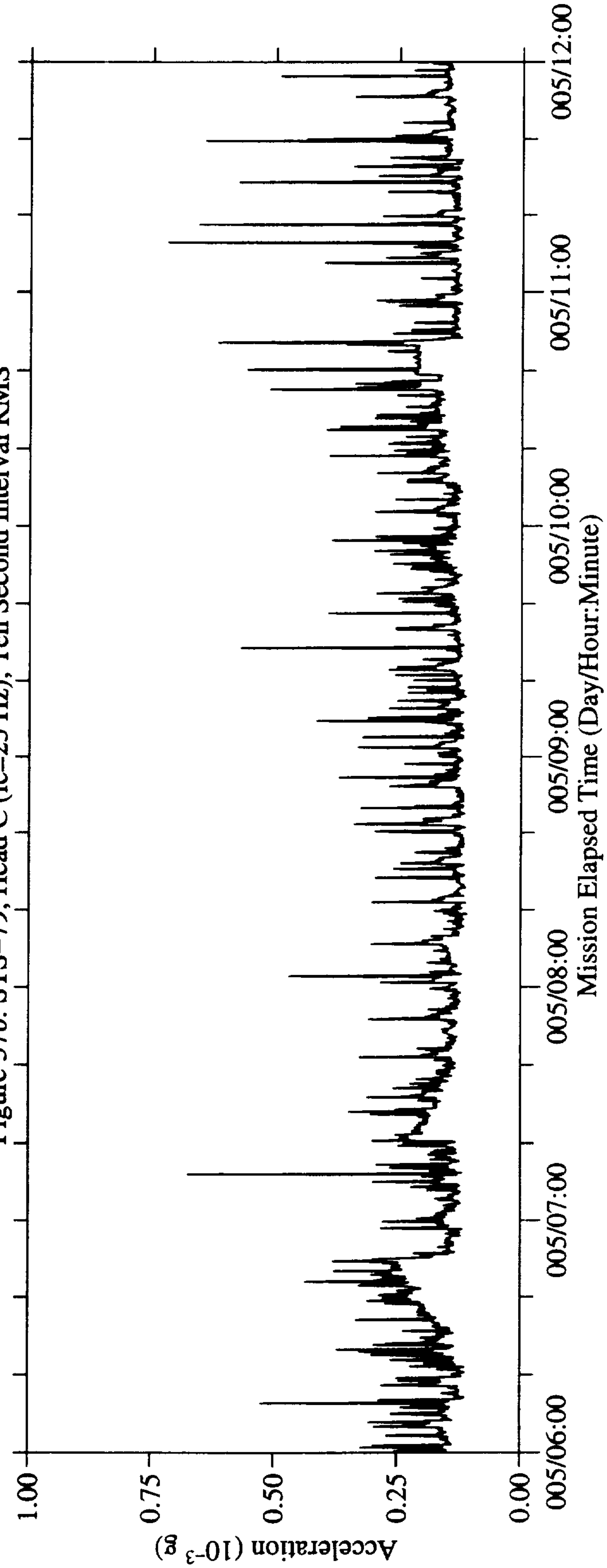

Figure 38: STS–79, Head C (fc=25 Hz)

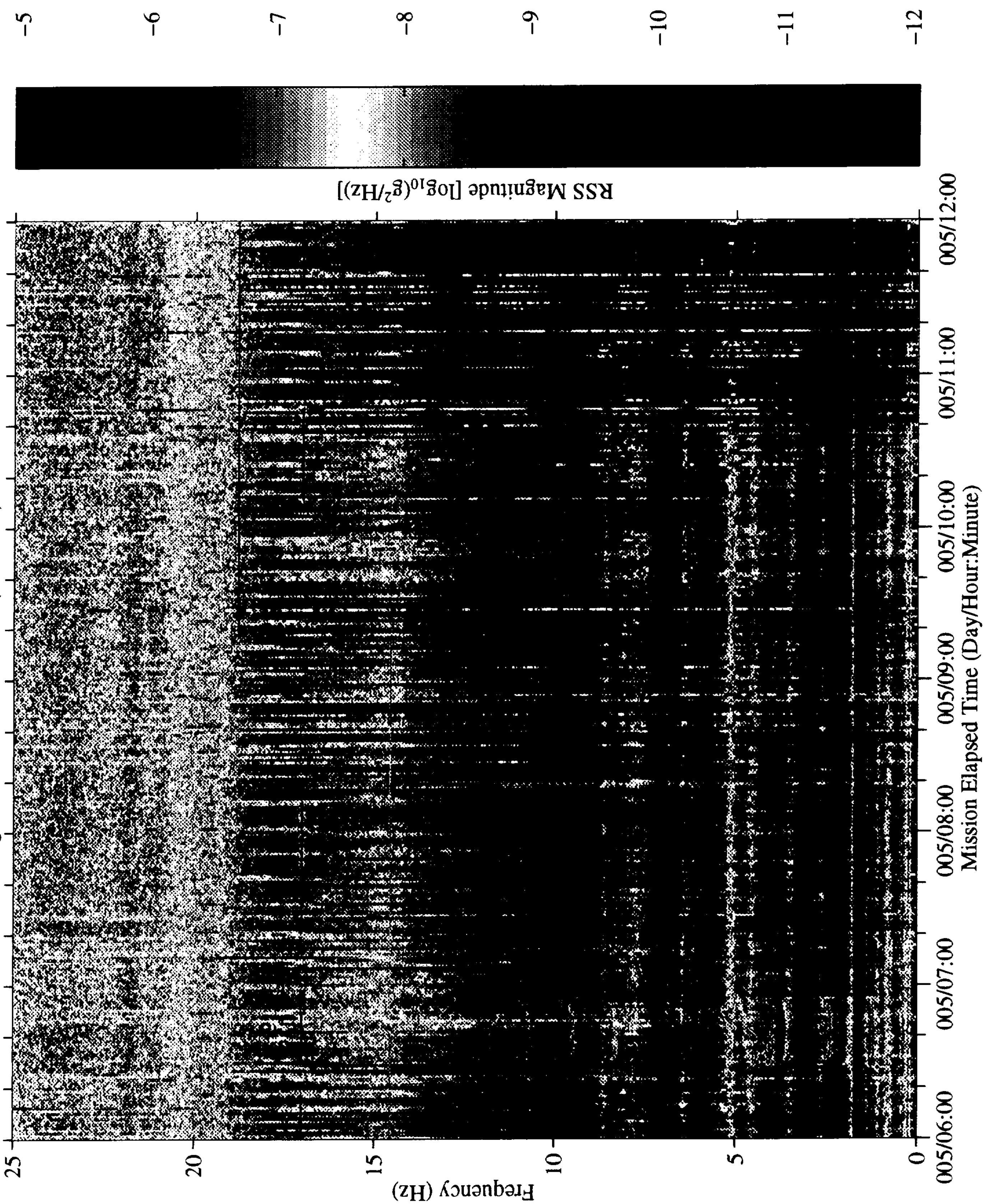

Figure 39a: STS-79, Head C (fc=25 Hz), Ten Second Interval Average

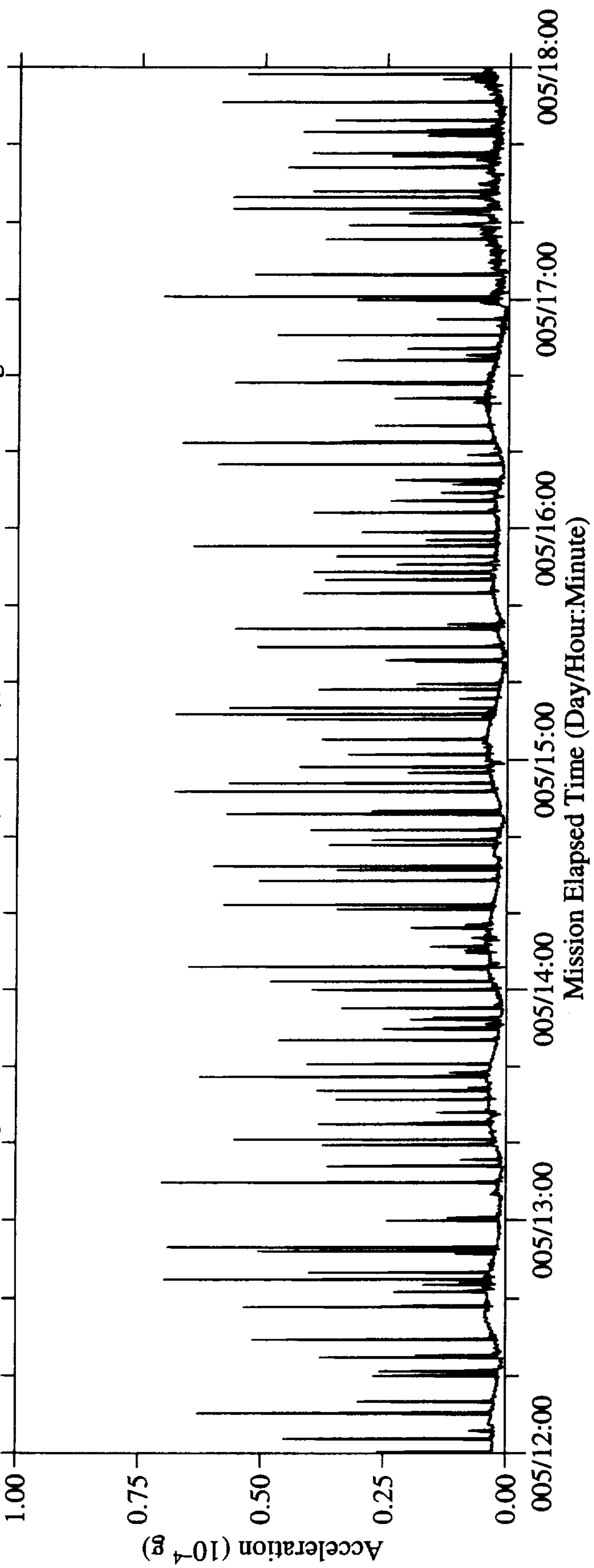

Figure 39b: STS-79, Head C (fc=25 Hz), Ten Second Interval RMS

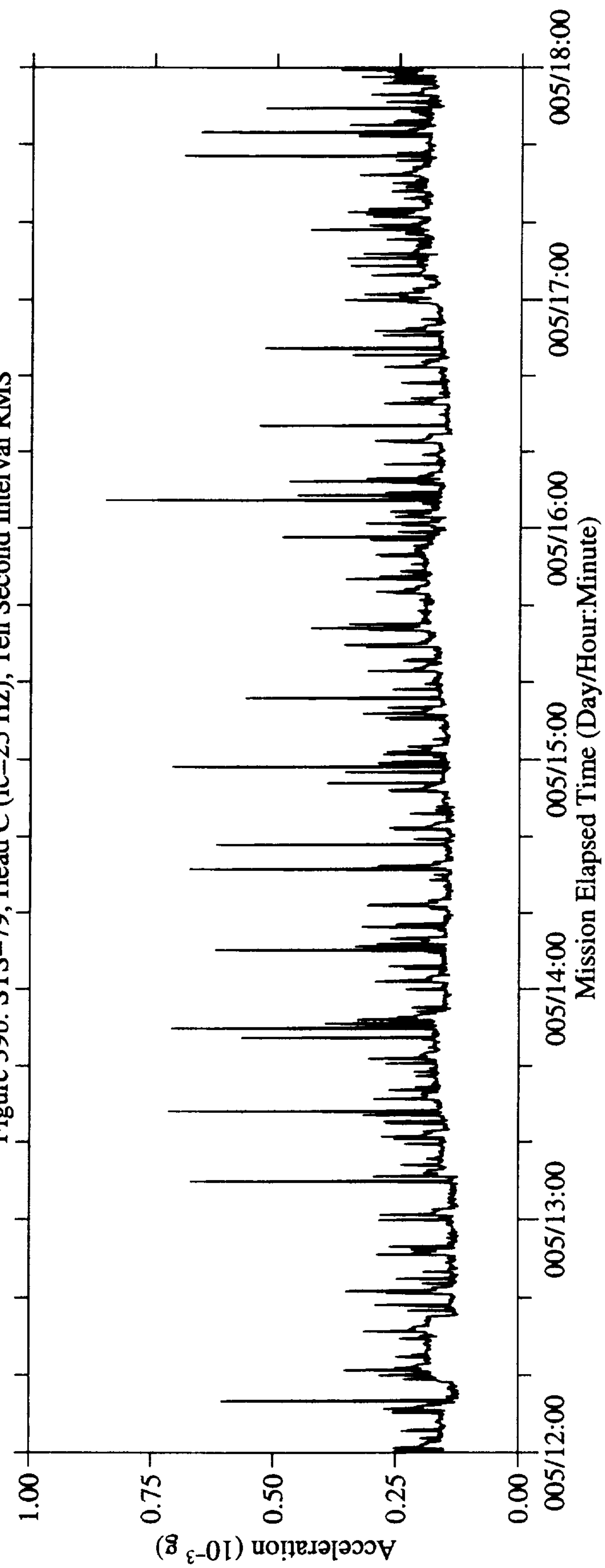

Figure 40: STS-79, Head C (fc=25 Hz)

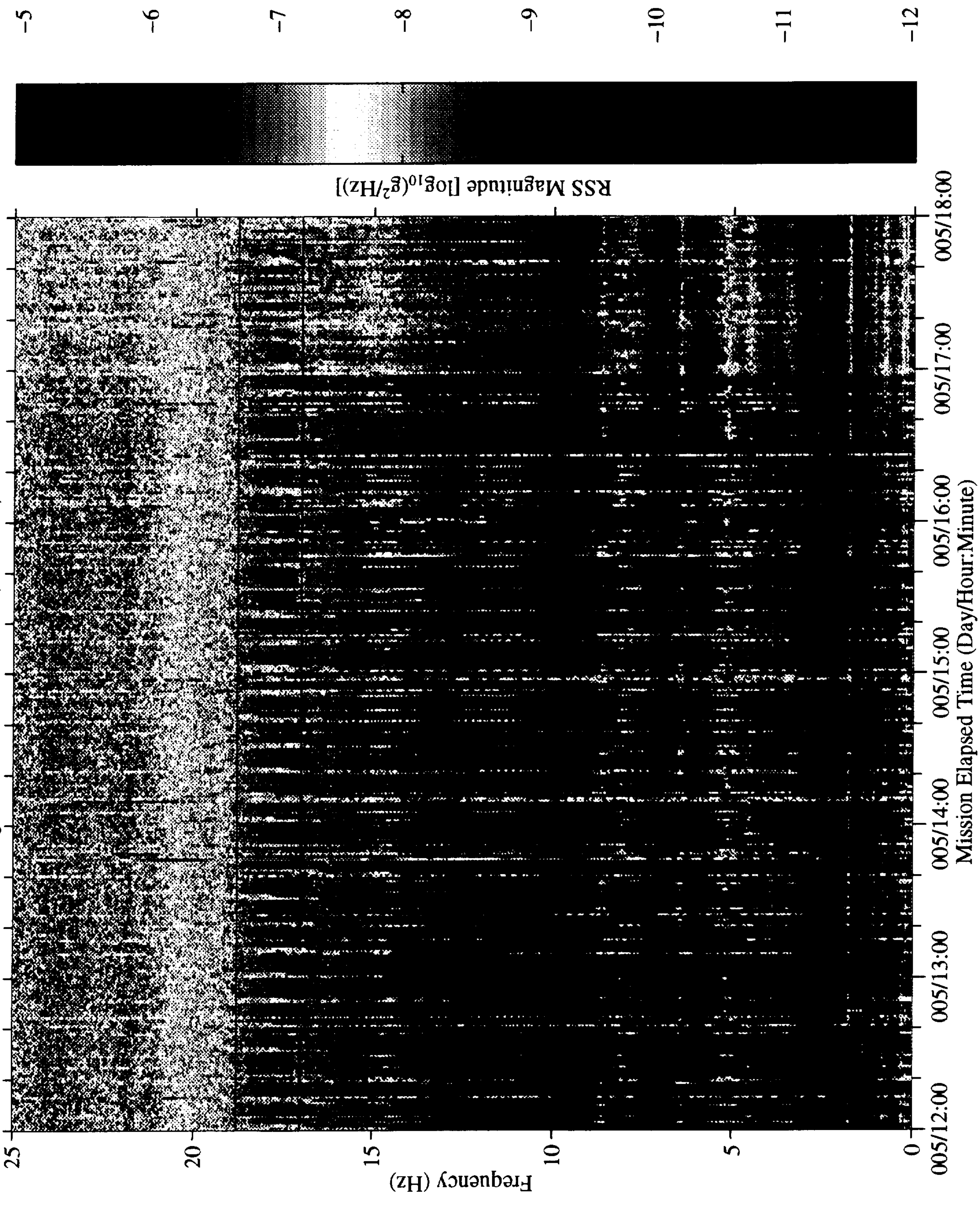

Figure 41a: STS−79, Head C (fc=25 Hz), Ten Second Interval Average

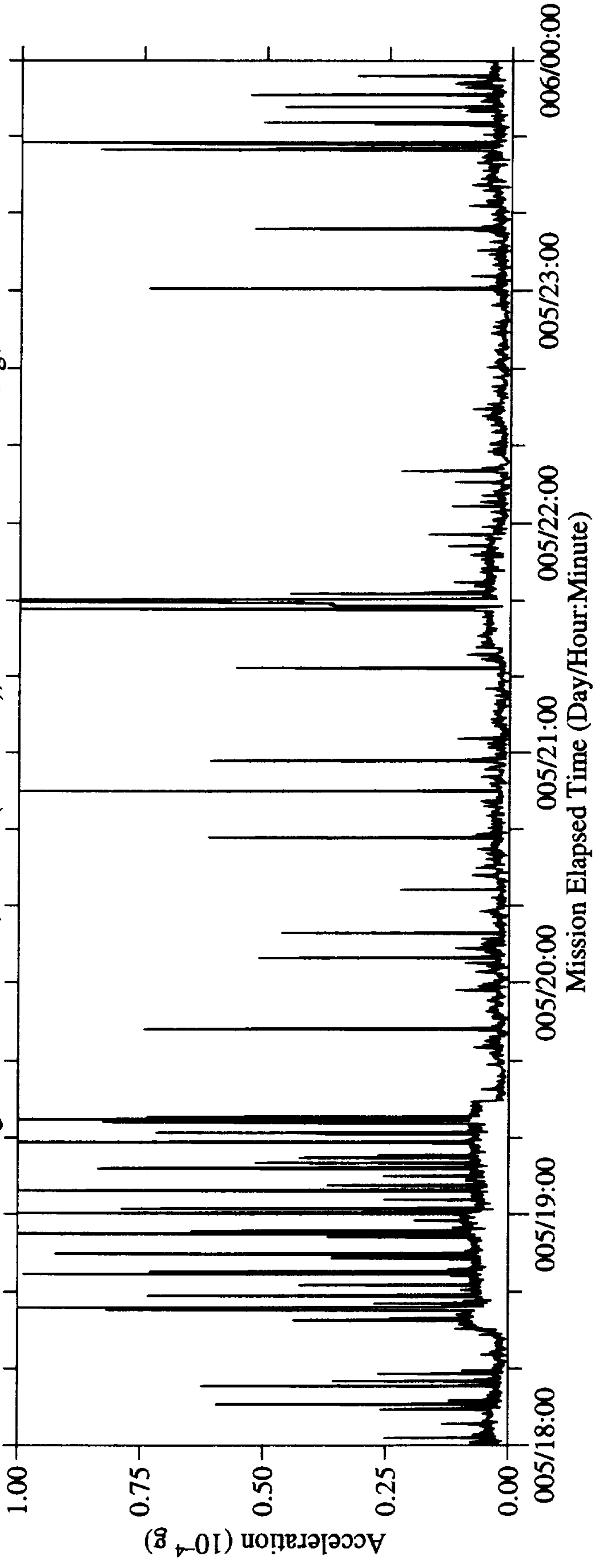

Figure 41b: STS−79, Head C (fc=25 Hz), Ten Second Interval RMS

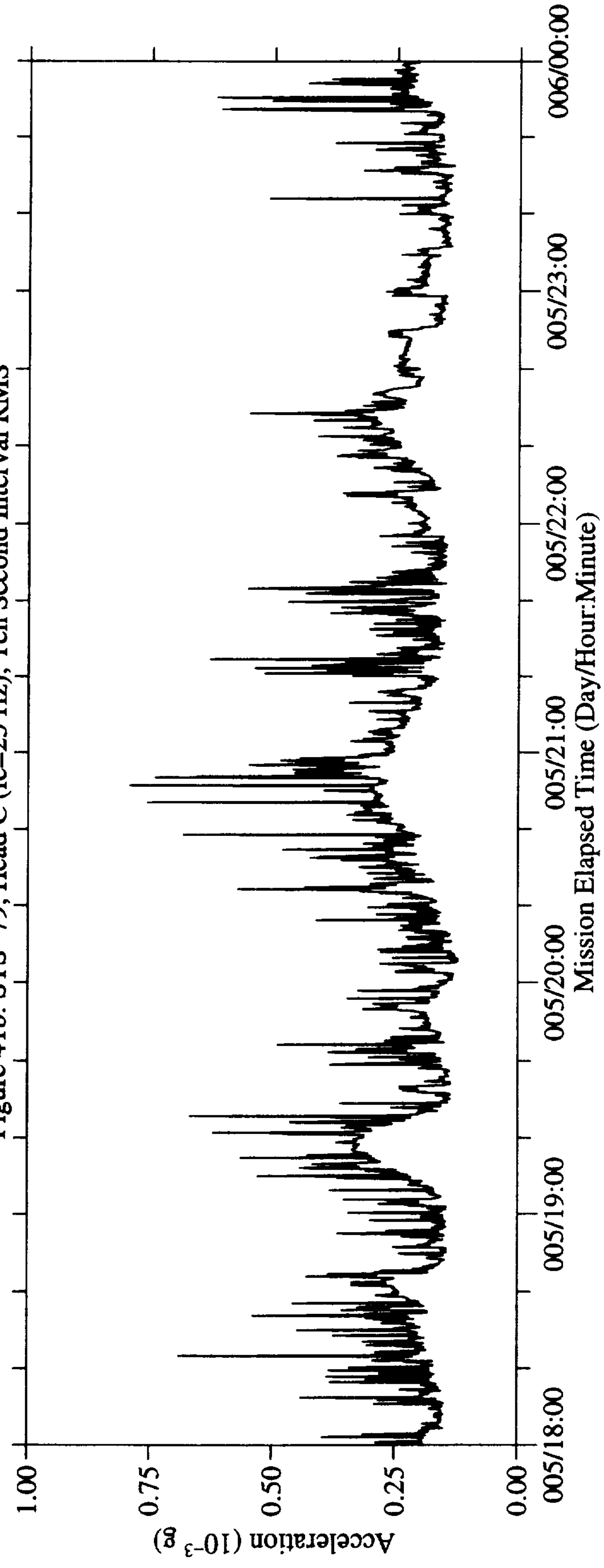

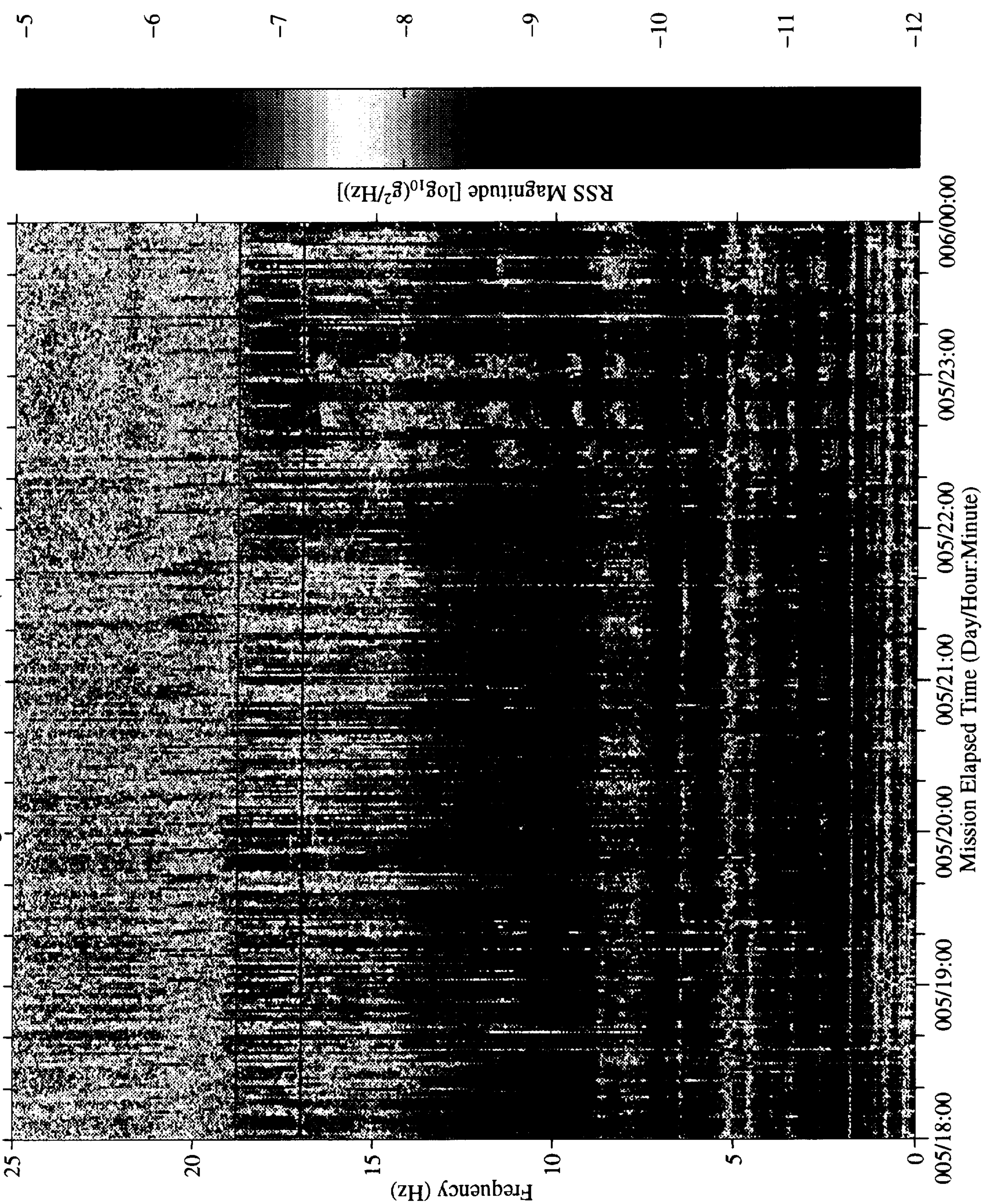

Figure 42: STS–79, Head C (fc=25 Hz)

Figure 43a: STS–79, Head C (fc=25 Hz), Ten Second Interval Average

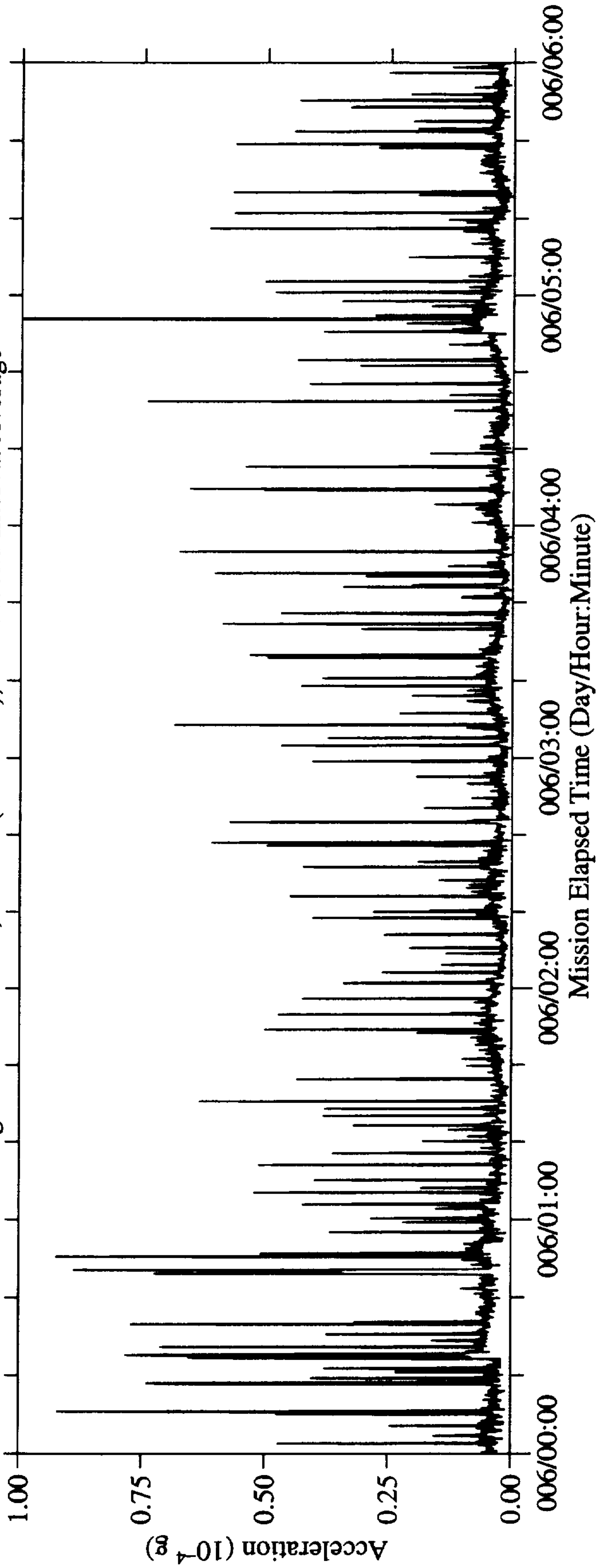

Figure 43b: STS–79, Head C (fc=25 Hz), Ten Second Interval RMS

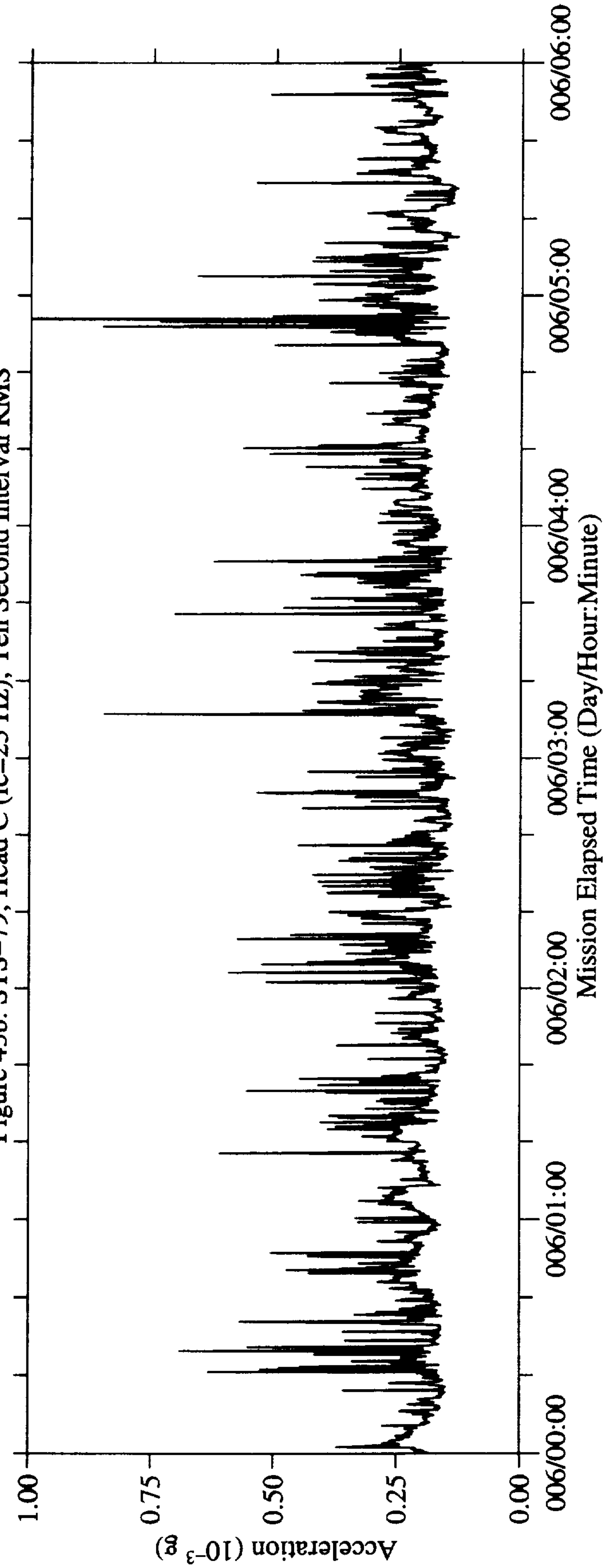

Figure 44: STS-79, Head C (fc=25 Hz)

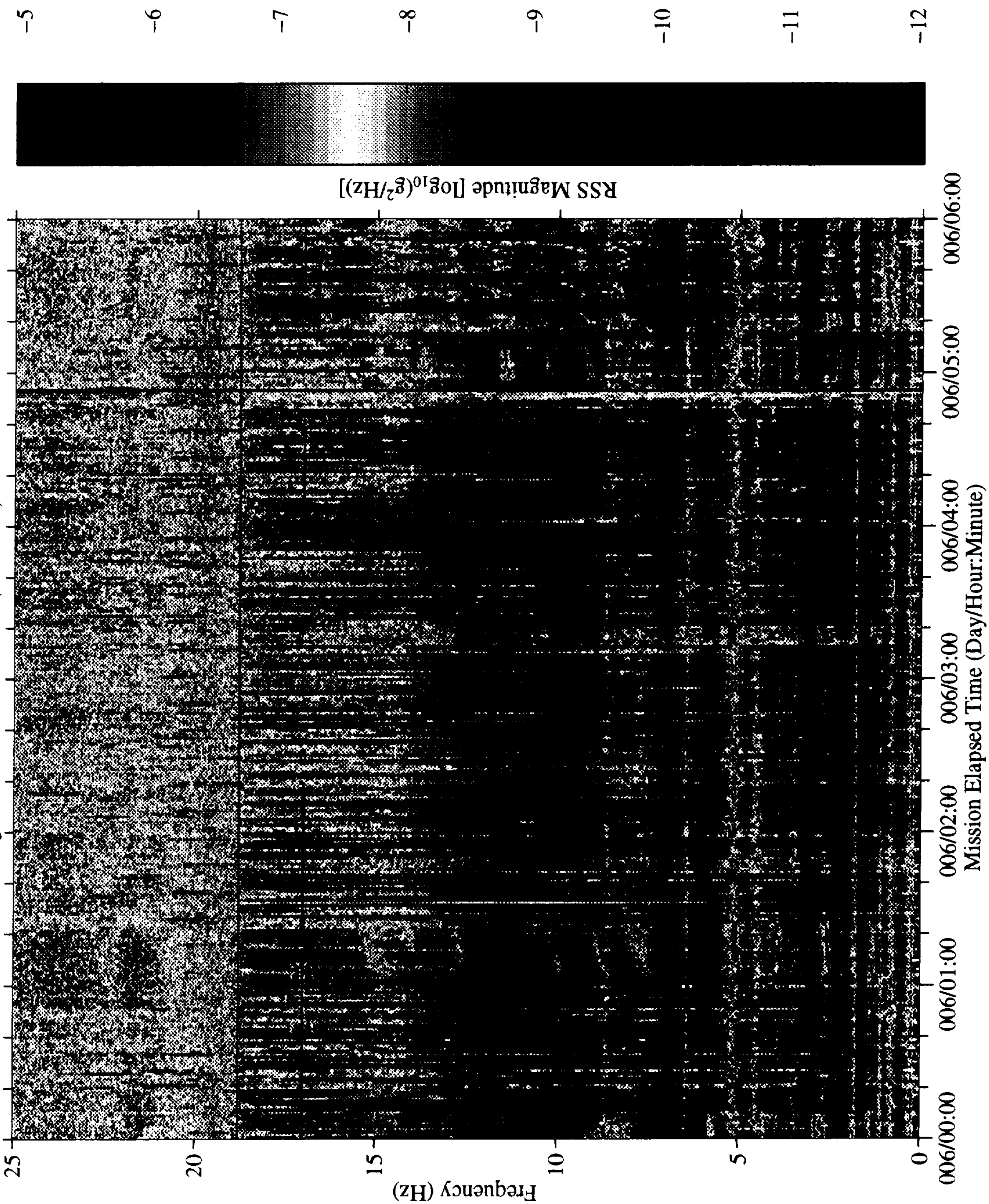

Figure 45a: STS–79, Head C (fc=25 Hz), Ten Second Interval Average

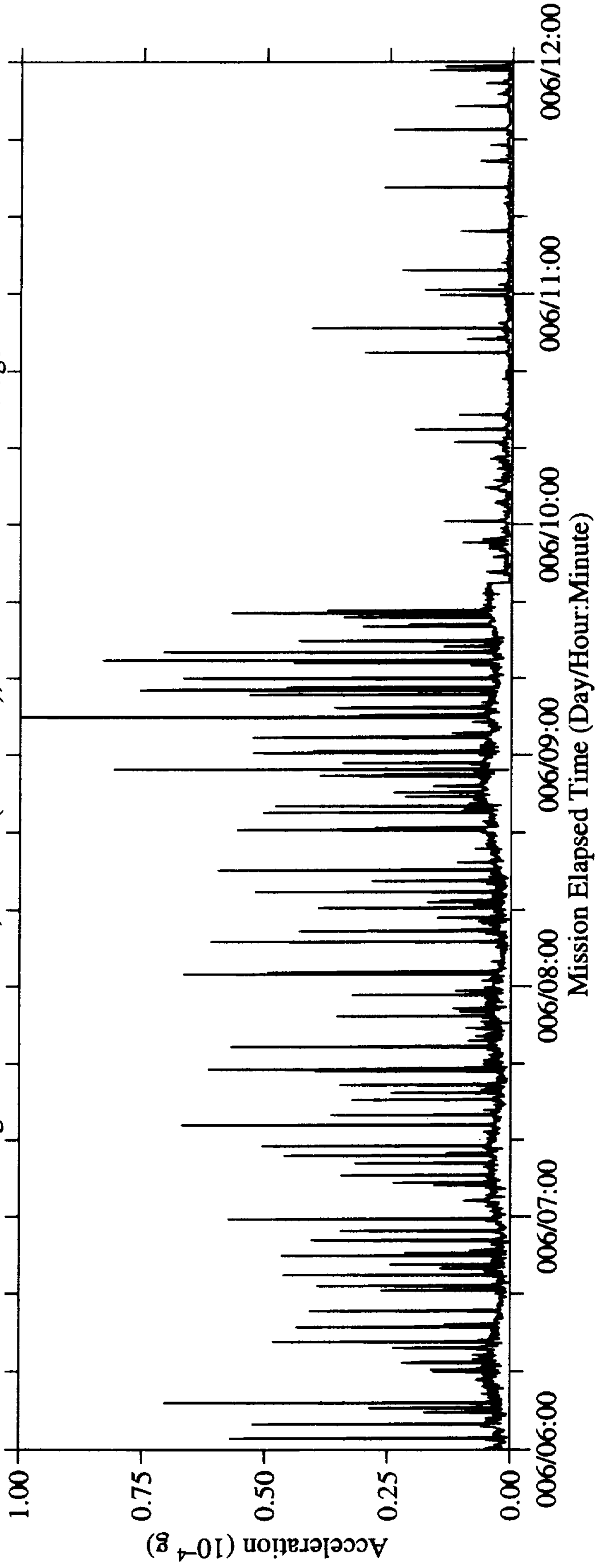

Figure 45b: STS–79, Head C (fc=25 Hz), Ten Second Interval RMS

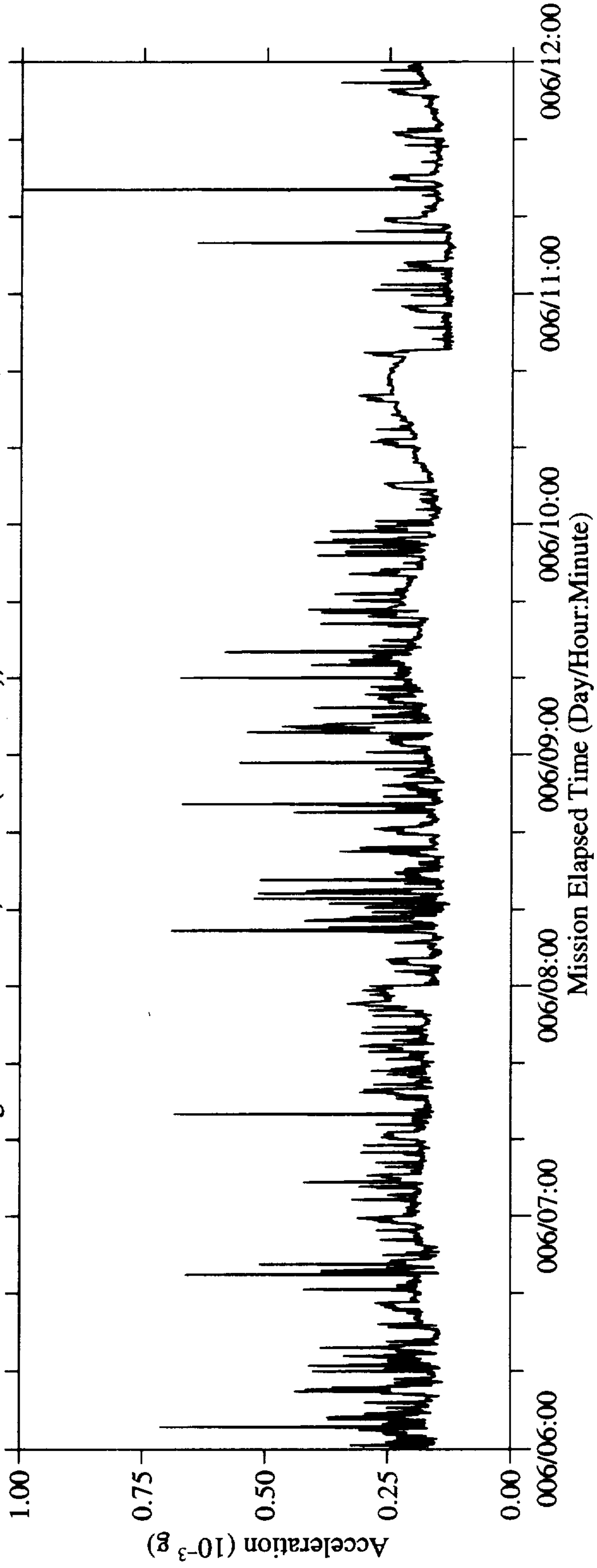

Figure 46: STS-79, Head C (fc=25 Hz)

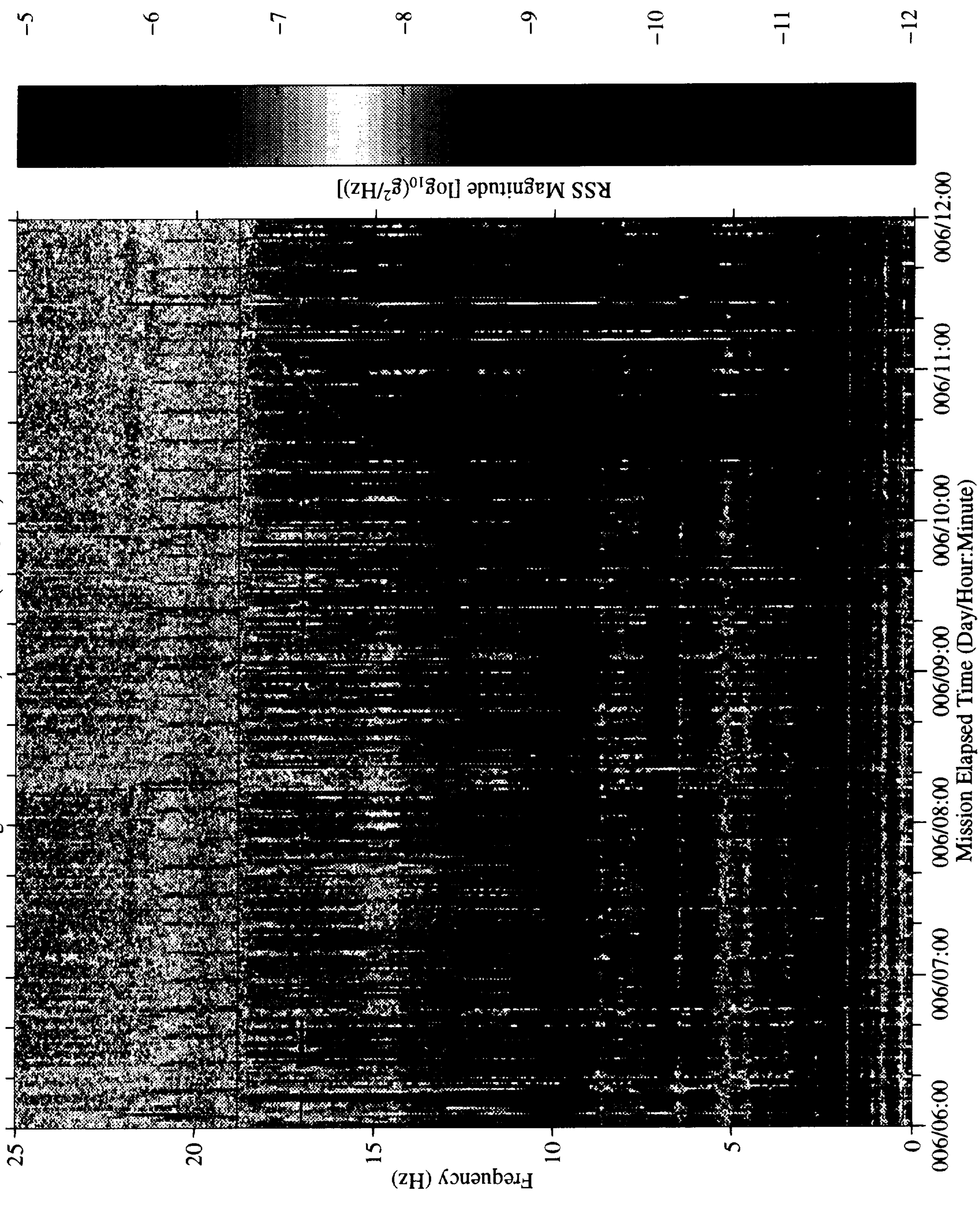

Figure 47a: STS–79, Head C (fc=25 Hz), Ten Second Interval Average

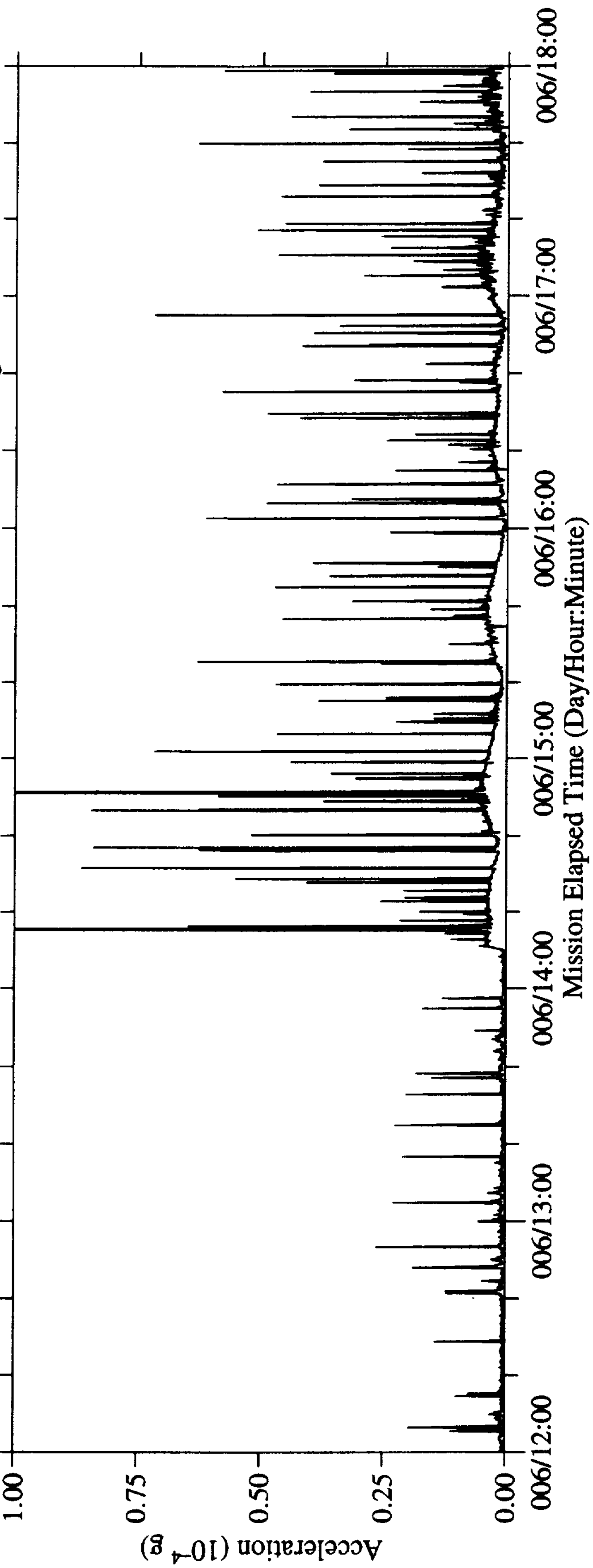

Figure 47b: STS–79, Head C (fc=25 Hz), Ten Second Interval RMS

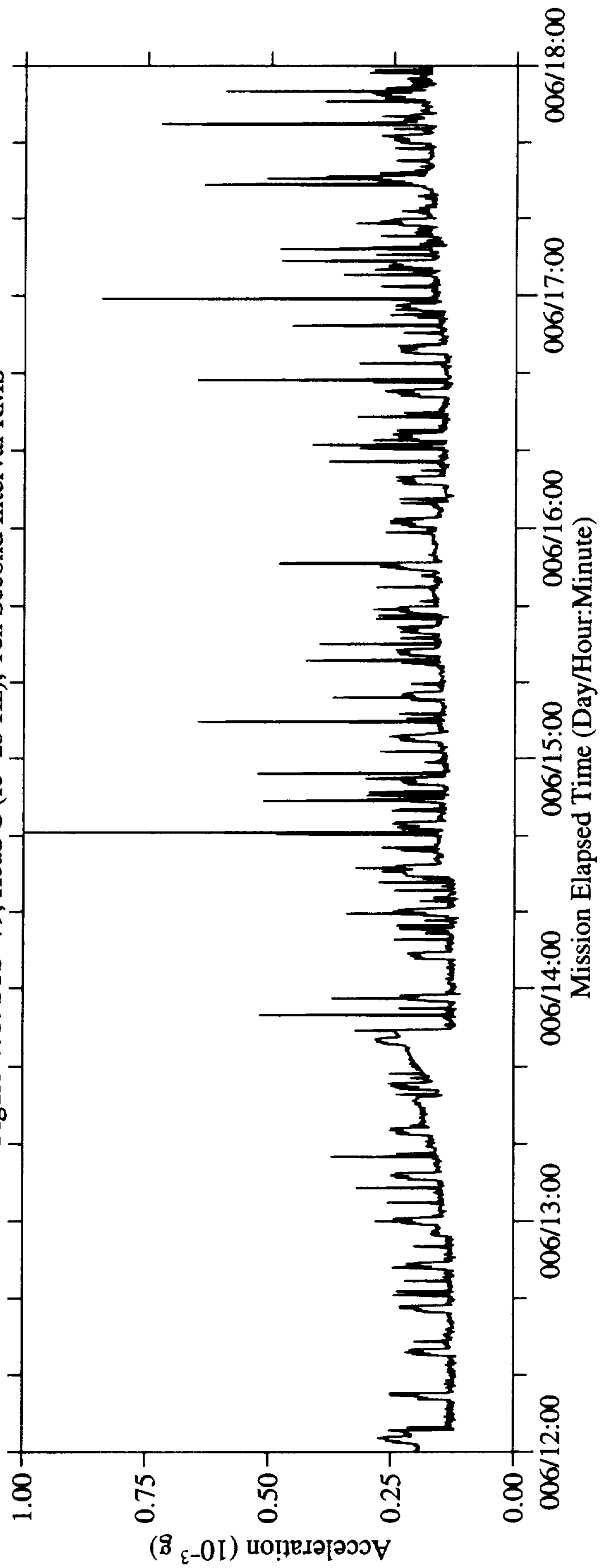

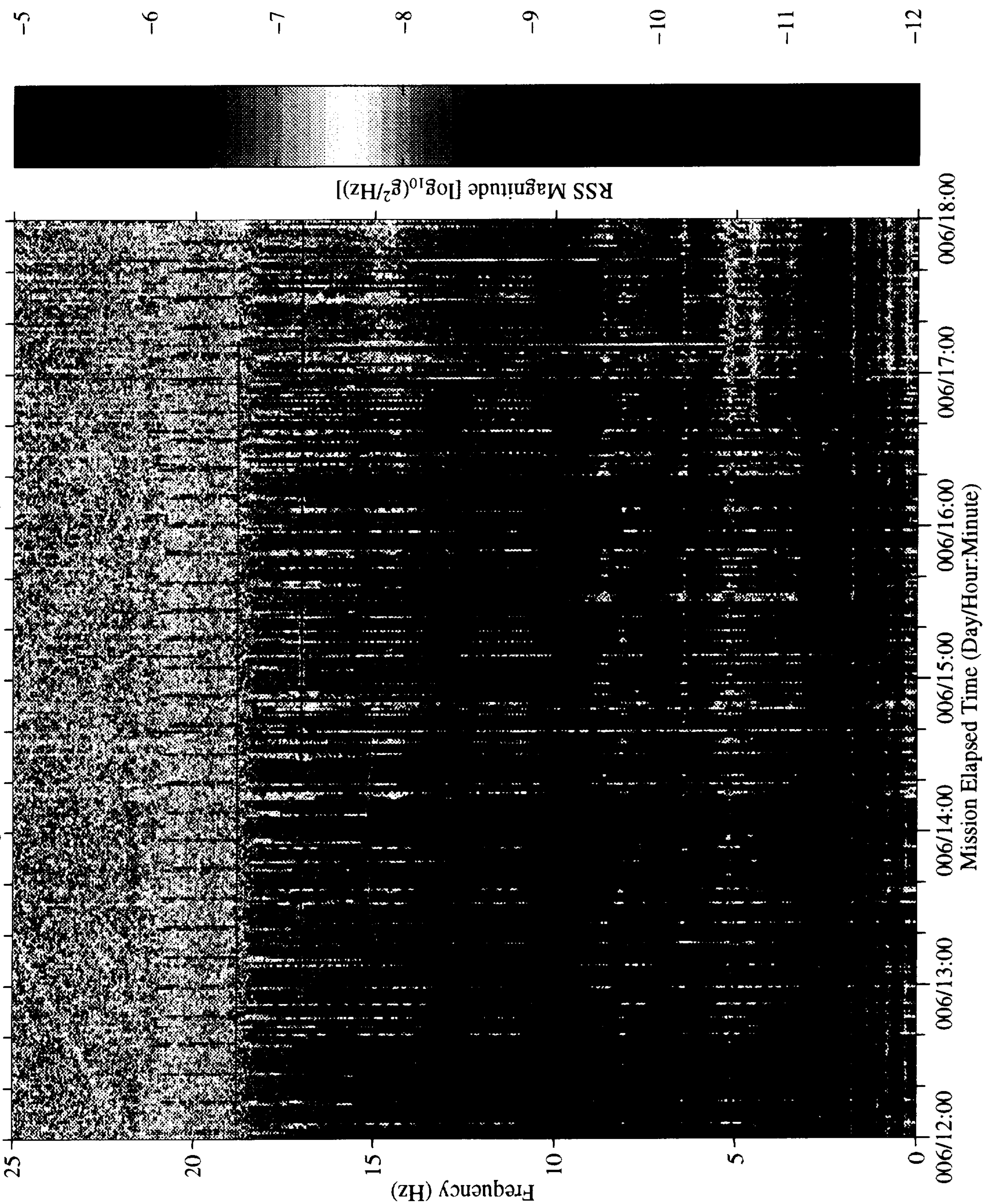

Figure 48: STS-79, Head C (fc=25 Hz)

Figure 49a: STS–79, Head C (fc=25 Hz), Ten Second Interval Average

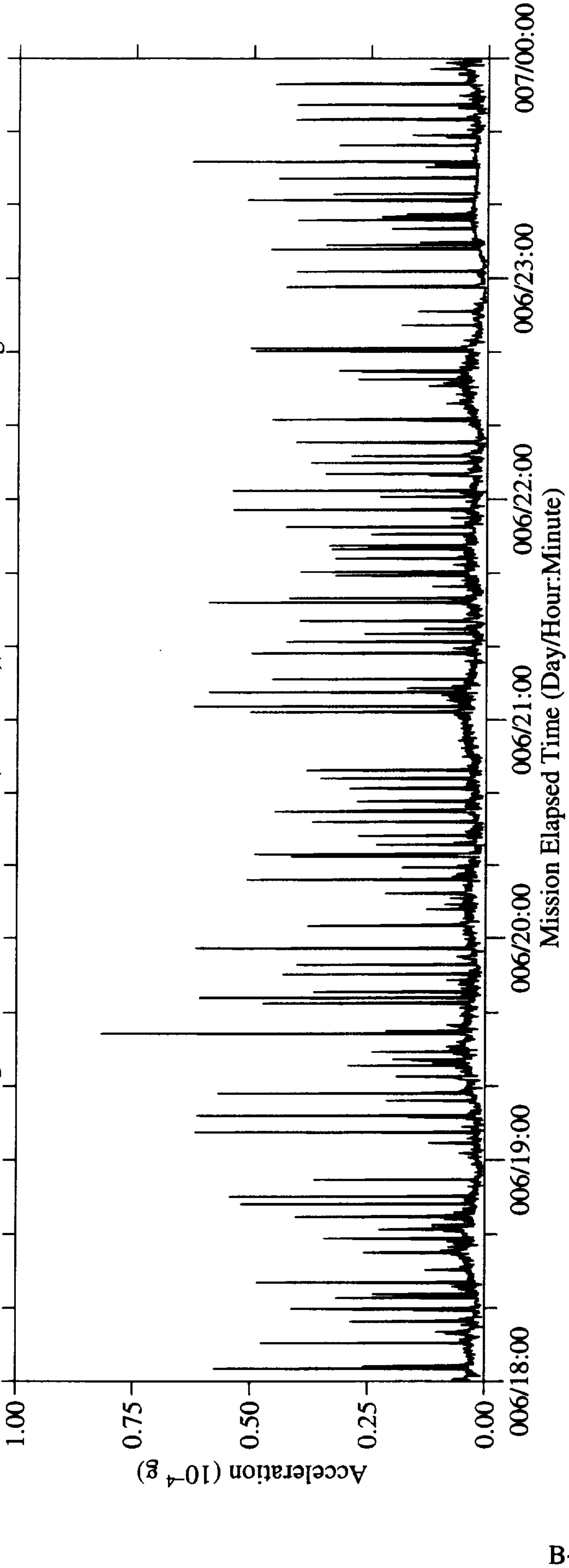

Figure 49b: STS–79, Head C (fc=25 Hz), Ten Second Interval RMS

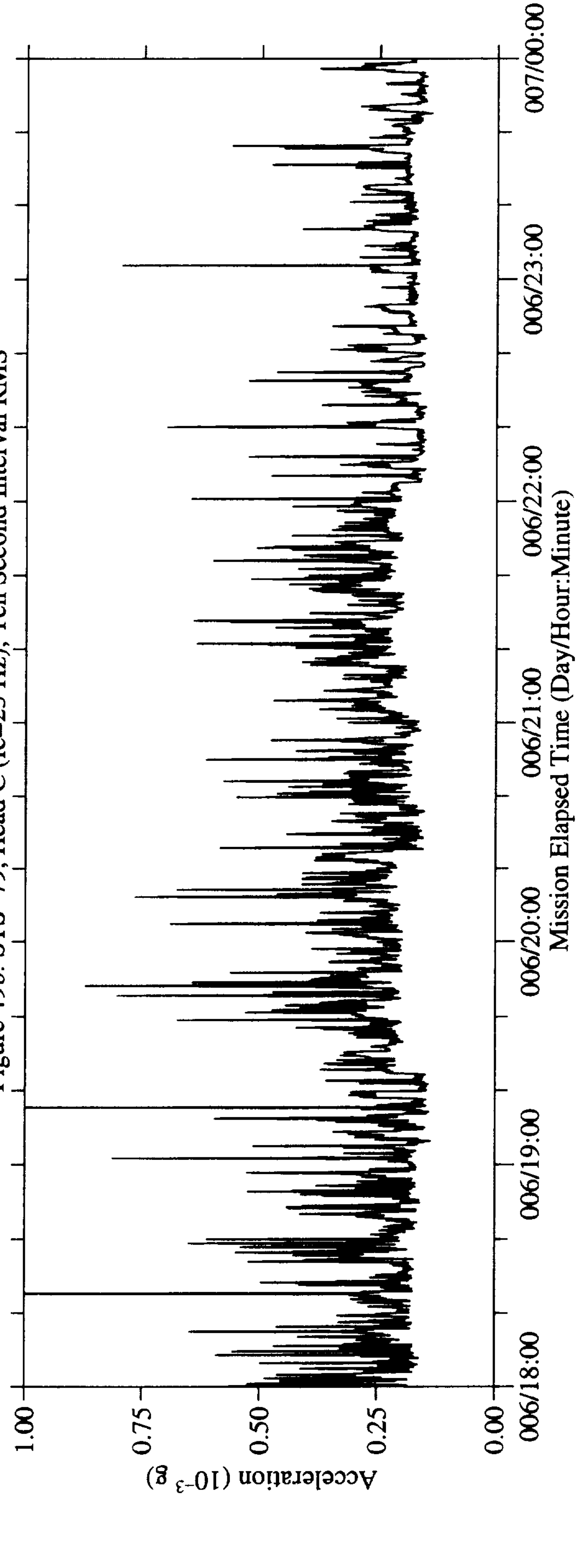

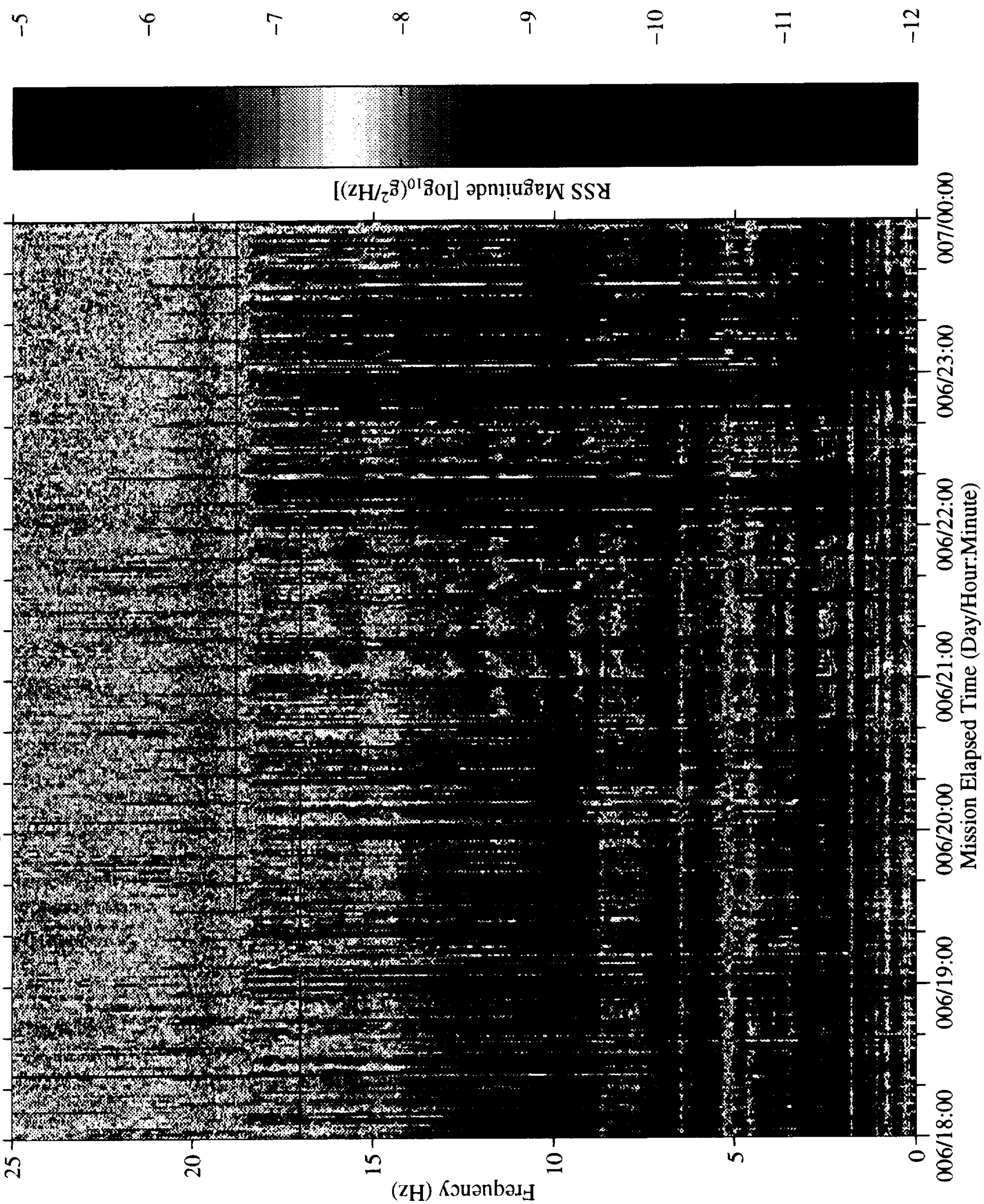

Figure 50: STS-79, Head C (fc=25 Hz)

Figure 51a: STS–79, Head C (fc=25 Hz), Ten Second Interval Average

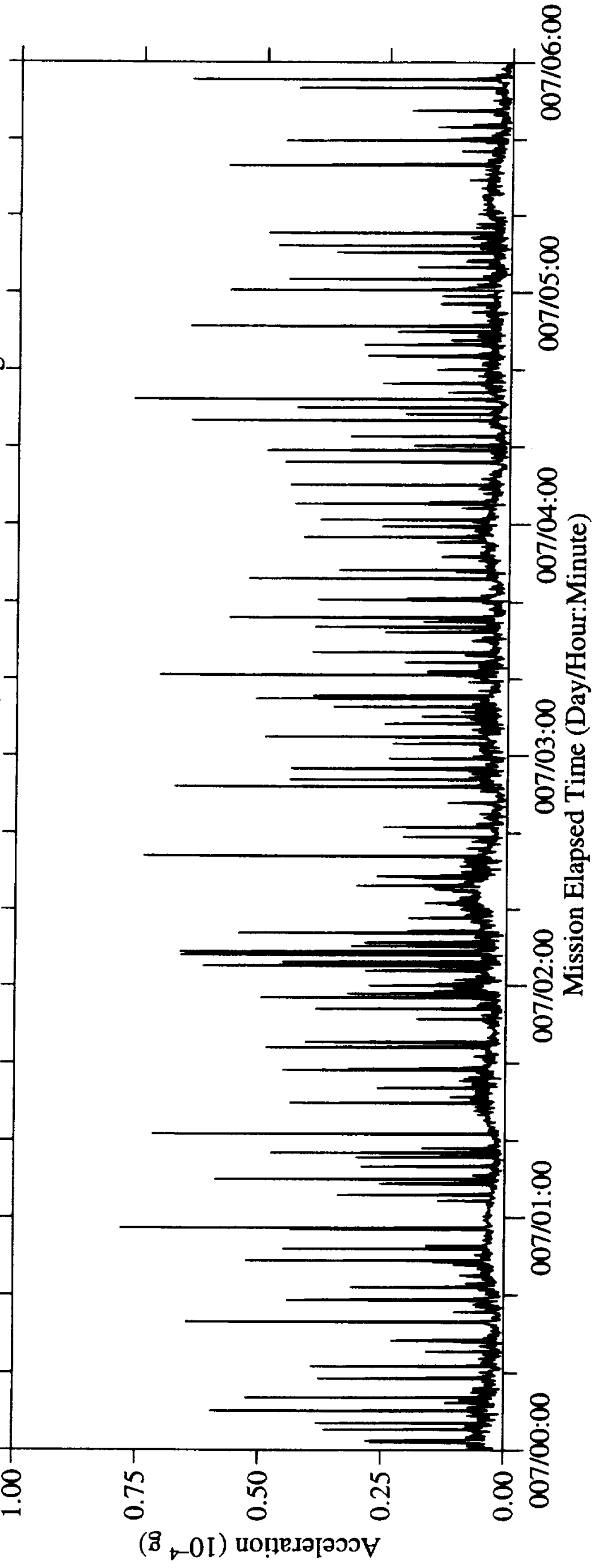

Figure 51b: STS–79, Head C (fc=25 Hz), Ten Second Interval RMS

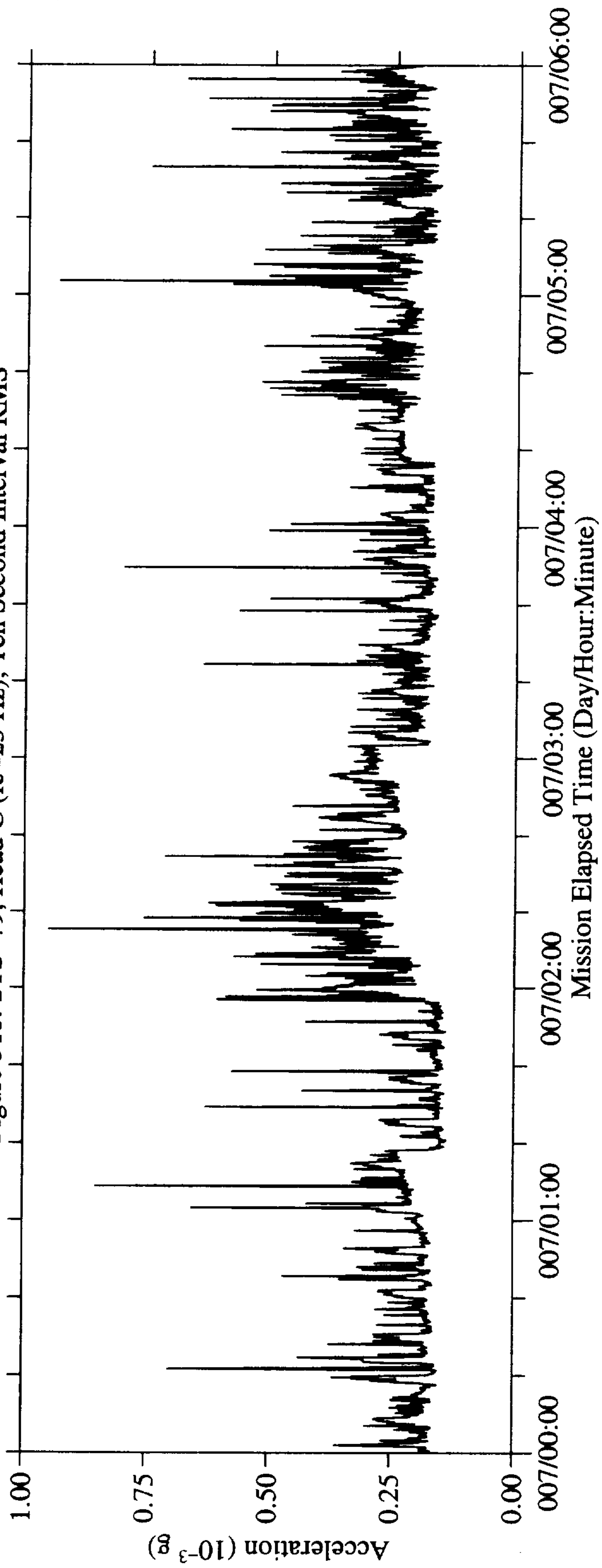

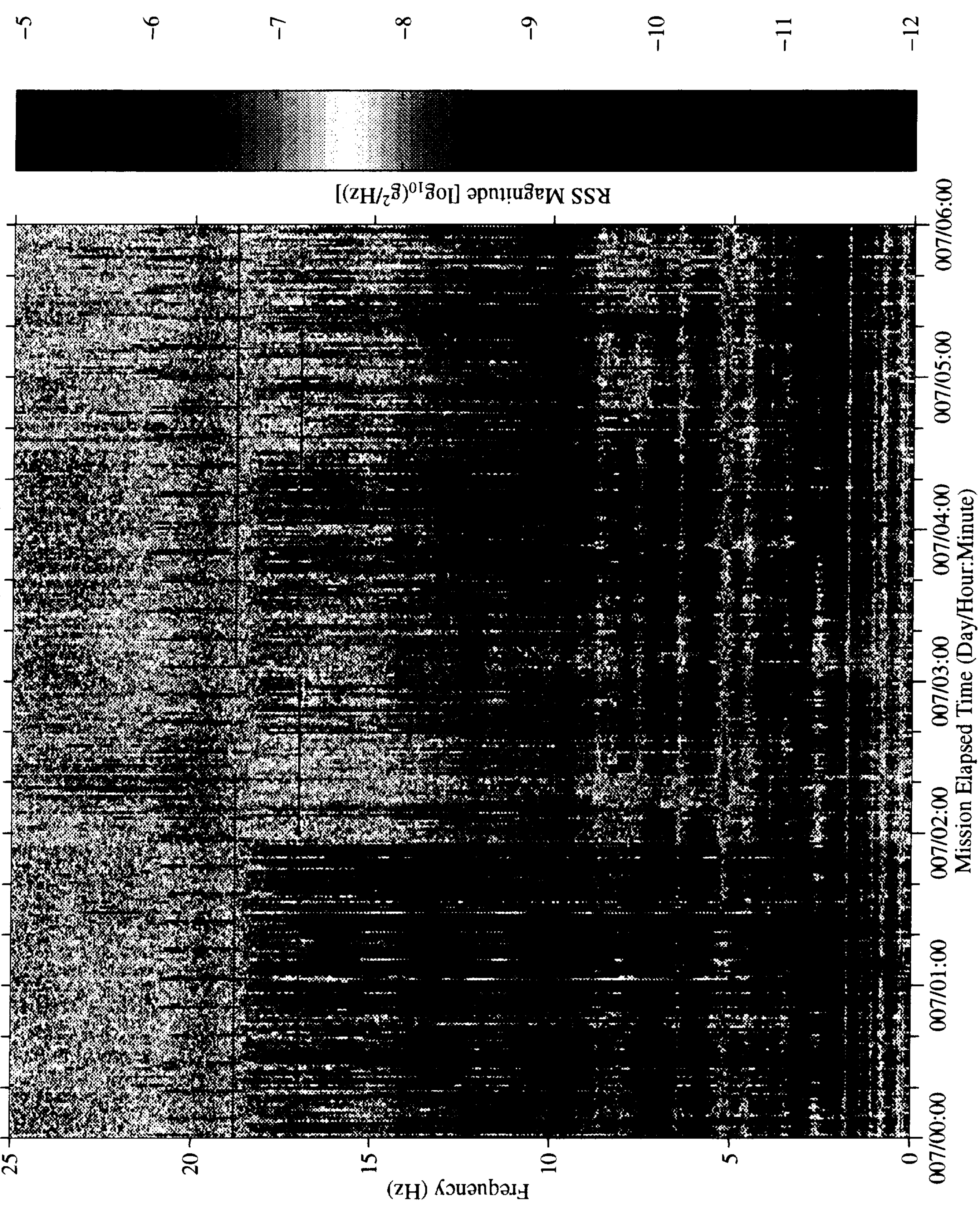

Figure 52: STS–79, Head C (fc=25 Hz)

Figure 53a: STS-79, Head C (fc=25 Hz), Ten Second Interval Average

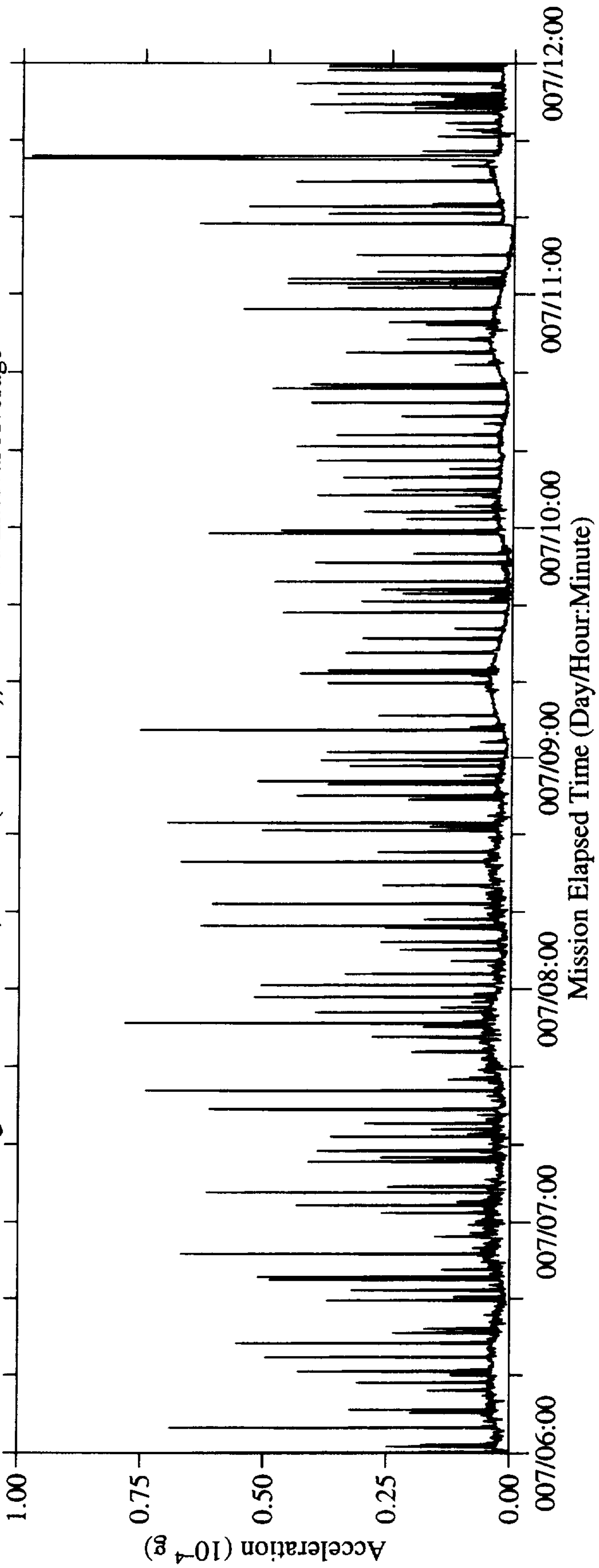

Figure 53b: STS-79, Head C (fc=25 Hz), Ten Second Interval RMS

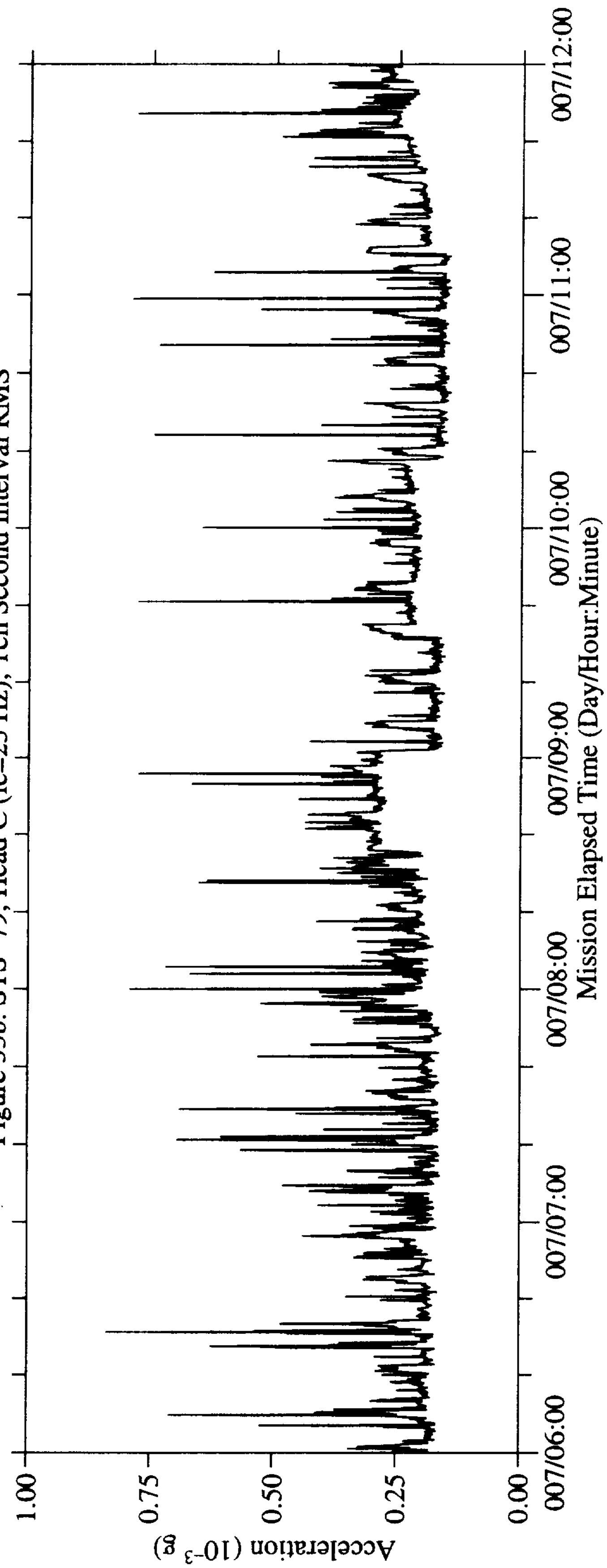

Figure 54: STS-79, Head C (fc=25 Hz)

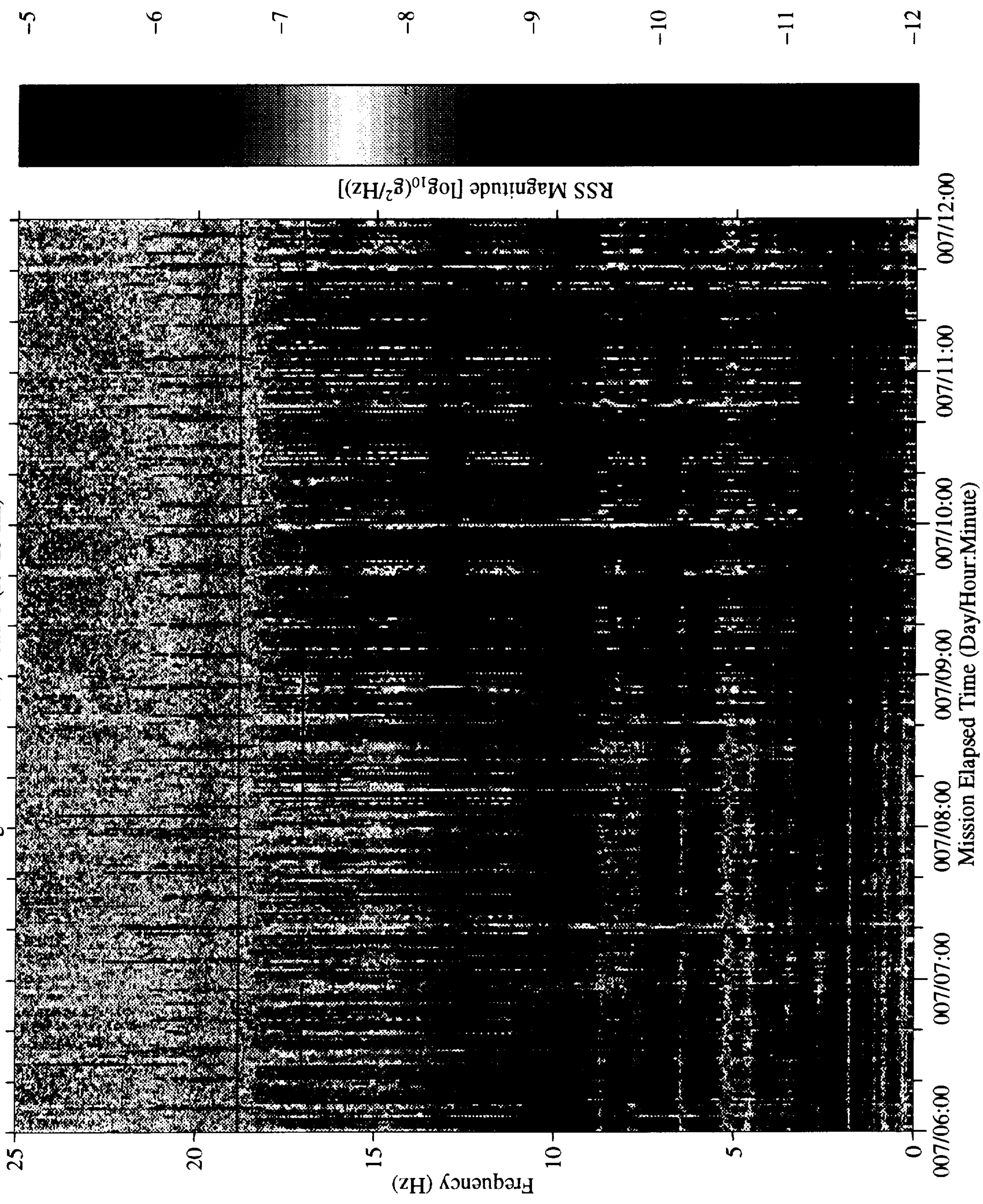

Figure 55a: STS-79, Head C (fc=25 Hz), Ten Second Interval Average

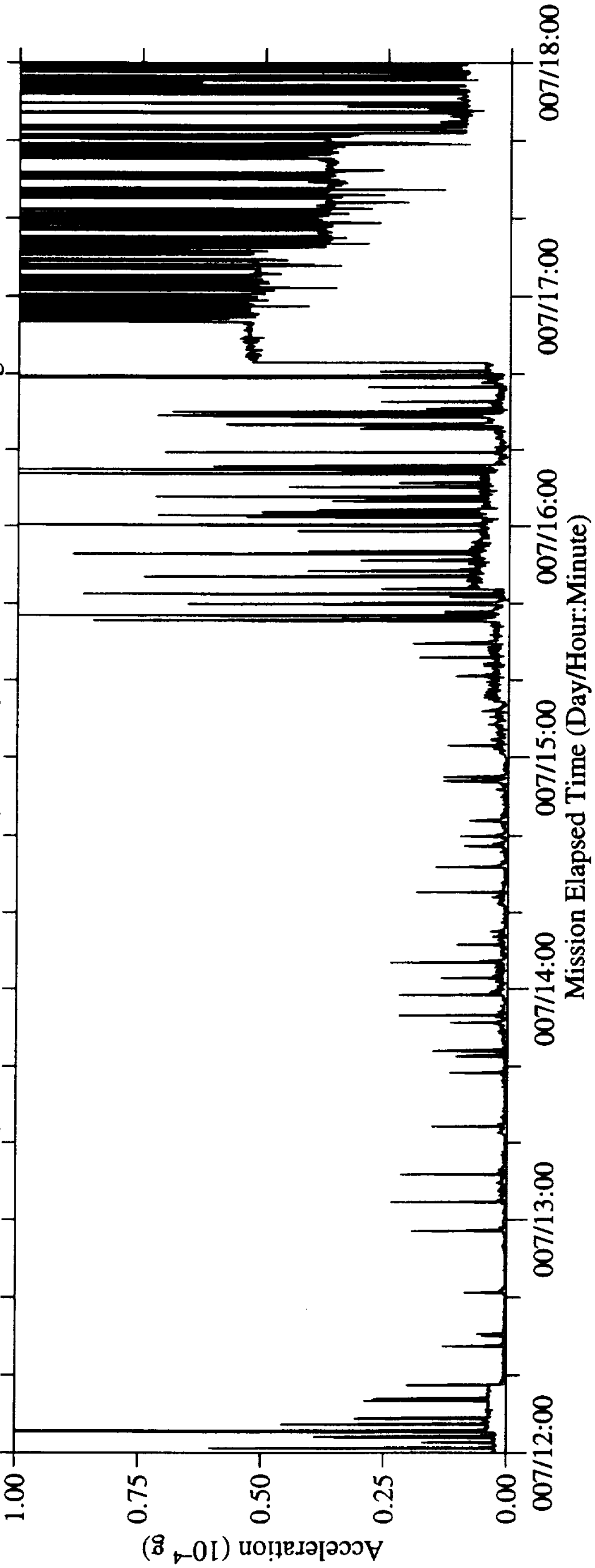

Figure 55b: STS-79, Head C (fc=25 Hz), Ten Second Interval RMS

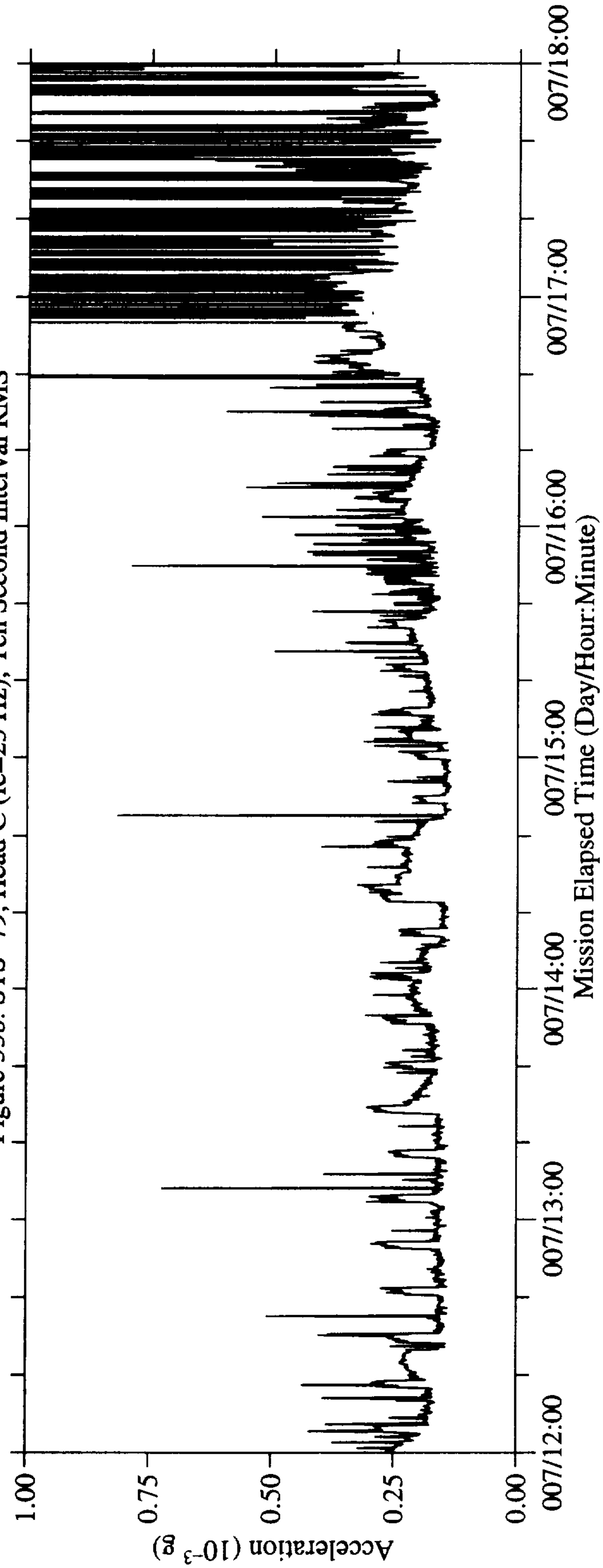

Figure 56: STS-79, Head C (fc=25 Hz)

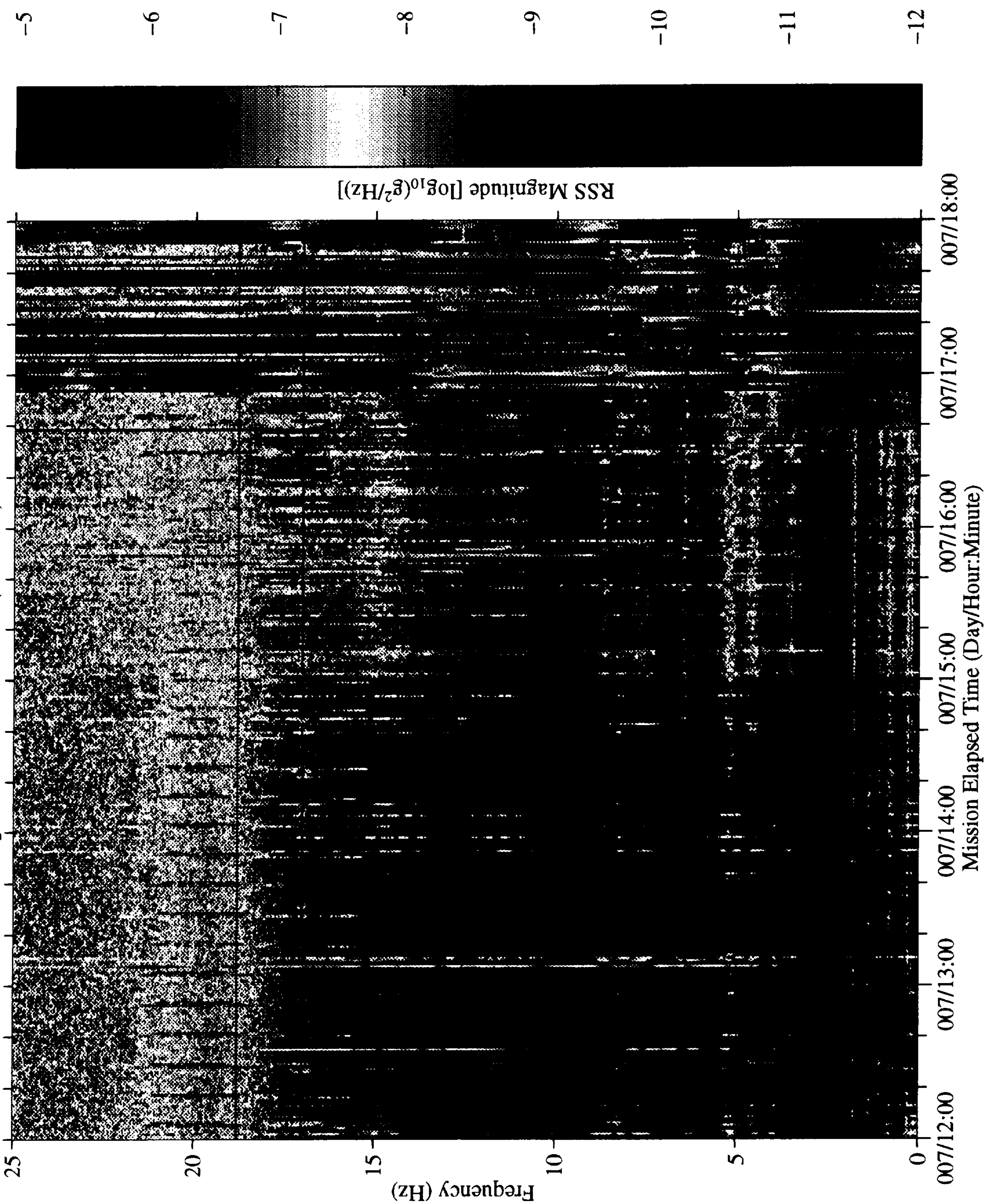

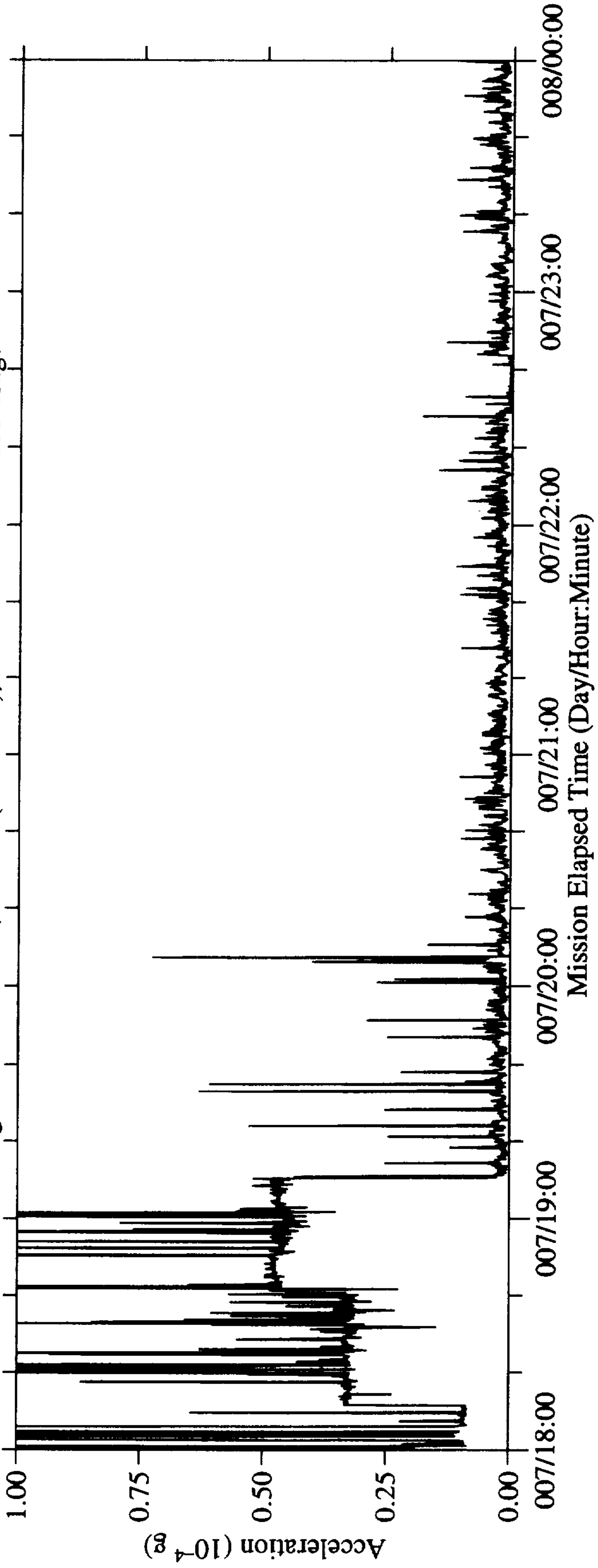

Figure 57a: STS–79, Head C (fc=25 Hz), Ten Second Interval Average

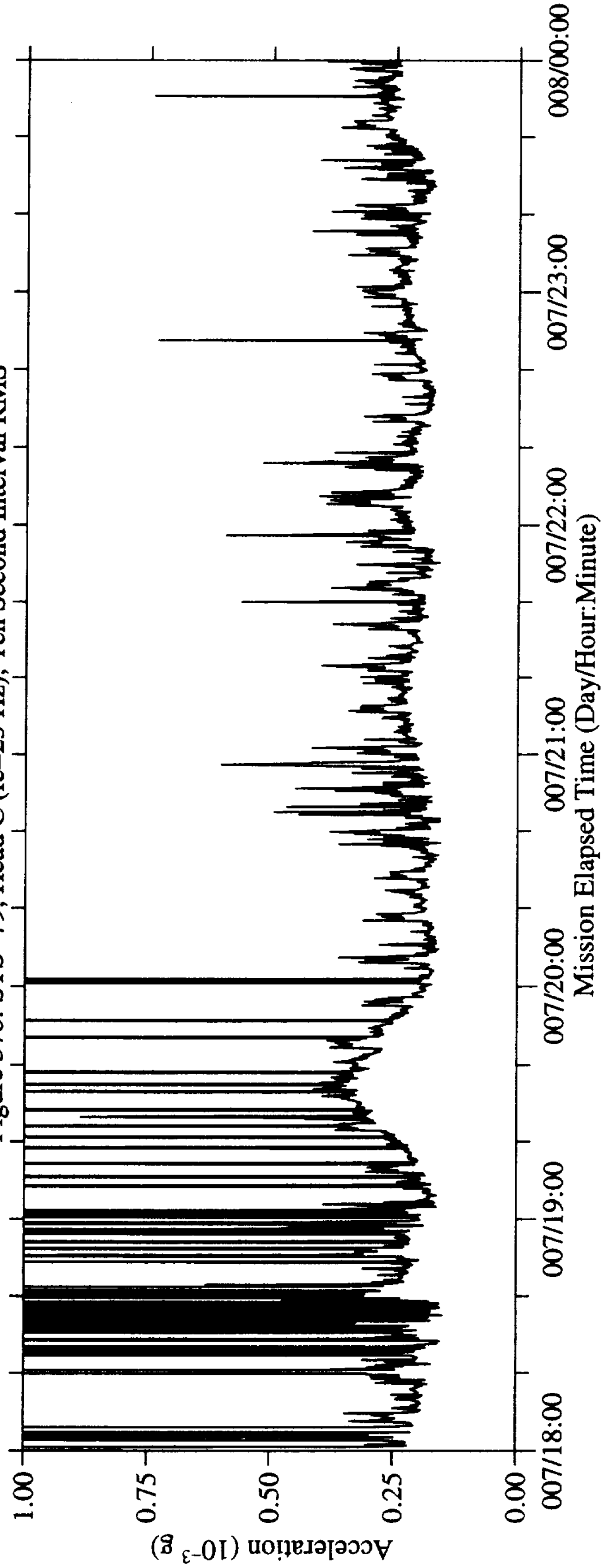

Figure 57b: STS–79, Head C (fc=25 Hz), Ten Second Interval RMS

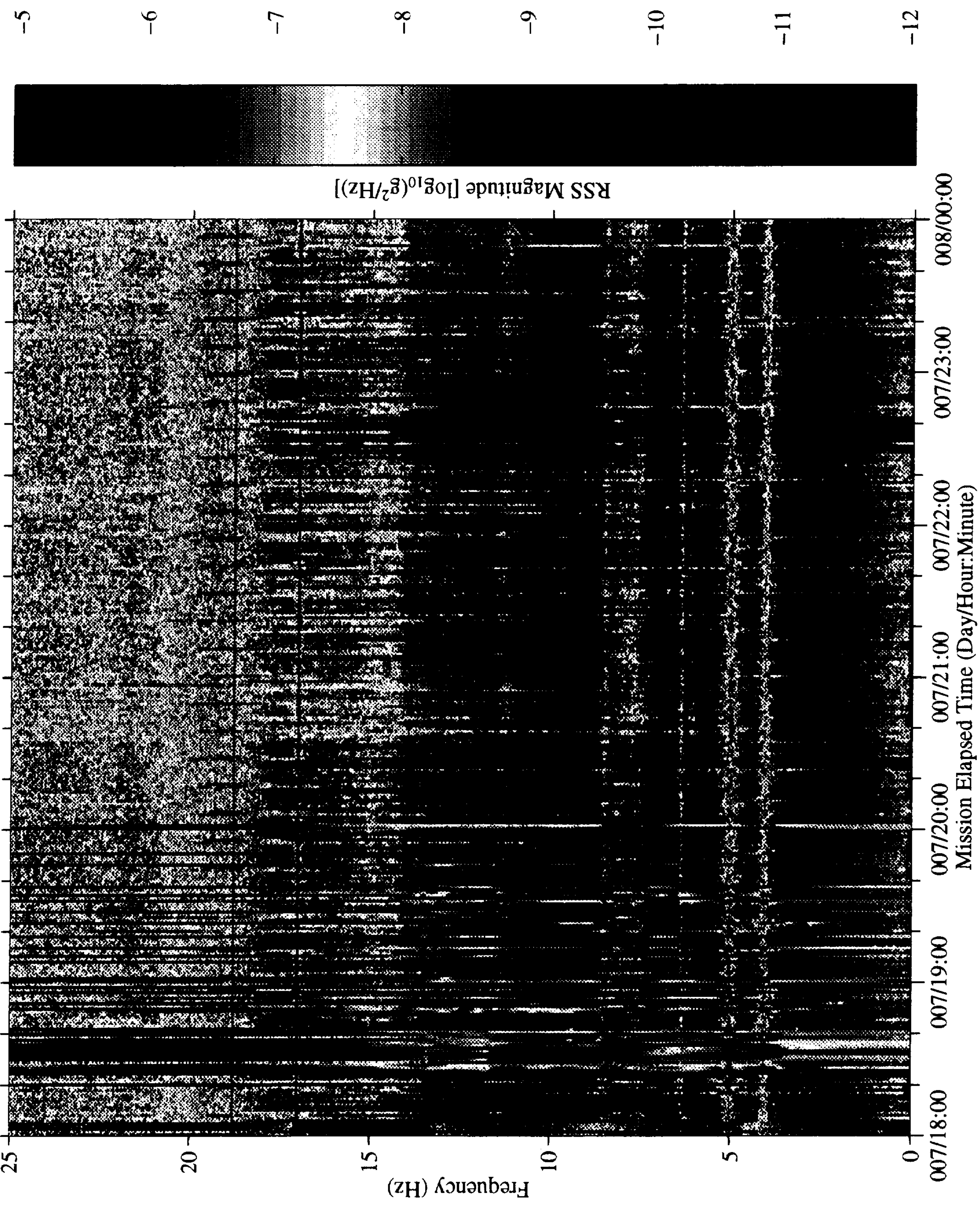

Figure 58: STS-79, Head C (fc=25 Hz)

Figure 59a: STS-79, Head C (fc=25 Hz), Ten Second Interval Average

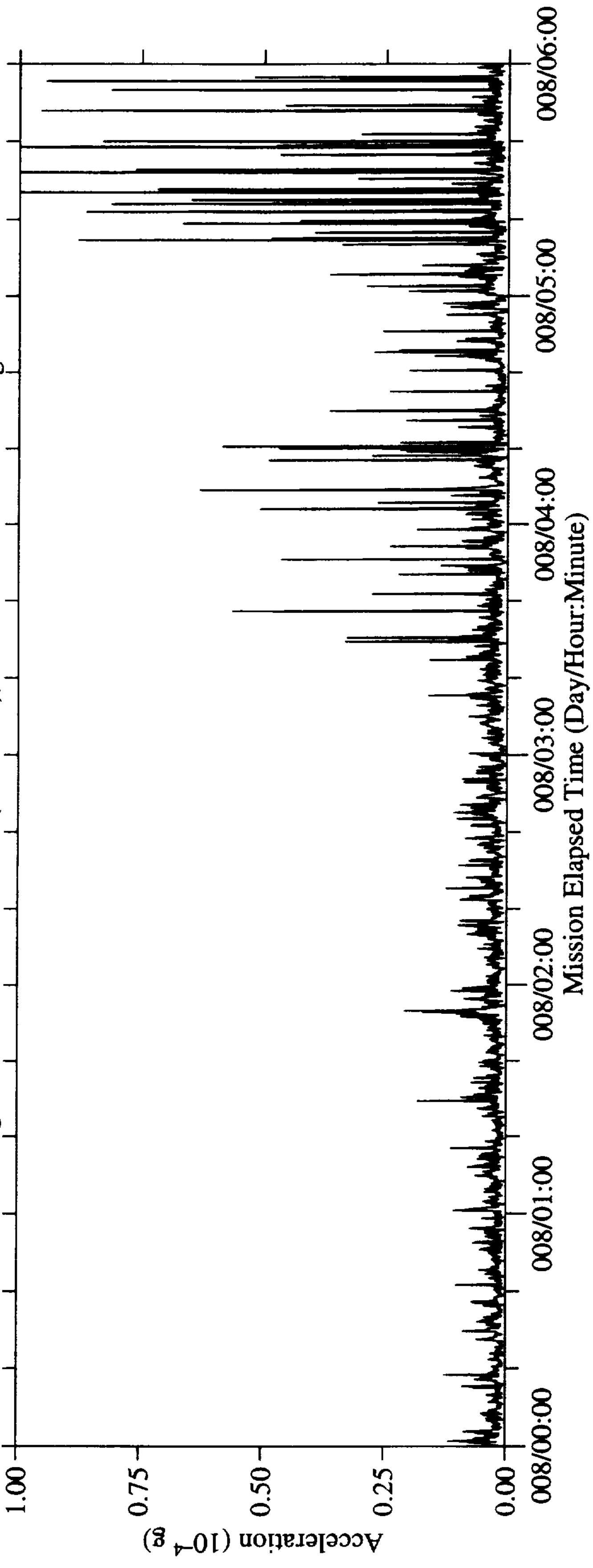

Figure 59b: STS-79, Head C (fc=25 Hz), Ten Second Interval RMS

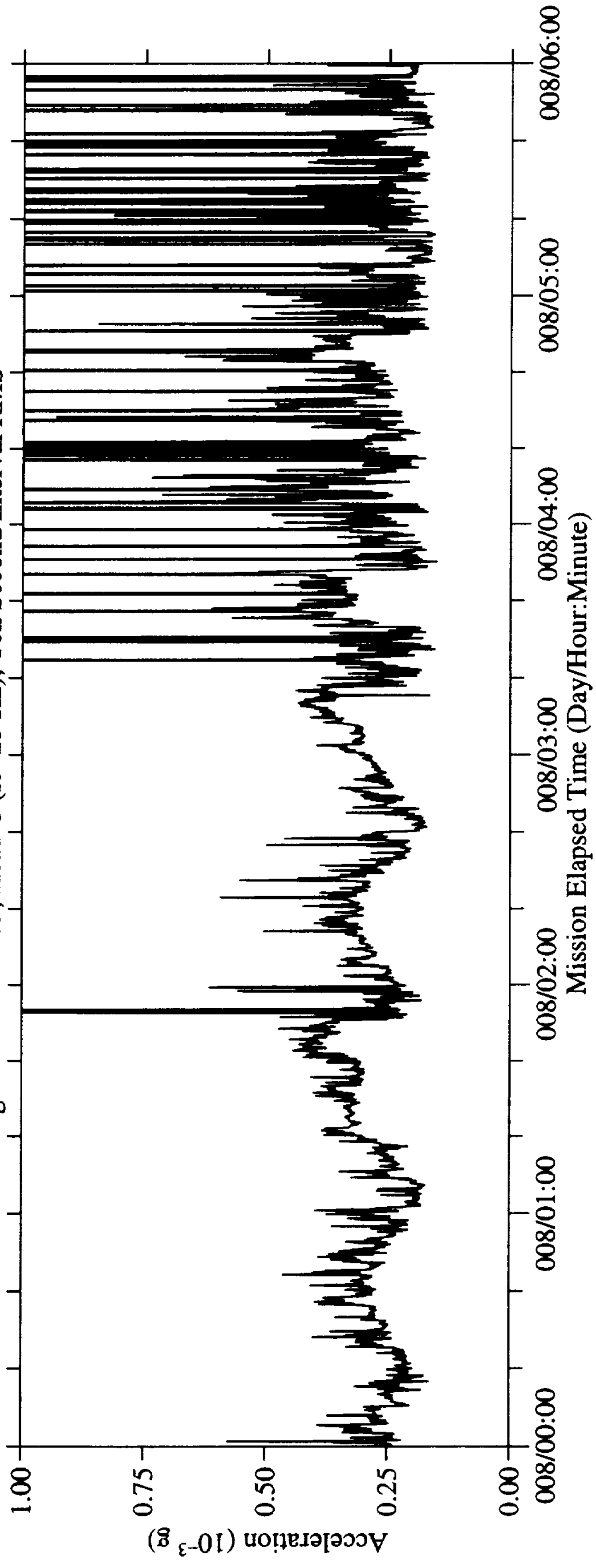

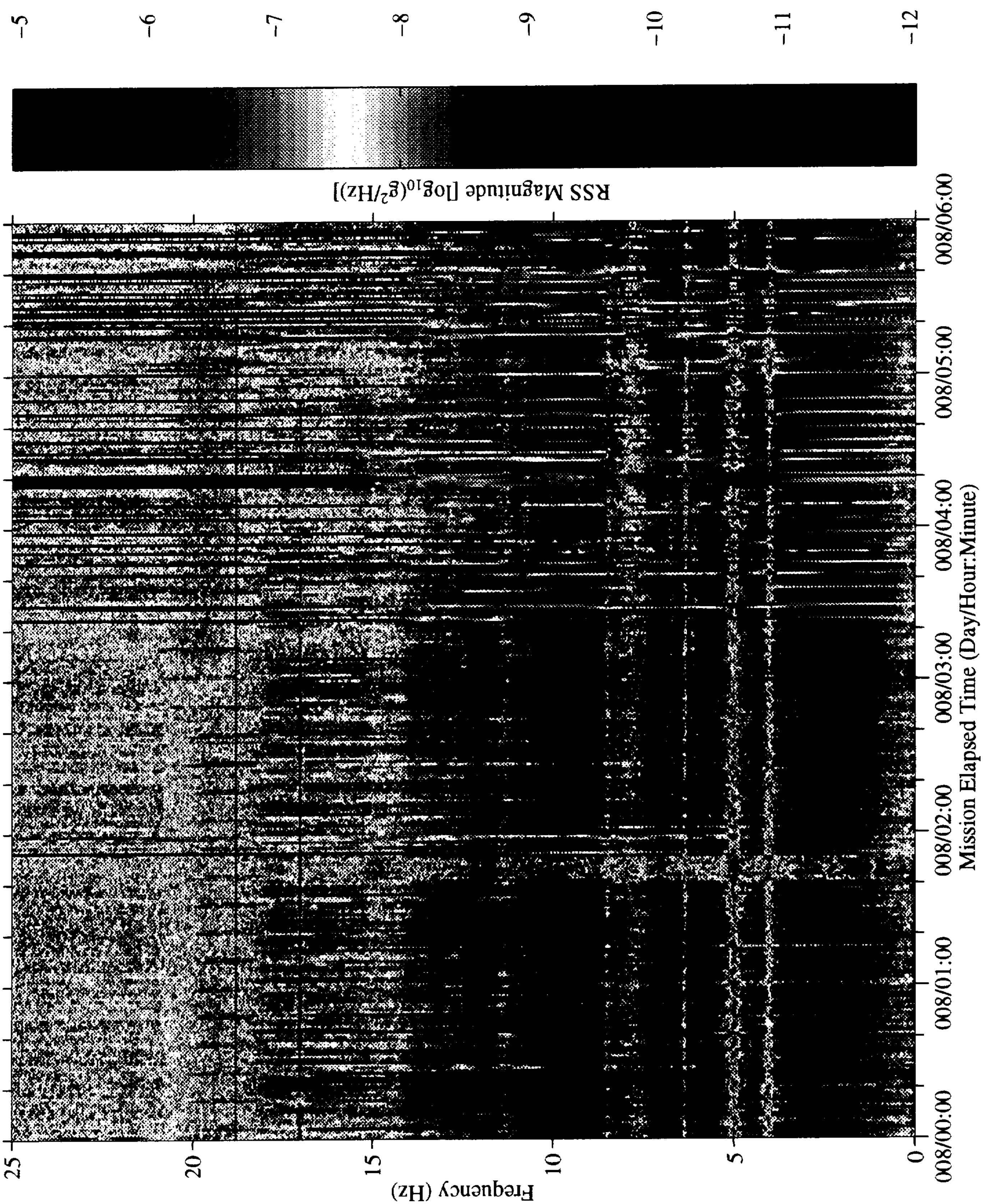

Figure 60: STS-79, Head C (fc=25 Hz)

Figure 61a: STS-79, Head C (fc=25 Hz), Ten Second Interval Average

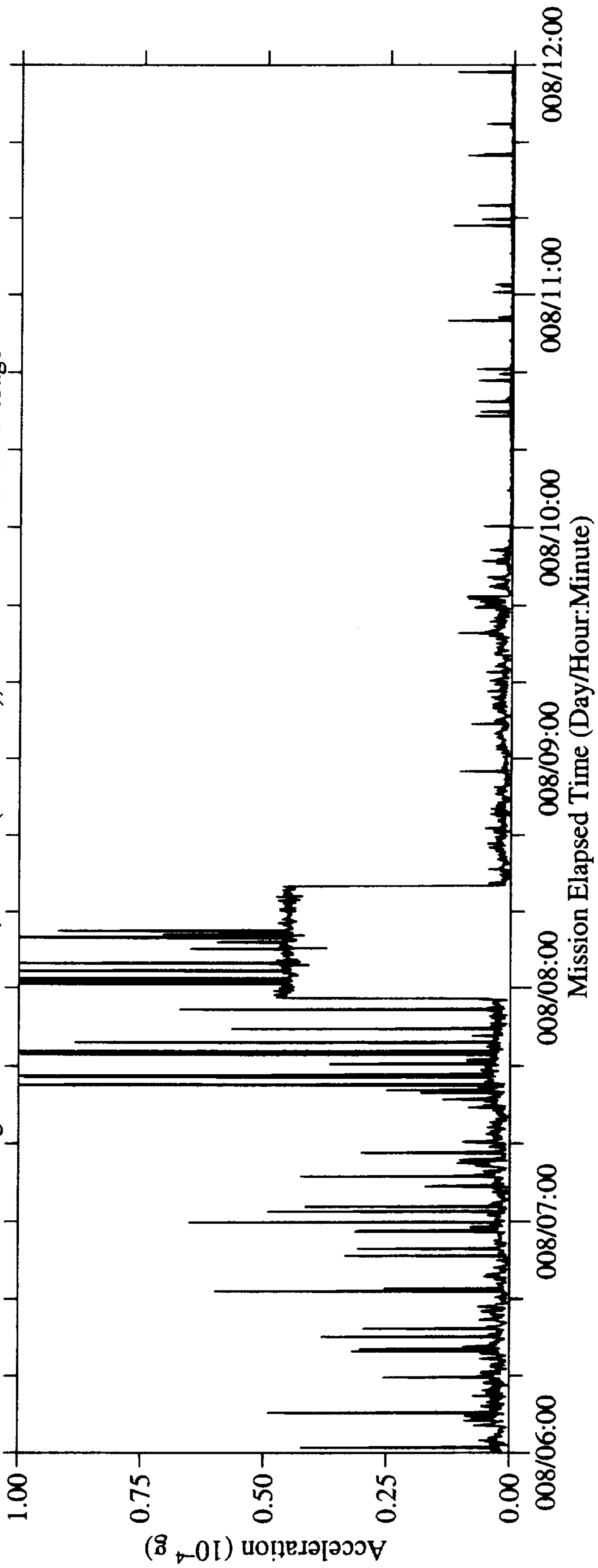

Figure 61b: STS-79, Head C (fc=25 Hz), Ten Second Interval RMS

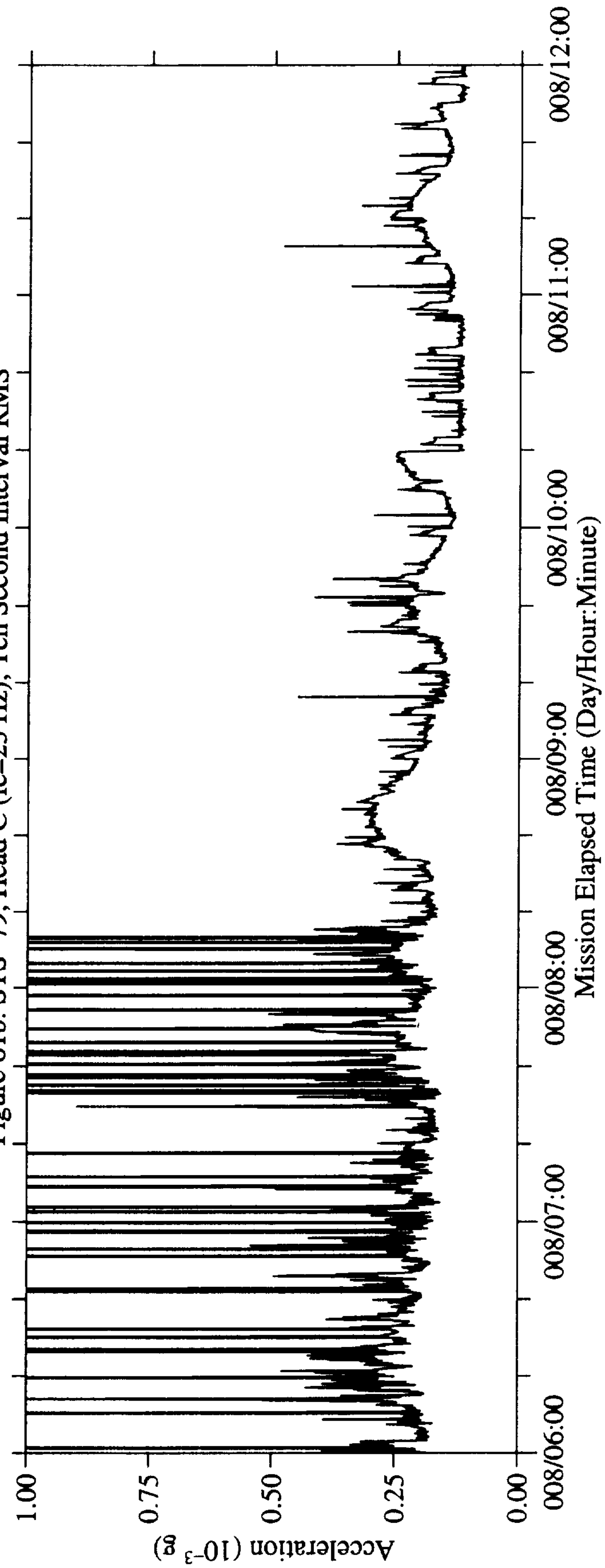

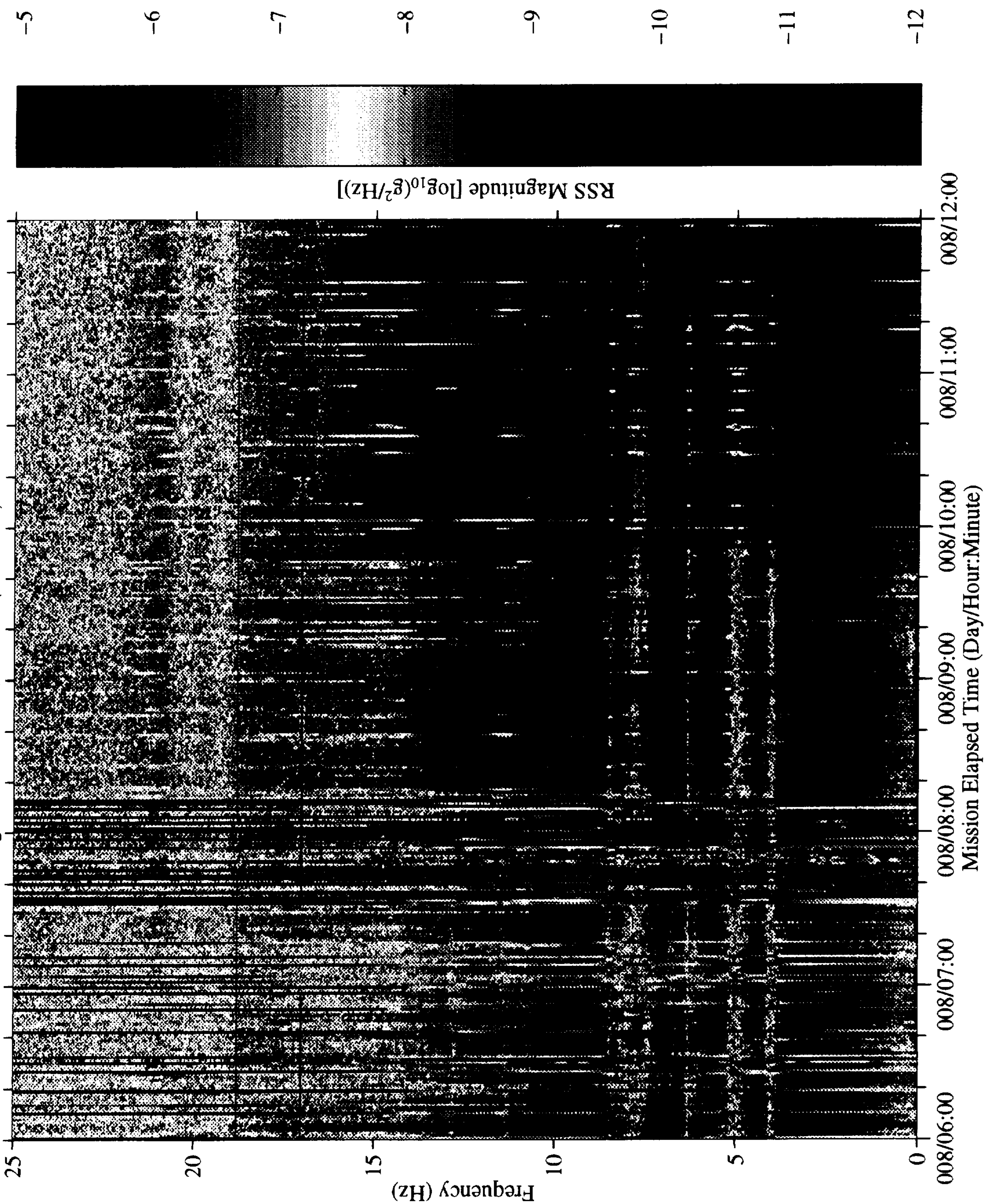

Figure 62: STS–79, Head C (fc=25 Hz)

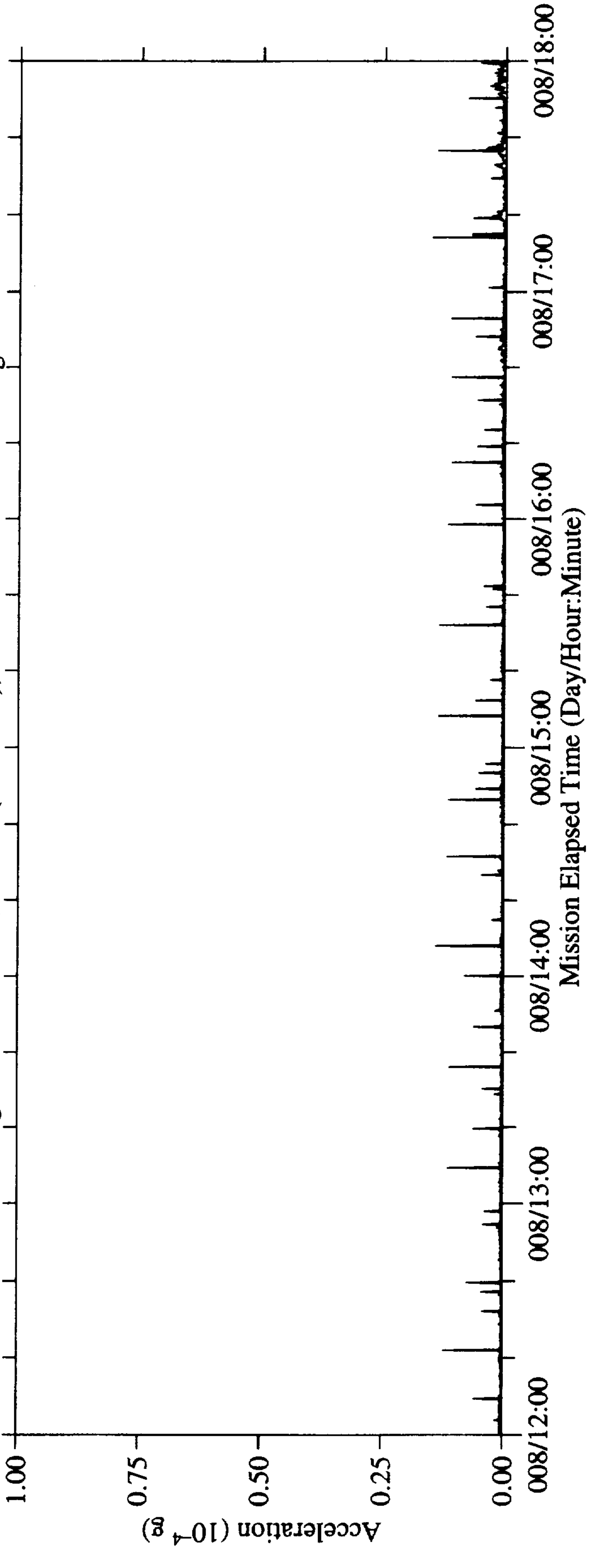

Figure 63a: STS-79, Head C (fc=25 Hz), Ten Second Interval Average

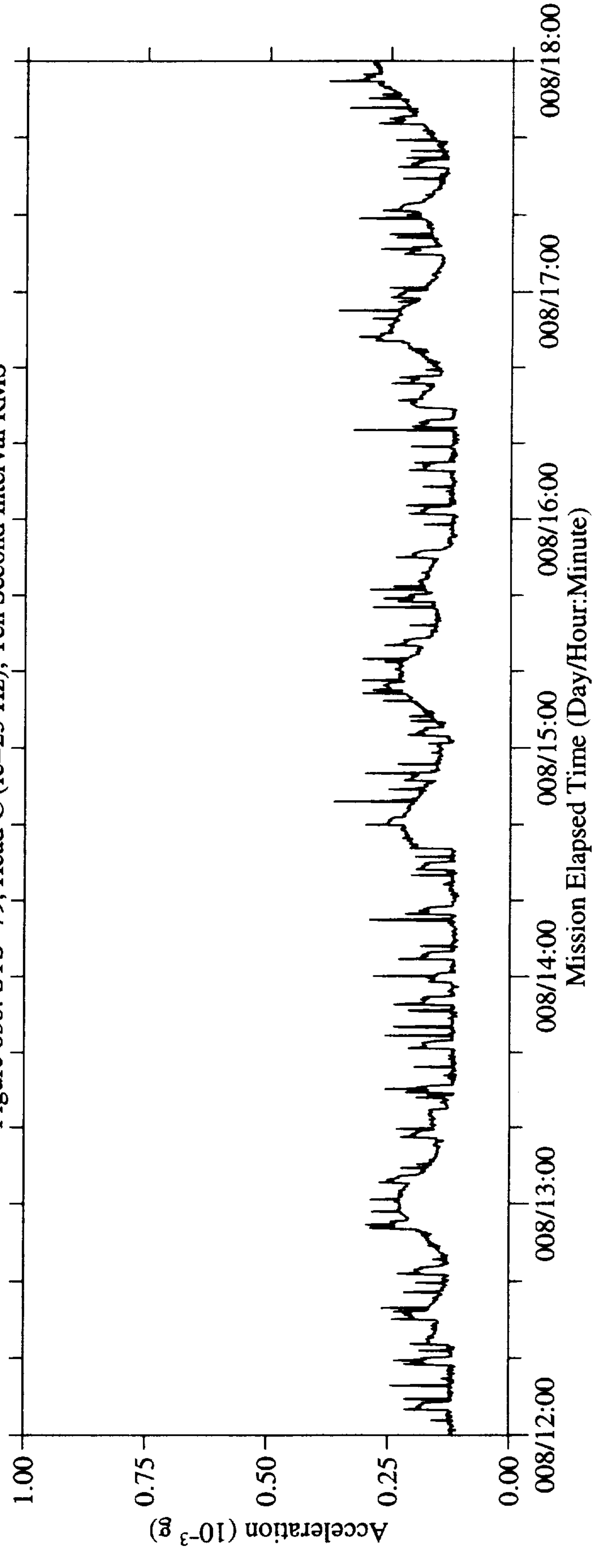

Figure 63b: STS-79, Head C (fc=25 Hz), Ten Second Interval RMS

Figure 64: STS-79, Head C (fc=25 Hz)

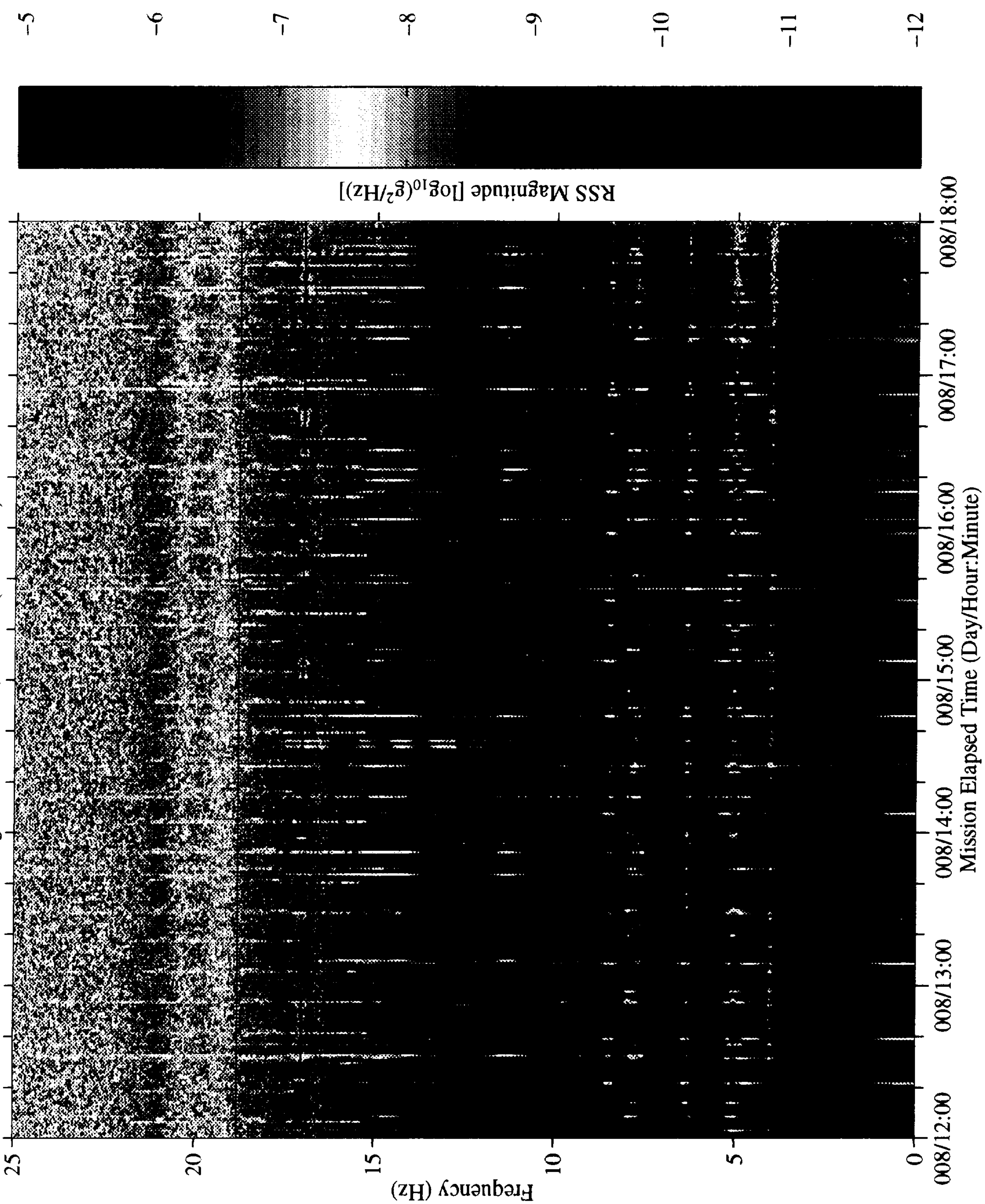

Figure 65a: STS–79, Head C (fc=25 Hz), Ten Second Interval Average

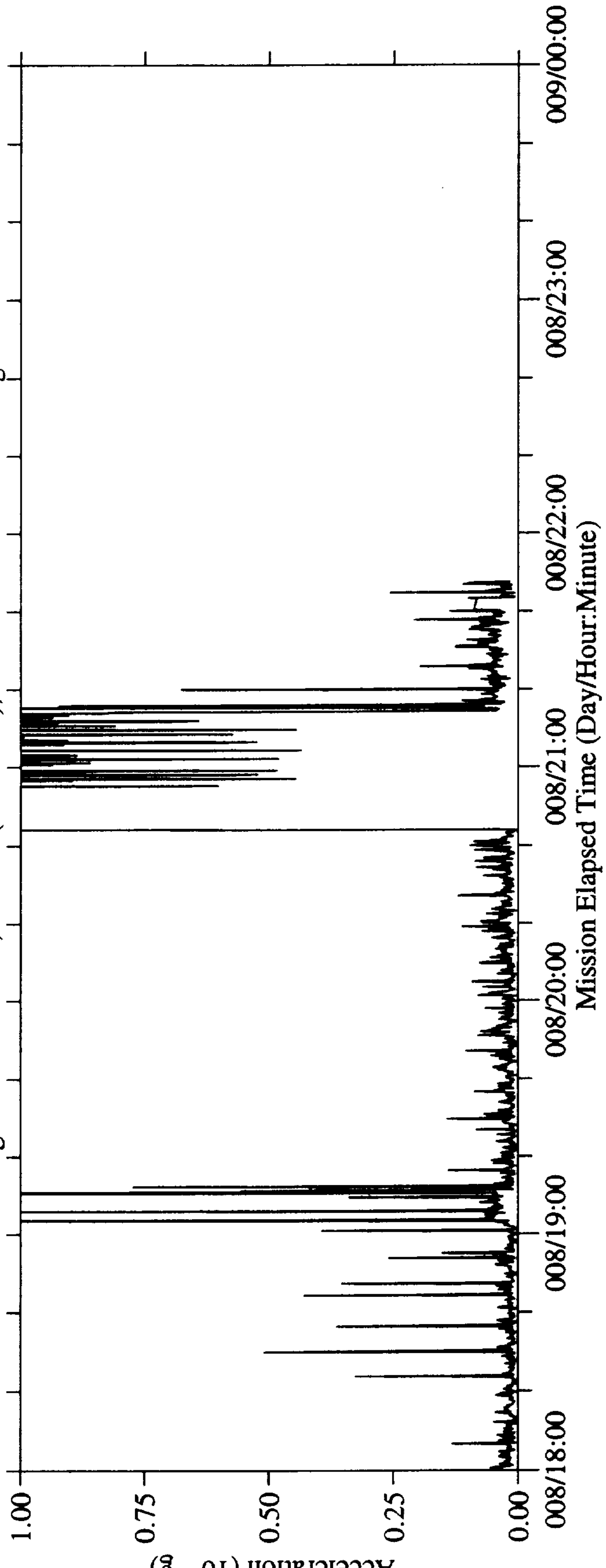

Figure 65b: STS–79, Head C (fc=25 Hz), Ten Second Interval RMS

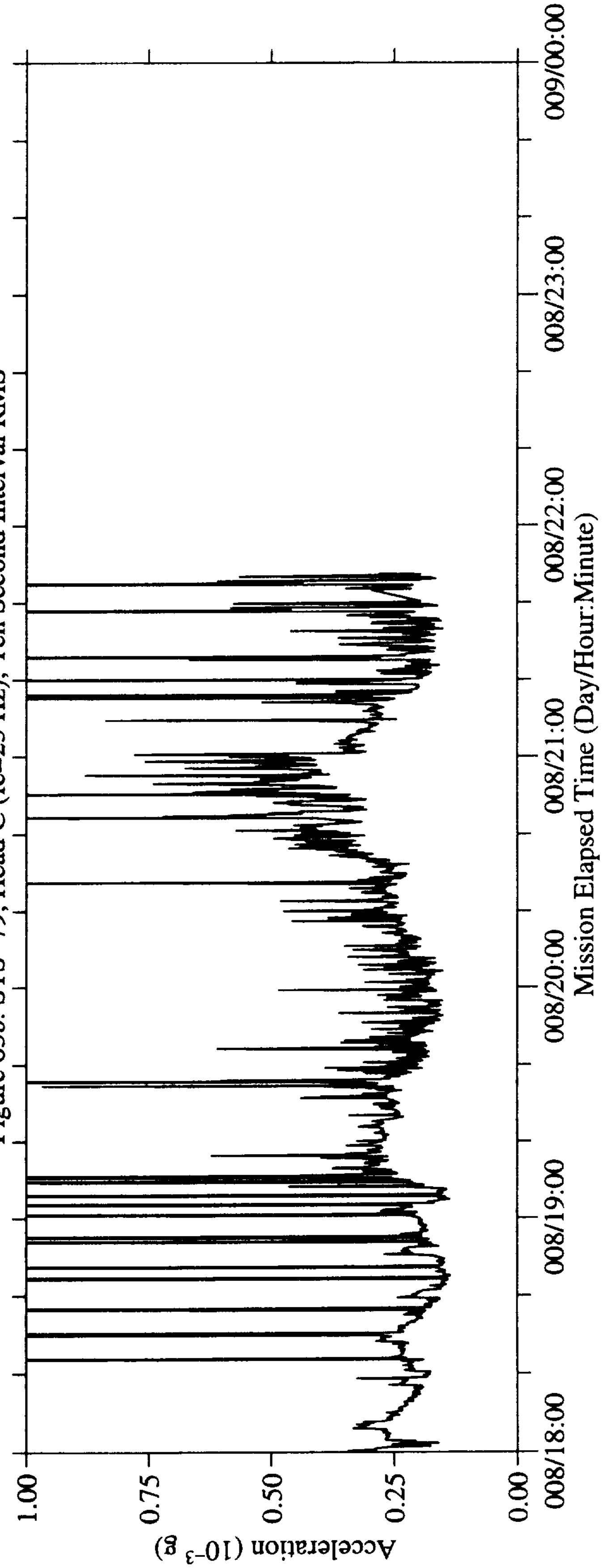

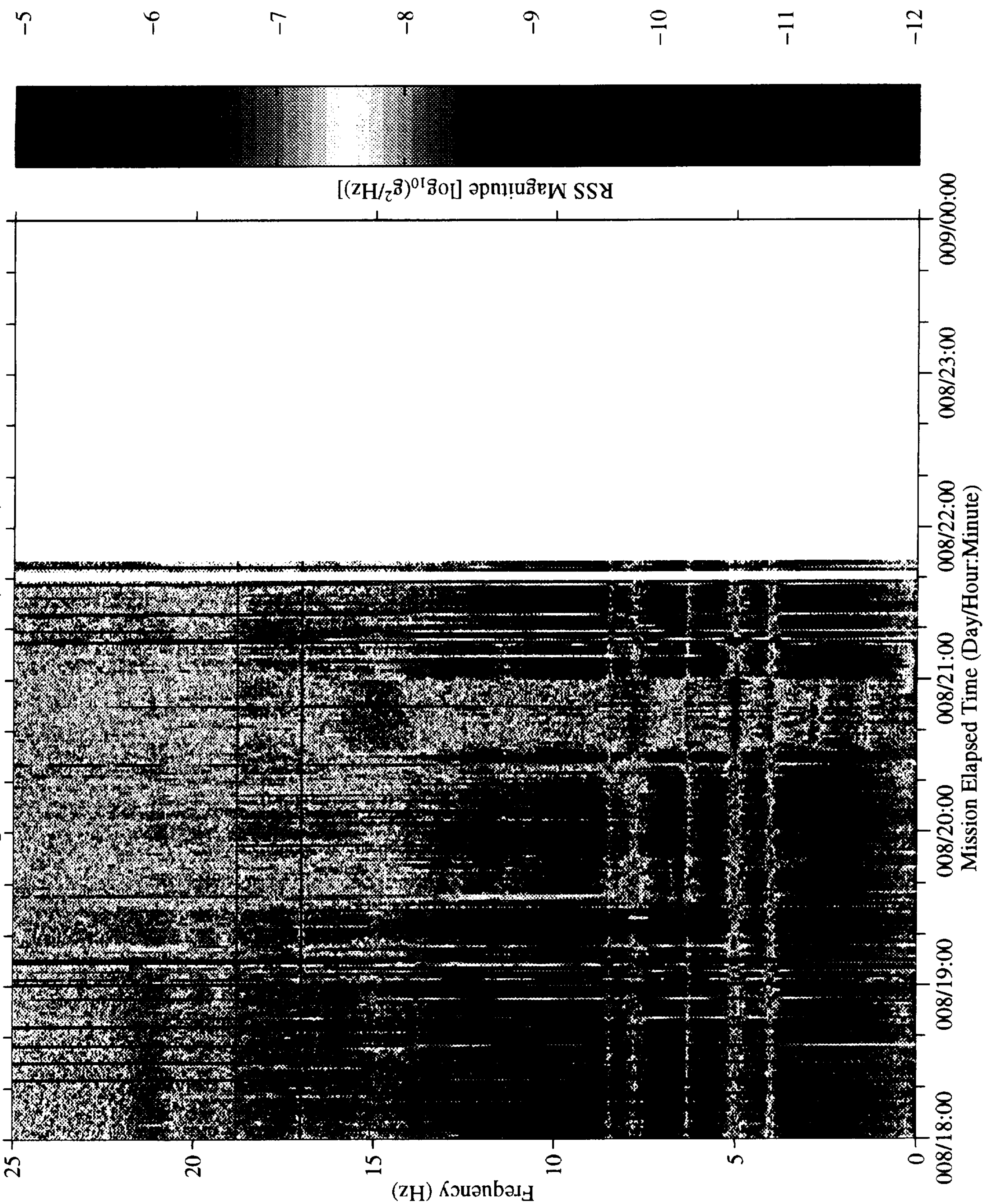

Figure 66: STS–79, Head C (fc=25 Hz)

Appendix C: User Comment Sheet

We would like you to give us some feedback so that we may improve the Mission Summary Reports. Please answer the following questions and give us your comments.

1. Do the Mission Summary Reports fulfill your requirements for acceleration and mission information?
______Yes ______No If not why not?

Comments:
____
____

2. Is there additional information which you feel should be included in the Mission Summary Reports?
______Yes ______No If so what is it?

Comments:
____
____

3. Is there information in these reports which you feel is not necessary or useful?

______Yes ______No If so, what is it?

Comments:
____
____

4. Do you have internet access via: (____)ftp (____)WWW (____)gopher (____)other? Have you already accessed SAMS data or information electronically?

______Yes ______No

Comments:
____
____

Completed by: Name:______________________ Telephone____________________

Address:______________________ Facsimile____________________

______________________ E-mail addr____________________

Return this sheet to:
Duc Truong
NASA Lewis Research Center
21000 Brookpark Road MS 500-216
Cleveland, OH 44135

or
FAX to PIMS Project: 216-433-8660
e-mail to: pims@lerc.nasa.gov.

REPORT DOCUMENTATION PAGE

Form Approved
OMB No. 0704-0188

1. AGENCY USE ONLY (*Leave blank*)	2. REPORT DATE	3. REPORT TYPE AND DATES COVERED
	March 1997	Final Contractor Report

4. TITLE AND SUBTITLE

Summary Report of Mission Acceleration Measurements for STS–79
Launched September 16, 1996

5. FUNDING NUMBERS

WU–963–60–0D
C–NAS3–27254

6. AUTHOR(S)

Melissa J.B. Rogers, Milton E. Moskowitz, Kenneth Hrovat, and Timothy A. Reckart

7. PERFORMING ORGANIZATION NAME(S) AND ADDRESS(ES)

Tal-Cut Company
24831 Lorain Road, Suite 203
North Olmsted, Ohio 44070

8. PERFORMING ORGANIZATION REPORT NUMBER

E–10661

9. SPONSORING/MONITORING AGENCY NAME(S) AND ADDRESS(ES)

National Aeronautics and Space Administration
Lewis Research Center
Cleveland, Ohio 44135–3191

10. SPONSORING/MONITORING AGENCY REPORT NUMBER

NASA CR–202325

11. SUPPLEMENTARY NOTES

Project Manager, Duc K. Truong, Microgravity Science Division, NASA Lewis Research Center, organization code 6727, (216) 433–8394.

12a. DISTRIBUTION/AVAILABILITY STATEMENT

Unclassified - Unlimited
Subject Categories 20, 35, and 18

This publication is available from the NASA Center for AeroSpace Information, (301) 621–0390.

12b. DISTRIBUTION CODE

13. ABSTRACT (*Maximum 200 words*)

The Space Acceleration Measurement System (SAMS) collected acceleration data in support of the Mechanics of Granular Materials experiment during the STS–79 Mir docking mission, September 1996. STS–79 was the first opportunity to record SAMS data on an Orbiter while it was docked to Mir. Crew exercise activities in the Atlantis middeck and the Mir base module are apparent in the data. The acceleration signals related to the Enhanced Orbiter Refrigerator Freezer had different characteristics when comparing the data recorded on Atlantis on STS–79 with the data recorded on Mir during STS–74. This is probably due, at least in part, to different transmission paths and SAMS sensor head mounting mechanisms. Data collected on Atlantis during the STS–79 docking indicate that accelerations due to vehicle and solar array structural modes from Mir transfer to Atlantis and that the structural modes of the Atlantis-Mir complex are different from those of either vehicle independently. A 0.18 Hz component of the SAMS data, present while the two vehicles were docked, was probably caused by the Mir solar arrays. Compared to Atlantis structural modes of about 3.9 and 4.9 Hz, the Atlantis-Mir complex has structural components of about 4.5 and 5.1 Hz. After docking, apparent structural modes appeared in the data at about 0.8 and 1.8 Hz. The appearance, disappearance, and change in the structural modes during the docking and undocking phases of the joint Atlantis-Mir operations indicates that the structural modes of the two spacecraft have an effect on the microgravity environment of each other. The transfer of structural and equipment related accelerations between vehicles is something that should be considered in the International Space Station era.

14. SUBJECT TERMS

Microgravity environment; SAMS; Acceleration; STS–79; Mir; Atlantis; Spacehab–05

15. NUMBER OF PAGES

105

16. PRICE CODE

A06

17. SECURITY CLASSIFICATION OF REPORT	18. SECURITY CLASSIFICATION OF THIS PAGE	19. SECURITY CLASSIFICATION OF ABSTRACT	20. LIMITATION OF ABSTRACT
Unclassified	Unclassified	Unclassified	